2011

Human brain hexokinase: Determinants of mitochondrial binding and mechanism of nucleotide release

Nimer Mehyar
Iowa State University

Human brain hexokinase: Determinants of mitochondrial binding and mechanism of nucleotide release

by

Nimer Mehyar

A dissertation submitted to graduate faculty

in partial fulfillment of the requirements for the degree of

DOCTOR OF PHILOSOPHY

Major: Biochemistry

Program of Study Committee:
Richard B. Honzatko, Major Professor
Michael Shogren-Knaak
Mark Hargrove
Reuben Peters
Joan Cunnick

Iowa State University

Ames, Iowa

2011

To Ghada

TABLE OF CONTENTS

CHAPTER 1: GENERAL INTRODUCTION

Introduction

The first step of glycolysis is catalyzed by hexokinase (ATP: D-hexose-6-phosphotransferase, EC 2.7.1.1). Hexokinases catalyze the transfer of γ-phosphoryl group from adenosine triphosphate-magnesium complex ($[ATP\text{-}Mg]^{2-}$) to glucose at the 6-hydroxyl position producing glucose-6-phosphate (Glc-6-P) and adenosine diphosphate (ADP) (1-3). Four hexokinase isozymes are identified in mammalian tissue: I, II, III and IV (1,4) (Table 1.1). Hexokinases I-III have molecular weights of 100 kDa and approximately 70% sequence identity (5). Hexokinase IV is a 50 kDa protein with sequences similar to the C- and N-halves of hexokinases I-III (5). Hexokinase I (HKI) or brain hexokinase is recognized as the "pacemaker of glycolysis" in brain tissue and the red blood cell (6). HKI is highly expressed in kidneys, liver, intestines and lungs (3,7). Heart, muscles, lungs, intestines and adipose tissue are the major tissues that produce HKII (3,7). HKIII is relatively abundant in lungs, liver and spleen (3,7). Presumably, hexokinases I-III have evolved by the duplication and fusion of a primodial gene similar to that of yeast hexokinase (8,9). The N-and C-terminal halves of HKI and HKII exhibit significant sequence similarities (10). Both halves of HKII support catalysis and are each sensitive to inhibition by Glc-6-P (11), whereas only the C-terminal half of HKI supports activity (12). Solution studies of native HKI reveal only one high-affinity binding site for Glc-6-P (13-15). X-ray crystal structure of HKI, however, shows Glc-6-P binding to

Table 1.1. Mammalian hexokinase isoenzymes.

Properties	HKI	HKII	HKIII	HKIV
MW (kDa)	~100	~100	~100	~50
K_m^{Glc} (mM)	0.03	0.3	0.003	6
K_m^{ATP} (mM)	0.5	0.7	1.0	0.6
C-half activity	+	+	+	
N-half activity	-	+	-	
$K_i^{AnGlc\text{-}6\text{-}P}$ (mM)	0.02	0.02	0.1	-
Glc-6-P inhibition (C-half)	+	+	?	
Glc-6-P inhibition (N-half)	+	+	?	
P_i relief of Glc-6-P inhibition	+	-	-	-
Tissue	Brain, kidney, red blood cells	Muscles, lung, adipose	Lung, liver, spleen	Liver, pancrease
Mitochondrial binding	+	+	-	-

both N- and C- terminal halves (16-18). Previous observations are in agreement with only one of the two Glc-6-P sites is available for functional ligand binding in solution. Two models are proposed to explain HKI inhibition by Glc-6-P and the relief of inhibition by phosphate (Pi). In the first model, Glc-6-P binds to N-terminal half causing inhibition of the catalytically active C-terminal half by an allosteric mechanism (12). Pi binding to N-terminal half is mutually exclusive with Glc-6-P (18-20). In the second model, Glc-6-P directly binds the catalytically active C-terminal half (19-21). Pi binds to N-terminal half and reliefs Glc-6-P inhibition by an allosteric mechanism (18-20). It is proposed that Glc-6-P sensitive binding site has evolved from an ancestral catalytic site (8). At high concentrations, P_i can bind to the active site and inhibit HKI (17). P_i does not relieve Glc-6-P inhibition of the HKII (18). ADP is a mixed inhibitor for both HKI and HKII (7). ADP inhibits HKI by binding to both the active site and a second allosteric site (2,22-26). Free adenosine triphosphate $[ATP]^{4-}$ is a competitive inhibitor in relation to $[ATP\text{-}Mg]^{2-}$, the true substrate for HKI.

The X-ray crystal structure of recombinant human HKI reveals a dimer of identical HKI molecules (Fig.1.1). The subunit consists of C- and N- terminal domains separated by a transition helix (16). In the crystalline complex of HKI with glucose (Glc) and Glc-6-P, both ligands bind in proximity to each other at the C- and N-terminal halves (16,18) (Fig. 1.2). Mutational analysis showed that C-and N-terminal Glc-6-P sites, can independently inhibit HKI (27). Crystallizing HKI with Glc and P_i revealed a binding site for P_i at N-terminal half (16) (Fig. 1.3). Mutations in the Glc-6-P pocket at N-half did not prevent Glc-6-P inhibition; however, P_i-relief

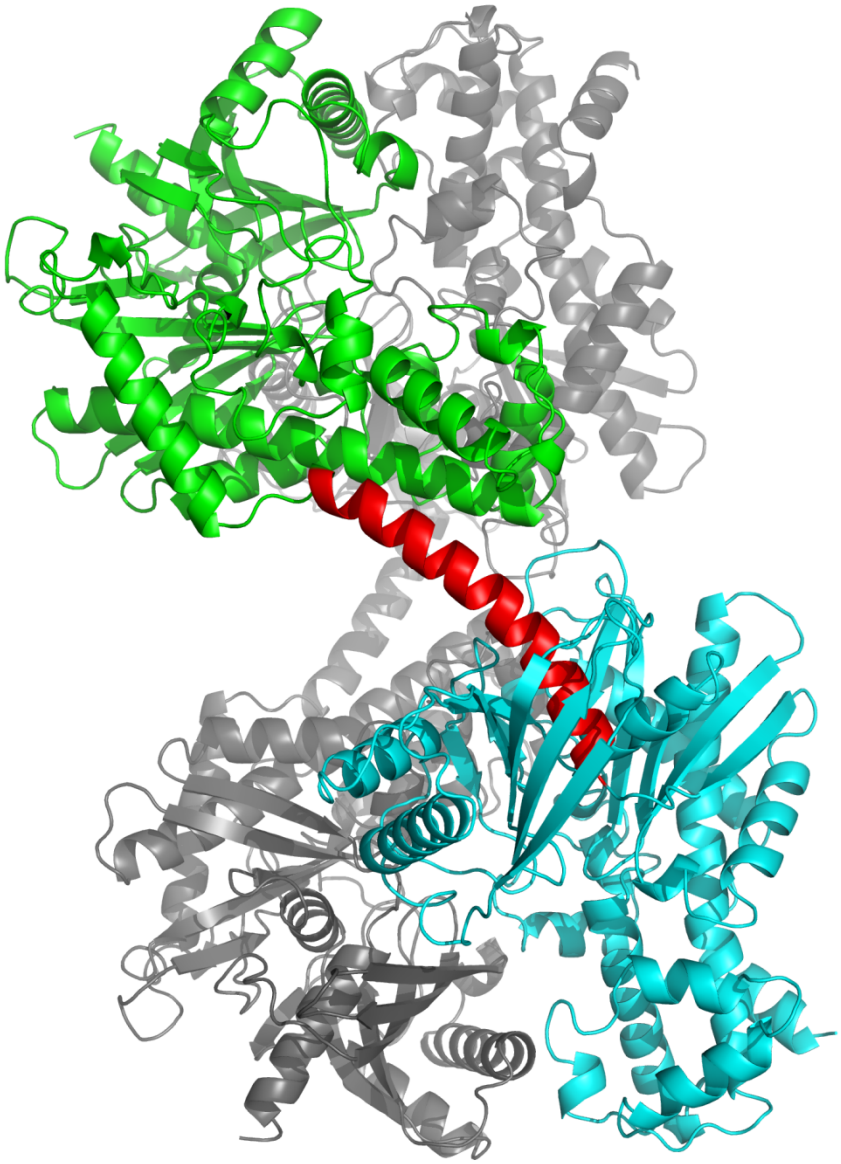

Fig. 1.1. Hexokinase x-ray structure (PDB 1HKB). C-half (green), N-half (cyan), and transition helix (red).

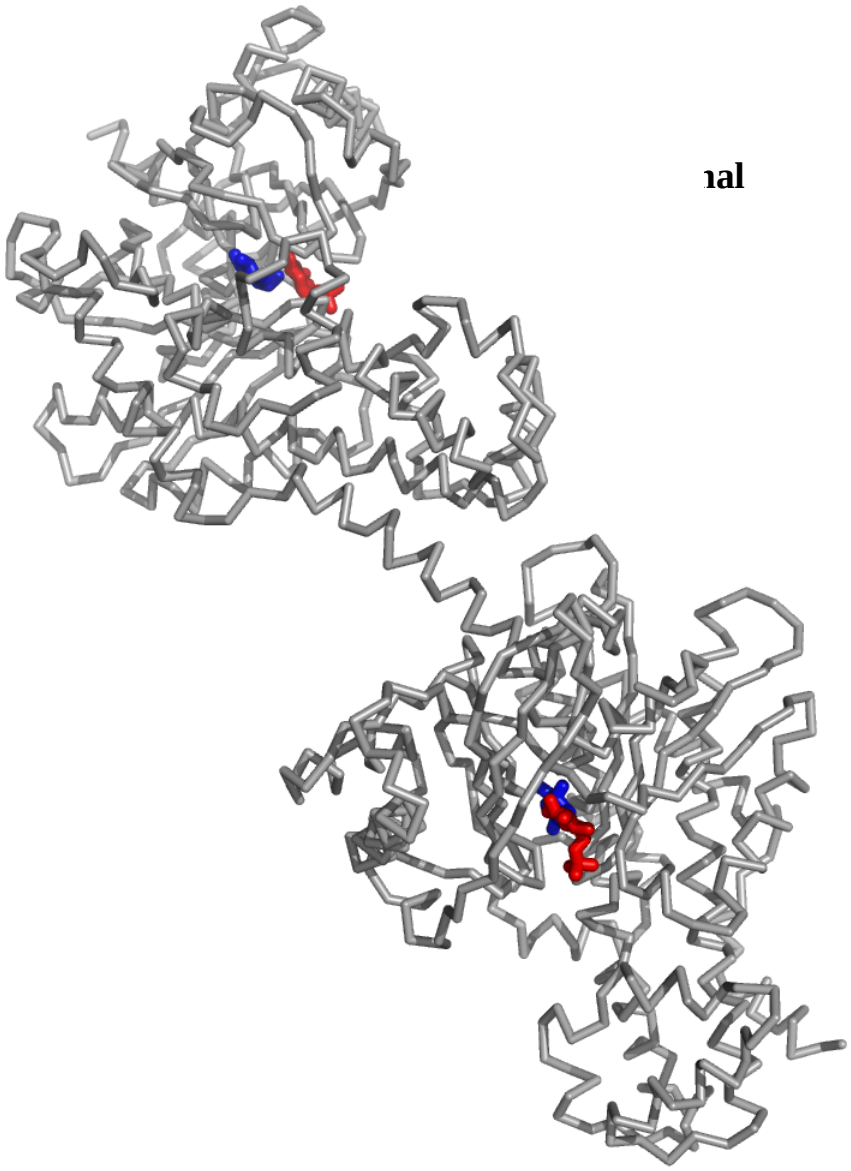

Fig. 1.2. Ligand binding to HKI. HKI complexed with Glc (blue) and Glc-6-P (red) (1HKB).

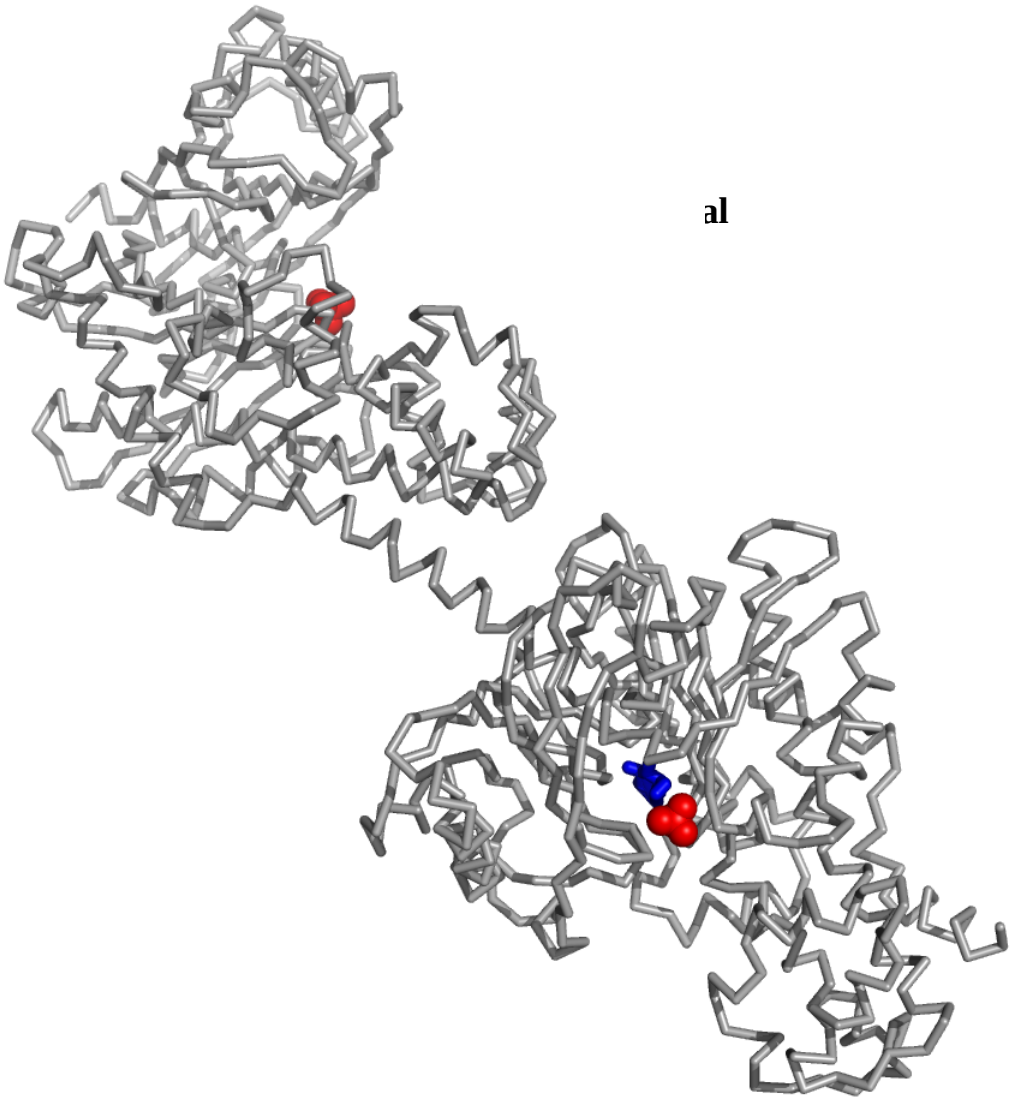

Fig. 1.3. Ligand binding to HKI. HKI complexed with Pi (red spheres) and Glc (blue) (1HKC).

of Glc-6-P inhibition was compromised (27). Mutating residues in Glc-6-P binding pocket at the C-terminal half did not affect Glc-6-P inhibition or P_i-relief of Glc-6-P inhibition (27). Similar to yeast hexokinase, the C-terminal of HKI has two conformational states: open and closed (16,18) (Fig. 1.2, Fig. 1.3). The 6-phosphoryl moiety of the Glc-6-P overlaps the binding site of the α-phosphoryl group of ATP in the C-terminal half (18,21). On the other hand, the same group overlaps the binding site of P_i in the N-terminal half (16,18). Homology modeling with yeast hexokinase and other adenine nucleotide binding proteins was used to develop a model for ATP binding site in HKI (28). Many residues in ATP binding pocket were tested by site directed mutation and proved to be essential for transition state product ADP-hexokinase stabilization (29-31). Corresponding mutations in the vestigial adenine nucleotide binding site at N-half caused significant loss of P_i induced relief of Glc-6-P inhibition (31). Subsequently crystals of an engineered monomer of HKI revealed ADP binding to the active site of the C-terminal half and an additional nucleotide binding sites at the N-half that is remote from the vestigial active site (21) (Fig. 1.4).

HKI binds the outer mitochondrial membrane (OMM) in brain tissue (32). Mitochondria-associated HKI has preferential access to newly formed mitochondrial ATP (32). HKI binding to the mitochondrion prevents the opening of the permeability transition pore (PTP) (33). The PTP putatively consists of the adenylate translocator (ANT) of the inner mitochondrion membrane, and the voltage dependent anion channel (VDAC) of the outer mitochondrion membrane (34-39). The PTP is regulated by cyclophilin D of the inner mitochondrion matrix and the binding of hexokinase I and II (40-42). HKI likely interacts with VDAC to close PTP opening

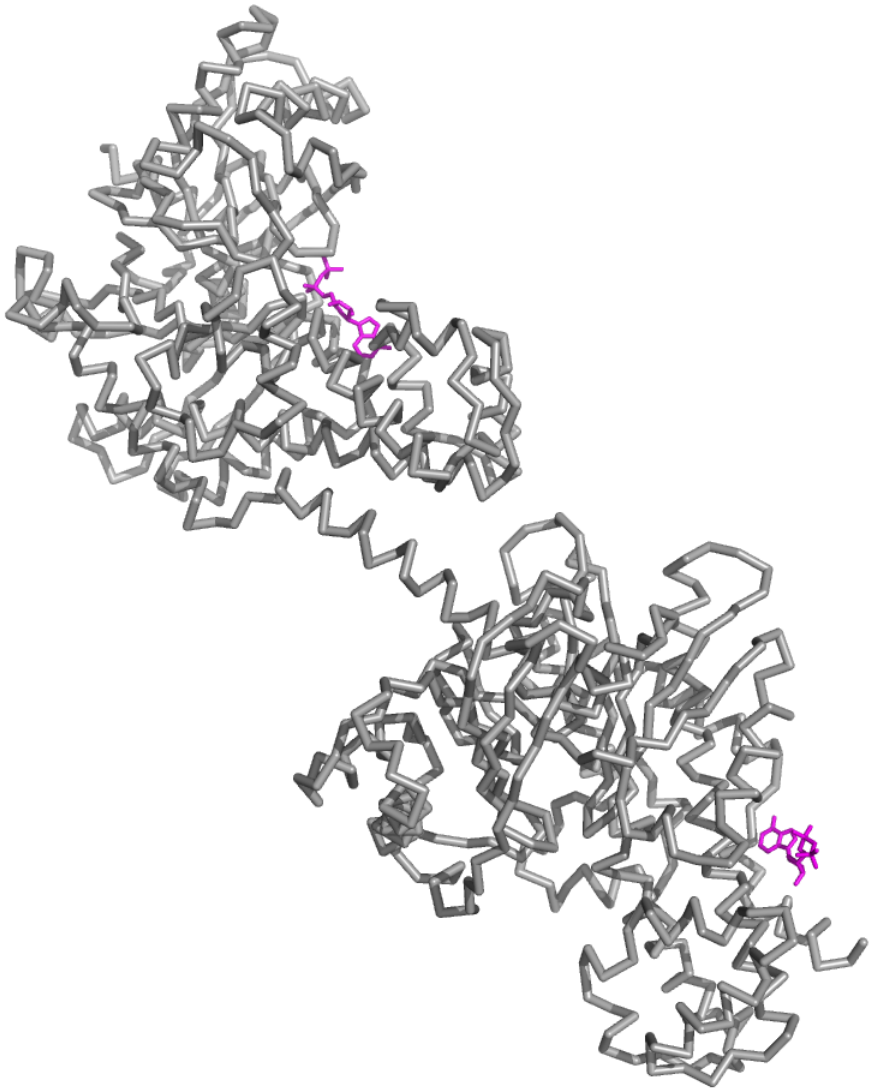

Fig. 1.4. Nucleotide binding to HKI (PDB 1CZA). HKI complexed with ADP (magenta).

(34-35). Open PTP results in loss of membrane potential, organelle swelling, cytosolic acidification, and the release of cytochrome c (33,40). Released cytochrome c activates the caspase family of proteases and initiates apoptosis (42-44). Another line of evidence suggests that pro-apoptotic proteins such as Bax trigger cytochrome c release without mitochondrial swelling (40,45,46). Pro-apoptotic proteins (Bax, Bak, and Bim) assemble with VDAC in large channels used to release of cytochrome c (45-47). Mitochondrion-associated hexokinase II antagonizes the formation of these channels (48-50). Overexpression of VDAC-1 causes apoptotic cell death (51,52), however, over expression of N-terminally truncated VDAC-1 did not induce cells to release cytochorme c and the cells were resistant to apoptosis (53). N-terminus peptide and other VDAC-1 based peptides bind to immobilized HKI (54). These peptides prevented HKI protection of cells (53,54). Chemical modification or mutation of residue Glu 72 prevented HKI binding to mitochondria and prevented it protection against apoptosis in different cancer cells (51,55). HKI binding to VDAC-1 in reconstituted in lipid membrane decreased channel conductance (33). HKI failed to bind to mutant mVDAC E72Q in reconstituted in lipid membrane (55).

HKI association with mitochondria requires fifteen, largely hydrophobic amino acid residues at the N-terminus (56). Exposing HKI to proteases results in loss of mitochondrial binding (57). Using rapid purification procedures such as HPLC decreases the mitochondria non-binding portion of rat brain hexokinase (58,59). Hydrophobicity of mitochondria-binding rat brain hexokinase is higher than that non-binding form (60). Mitochondria binding and non-binding forms of HKI have similar molecular weight and kinetic properties (61). The N-terminal peptide from rat brain

does not yield to chemical sequencing (62), being blocked most probably by an acetyl group (63). The first 11 residues of HKI N-terminus are proposed to have a helical conformation (62). A helical conformation facilitates the insertion of the N-terminal segment in the OMM in lipid bilayer (62-64). Monoclonal antibodies against rat brain hexokinase inhibited both mitochondrial binding and Glc-6-P induced release (65,66). Structural determinants for HKI-association must be contained in the hydrophobic tail, but single-residue determinants have not been identified. A contribution of thesis work here is the discovery of single-residue determinants essential for the binding of HKI to mitochondria.

Many small and physiological important ligands dissociate HKI from the OMM. The most relevant releasing ligands are nucleotides and Glc-6-P (32). Using a wild-type recombinant HKI with properties comparable to native brain hexokinase, including those of mitochondrial-binding and release, Skaff *et al.* (67) demonstrated that Glc-6-P-induced release of mitochondria-bound HKI follows a simple equilibrium model. In this model, ligand-bound HKI partitions between solution and OMM. Mutating the Glc-6-P binding site at N-terminal half of HKI, increased the Glc-6-P concentration necessary for 50% release of mitochondria-bound HKI by 7-fold. Although nucleotide-induced release of HKI from mitochondria was observed as early as Glc-6-P release (32,68-70), the mechanism of nucleotide release remained unclear. Adenine nucleotides can induce mitochondrial release by either binding to HKI itself or to VDAC. Three possible sites exist on HKI: (a) the active site at the C-terminal half (5), (b) the P_i binding site at the N-terminal half (21), and (c) the nucleotide pocket of unknown function near the N-terminal membrane targeting

element (21,71). VDAC-1, on the other hand, has multiple nucleotide binding sites as shown by photoactive ATP analog, Bz-ATP (benzoyl-benzoyl-ATP), studies (72). Mutated nucleotide-binding VDAC-1 affects cellular growth levels negatively (73). We propose that nucleotide-induced release of HKI mitochondria follows a mutually exclusive binding model. In this model HKI and nucleotides compete for a common binding site on VDAC1 at the OMM.

The major contribution of this dissertation is to establish an ATP induced release model and to identify binding determinants in the HKI hydrophobic tail. Properties of binding of fluorescent nucleotide analogs to HKI were also investigated.

Dissertation Organization

This dissertation is organized into five chapters. Chapter 1 covers the literature related to the research project. Problems and objectives of the thesis research are provided as well. Chapters 2, 3 and 4 are papers prepared for submission for publication in peer reviewed journals. Chapter 2 is a determination of the mechanism of nucleotide release of HKI from OMM. Chapter 3 shows that the N-terminal hydrophobic tail has specific and essential amino-acid determinants that stabilize the binding of HKI to the mitochondrion. Chapter 4 describes the specificity of nucleotide and TNP-nucleotide binding to HKI under different conditions of ligation. Conclusions and recommendations for future studies are in Chapter 5.

References

1. González, C; Ureta, T; Sánchez, R; Niemeyer, H. (1964) *Biochem. Biophys. Res. Commun.* **16**, 347-52.

2. Grossbard, L; Schimke, R T. (1966) *J. Biol. Chem*. **241**, 3546-60.

3. Katzen, H M. (1967) *Adv. Enzyme. Regul*. **5**, 335-56.

4. Katzen, H M; Schimke, R T. (1965) *Proc. Natl. Acad. Sci. U S A.* **54**, 1218-25.

5. Wilson, J E. (1995) *Rev. Physiol. Biochem. Pharmacol*. **126**, 65-198.

6. Lowry, O H; Passonneau, J V. (1964) *J. Biol. Chem*. **239**, 31-42.

7. Purich, D L; Fromm, H J; Rudolph, F B. (1973) *Adv. Enzymol. Relat. Areas. Mol. Biol*. **39**, 249-326.

8. Colowick, S P. (1973) in The enzymes. (Boyer, PD., ed) 9, 1-48, Academic New York, New York.

9. Wilson, J E. (2003) *J. Exp. Biol*. **206**, 2049-57.

10. Schwab, D A; Wilson, J E. (1989) *Proc Natl Acad Sci U S A*. **86**, 2563-2567.

11. Ardehali, H; Yano, Y; Printz, R L; Koch, S; Whitesell, R R; May, J M; Granner, D K. (1996) *J. Biol. Chem*. **271**, 1849-52.

12. White, T K; Wilson, J E. (1989) *Arch. Biochem. Biophys*. **274**, 375-93.

13. Chou, A C; Wilson, J E. (1974) *Arch. Biochem. Biophys*. **165**, 628-33.

14. Ellison, W R; Lueck, J D; Fromm, H J. (1975) *J. Biol. Chem*. **250**, 1864-71.

15. Mehta , A; Jarori , G K; Kenkare, U W. (1988) *J. Biol. Chem*. **263**, 15492-7.

16. Aleshin, A E; Zeng, C; Bourenkov, G P; Bartunik , H D; Fromm, H J; Honzatko, R.B. (1998) *Structure* **6**, 39-50.

17. Aleshin, A E, Fromm, H J and Honzatko, R B. (1998) *FEBS Lett*. **434**, 42-6.

18. Aleshin, A E; Zeng, C; Bartunik, H D; Fromm, H J; Honzatko, R B. (1998) *J. Mol. Biol.* **282**, 345-57.

19. Fang, T Y; Alechina, O; Aleshin, A E; Fromm, H J; Honzatko, R B. (1998) *J. Biol. Chem*. **273**, 19548-53.

20. Tsai, H J; Wilson, J E. (1995) *Arch. Biochem. Biophys*. **316**, 206-14.

21. Aleshin, A E; Kirby, C; Liu, X; Bourenkov, G P; Bartunik, H D; Fromm, H J; Honzatko, R B. (2000) *J. Mol. Biol*. **296**, 1001-15.

22. Fromm, H J; ZEWE, V. (1962) *J. Biol. Chem*. **237**, 1661-7.

23. Purich, D L; Fromm, H J. (1972) *Biochem. J.* **130**, 63-9.

24. Purich, D L; Fromm, H J. (1971) *J. Biol. Chem*. **246**, 3456-63.

25. Kosow, D P; Rose, I A. (1970) *J. Biol. Chem*. **245**, 198-204.

26. Copley , M; Fromm, H J. (1967) *Biochemistry* **6**, 3503-9.

27. Liu, X; Kim, C S; Kurbanov, F T; Honzatko, R B; Fromm, H J. (1999) *J. Biol. Chem*. **274**, 31155-9.

28. Zeng, C; Fromm, H J. (1995) *J. Biol. Chem*. **270**, 10509-13.

29. Baijal, M; Wilson, J E. (1995) *Arch. Biochem. Biophys*. **321**, 413-20.

30. Zeng, C; Aleshin, A E; Hardie, J B; Harrison , R W; Fromm, H J. (1996) *Biochemistry* **35**, 13157-64.

31. Zeng, C; Aleshin, A E; Chen, G; Honzatko, R B; Fromm, H J. (1998) *J. Biol. Chem.* **273**, 700-4.

32. Rose, I A; Warms, J V. (1967) *J. Biol. Chem*. **242**, 1635-45.

33. Azoulay-Zohar, H; Israelson, A; Abu-Hamad, S; Shoshan-Barmatz, V. (2004) *Biochem. J*. **377**, 347-55.

34. Lindén, M; Gellerfors, P; Nelson, B D. (1982) *FEBS Lett.* **141**, 189-92.

35. Fiek, C; Benz, R; Roos, N; Brdiczka, D. (1982) *Biochim. Biophys. Acta*. **688**, 429-40.

36. Beutner, G; Ruck, A; Riede, B; Welte, W; Brdiczka, D. (1996) *FEBS Lett*. **396**, 189-95.

37. Beutner, G; Rück, A; Riede, B; Brdiczka, D. (1997) *Biochem. Soc. Trans*. **25**, 151-7.

38. Vyssokikh, M Y; Brdiczka, D. (2003) *Acta. Biochim. Pol*. **50**, 389-404.

39. Vyssokikh, M Y; Goncharova, N Y; Zhuravlyova, A V; Zorova, L D; Kirichenko, W; Krasnikov, B F; Kuzminova, A E; Melikov, K C; Melik-Nubarov, N S; Samsonov, A V; Belousov, W; Prischepova, A E; Zorov, D B. (1999) *Biochemistry (Mosc)*. **64**, 390-8.

40. Machida, K; Ohta, Y; Osada, H. (2006) *J. Biol. Chem*. **281**, 14314-20.

41. Zoratti, M; Szabò, I. (1995) *Biochim. Biophys. Acta*. **1241**, 139-76.

42. Crompton, M; Virji, S; Doyle, V; Johnson, N; Ward, J M. (1999) *Biochem. Soc. Symp*. **66**, 167-79.

43. Zamzami, N; Kroemer, G. (2003) *Curr. Biol*. **13**, R71-3.

44. Lemasters, J J; Qian, T; Bradham, C A; Brenner, D A; Cascio, W E; Trost, L C; Nishimura, Y; Nieminen, A L; Herman, B. (1999) *J. Bioenerg. Biomembr*. **31**, 305-19.

45. Shimizu, S; Narita, M; Tsujimoto, Y. (2000) *Nature* **399**, 483-87.

46. Shimizu, S; Matsuoka, Y; Shinohara, Y; Yoneda, Y; Tsujimoto, Y. (2001) *J. Cell Biol*. **152**, 237-50.

47. Shimizu, S; Ide, T; Yanagida, T; Tsujimoto, Y. (2000) *J. Biol. Chem*. **275**, 12321-5.

48. Pastorino, J G; Shulga, N; Hoek, J B. (2002) *J. Biol. Chem*. **277**, 7610-8.

49. Majewski, N; Nogueira, V; Bhaskar, P; Coy, P E; Skeen, J E; Gottlob, K; Chandel, N S; Thompson, C B; Robey, R B; Hay, N. (2004) *Mol. Cell* **16**, 819-30.

50. Majewski, N; Nogueira, V; Robey, R B; Hay, N. (2004) *Mol. Cell. Biol*. **24**, 730-40.

51. Zaid, H; Abu-Hamad, S; Israelson, A; Nathan, I; Shoshan-Barmatz, V. (2005) *Cell Death Differ.* **12**, 751-60.

52. Abu-Hamad, S; Sivan, S; Shoshan-Barmatz, V. (2006) *Proc. Natl. Acad. Sci. U S A.* **103**, 5787-92.

53. Abu-Hamad, S; Arbel, N; Calo, D; Arzoine, L; Israelson, A; Keinan, N; Ben-Romano, R; Friedman, O; Shoshan-Barmatz, V. (2009) *J. Cell Sci*. **122**, 1906-16.

54. Arzoine, L; Zilberberg, N; Ben-Romano, R; Shoshan-Barmatz, V. (2009) *J. Biol. Chem.* **284**, 3946-55.

55. Shoshan-Barmatz, V; Zakar, M; Rosenthal, K; Abu-Hamad, S. (2009) *Biochim. Biophys. Acta*. **1787**, 421-30.

56. Xie, G C; Wilson, J E. (1988) *Arch. Biochem. Biophys*. **267**, 803-10.

57. Rose, I A; Warms, J V. (1967) *J. Biol. Chem*. **242**, 1635-45.

58. Felgner, P L; Wilson, J E. (1976) *Biochem. Biophys. Res. Commun*. **68**, 592-7.

59. Polakis, P G; Wilson, J E. (1982) *Biochem. Biophys. Res. Commun*. **107**, 937-43.

60. Kurokawa, M; Tokoyama, K; Kaneko, M; Ishibashi, S. (1983) *Biochem. Biophys. Res. Comm.* **115**, 1101-7.

61. Ceccaroli, P; Fiorani, M; Buffalini, M; Piccoli, G; Biagiarelli, B; Stocchi, V.

(1995) *Biochem. Mol. Biol. Int*. **37**, 665-74.

62. Xie, G C; Wilson, J E. (1988) *Arch. Biochem. Biophys*. **267**, 803-10.

63. Pittler, S J; Kozak, L P; Wilson, J E. (1985) *Biochim. Biophys. Acta*. **843**, 186-92.

64. Ehsani-Zonouz, A; Golestani, A; Nemat-Gorgani, M. (2001) *Mol. Cell. Biochem*. **223**, 81-7.

65. Finney, K G; Messer, J L; DeWitt, D L; Wilson, J E. (1984) *J. Biol. Chem*. **259**, 8232-7.

66. Smith, A D; Wilson, J E. (1991) *Arch. Biochem. Biophys*. **287**, 359-66.

67. Skaff, D A; Kim, C S; Tsai, H J; Honzatko, R B; Fromm, H J. (2005) *J. Biol. Chem*. **280**, 38403-9.

68. Wilson, J E. (1968) *J. Biol. Chem*. **243**, 3640-7.

69. Hochman, M S, Shimada, Y and Sacktor, B. (1974) *J. Neurochem*. **23**, 861-3.

70. Bustamante, E and Pedersen, P L. (1980) *Biochemistry* **19**, 4972-7.

71. Rosano, C; Sabini, E; M, Rizzi; Deriu, D; Murshudov, G; Bianchi, M; Serafini, G; M, Magnani; Bolognesi, M. (1999) *Structure* **7**, 1427-37.

72. Yehezkel, G; Hadad, N; Zaid, H; Sivan, S; Shoshan-Barmatz, V. (2006) *J. Biol. Chem*. **281**, 5938-46.

73. Yehezkel, G, Abu-Hamad, S and Shoshan-Barmatz, V. (2007) *J. Cell. Physiol*. **212**, 551-61.

CHAPTER 2. MECHANISM OF ATP-DEPENDENT RELEASE OF WILD-TYPE AND MUTANT HUMAN BRAIN HEXOKINASES FROM MITOCHONDRIA[1]

A paper to be submitted to the Journal of Biological Chemistry

Nimer Mehyar[2], Muneaki Watanabe, Lu Shen, Andrew D. Skaff, and Richard B. Honzatko[2,3]

Abstract

Adenosine 5′-triphosphate (ATP) can release hexokinase I (HKI) from its binding site on the outer mitochondrial membrane, but the mechanism of ATP release of HKI from mitochondria is unclear. ATP binds to the C-terminal half of HKI as a substrate and to the N-terminal half near the membrane binding element. ATP may also bind to the voltage dependent anion channel (VDAC), the integral membrane component that putatively targets HKI to the mitochondrion. The fluorescent nucleotide analogue 2′,3′-*O*-(2,4,6-trinitrophenyl) adenosine 5′-diphosphate (TNP-ADP) binds with high affinity to the C-terminal half of HKI (K_d = 0.79 ± 0.09 μM)

[1] This research was supported in part by National Institute of Health Research Grant NS 10546.

[2] Graduate student and professor, respectively, Department of Biochemistry, Biophysics and Molecular Biology, Iowa State University. Research conducted and manuscript written by Mehyar with assistance from Muneaki, Shen, Skaff and Honzatko.

[3] To whom correspondence should be addressed.

and to VDAC (K_d = 1.3 ± 0.1 μM), but not to the N-terminal half of HKI (K_d > 50 μM). ATP competes with TNP-ADP for binding sites on HKI (K_A = 190 ± 20 μM) and VDAC (K_A = 550 ± 40 μM), but CTP does not displace TNP-ADP from either HKI or VDAC. Other trinitophenyl nucleotides (TNP-ATP, TNP-AMP, and TNP-CTP) bind with high affinity to HKI and VDAC. ATP and trinitrophenyl nucleotides individually release wild-type HKI from mitochondria; however, CTP is ineffective as an agent of release. ATP and ADP-TNP release the truncated N-domain of HKI from mitochondria, excluding nucleotide binding to either the N- or C-half of HKI in the release mechanism. Results here are consistent with a release mechanism caused by the binding of ATP or TNP-ADP to VDAC.

Introduction

Mammalian tissue contains four hexokinase isozymes: I, II, III and IV (1). Hexokinase I (HKI) or brain hexokinase has long been recognized as the “pacemaker of glycolysis” in brain tissue and the red blood cell (2). Human brain comprises less than 2% of body weight and yet it utilizes at least one-quarter of the circulating blood glucose and approximately one-fifth of the oxygen consumed by the body (3). Nevertheless, HKI is at least 95% inhibited under normal physiological conditions in brain tissue (2). A number of ligands inhibit HKI; however, glucose 6-phosphate (Glc-6-P) is probably the primary physiological inhibitor of the Type-I enzyme (4). On the other hand, inorganic orthophosphate (P_i) is capable of ameliorating Glc-6-P inhibition under normal physiological conditions (5), although at elevated levels it inhibits HKI by binding to the active site (6). Hexokinase II (HKII) is functionally

similar to HKI; however, P_i does not relieve Glc-6-P inhibition of the Type-II isozyme (7).

HKI and HKII have evolved by the duplication and fusion of a primodial hexokinase gene similar to that of yeast hexokinase (8). Each half of HKI and HKII exhibits significant sequence similarities (9). For HKII both halves support catalysis and are each sensitive to inhibition by Glc-6-P (10), whereas only the C-terminal half of HKI supports activity (11). Nonetheless, both halves of HKI can bind Glc-6-P with high affinity, and moreover the binding of Glc-6-P to either half inhibits activity (12,13). P_i binds with high affinity to the N-terminal half of HKI (14-15), and relieves Glc-6-P inhibition by an allosteric mechanism that couples both halves of the enzyme (15).

HKI and HKII associate with the outer mitochondrial membrane in brain tissue (16). This interaction requires fifteen, largely hydrophobic amino acid residues at its N-terminus (17). HKI association with outer mitochondrial membrane allows preferential access to newly formed mitochondrial ATP (16). HKI likely interacts with the voltage-dependent anion channel (VDAC) of the outer mitochondrial membrane (18-19). HKI binding to the mitochondrion prevents the opening of the permeability transition pore (PTP) (20). The PTP is a multicomponent system that includes the adenylate translocator (ANT) of the inner mitochondrion membrane, and the voltage dependent anion channel (VDAC) of the outer mitochondrion membrane (18-24), and is regulated by cyclophilin D of the inner mitochondrion matrix and the binding of hexokinase I and II (25-27). Opening of the PTP results in loss of membrane potential, organelle swelling, cytosolic acidification, and the release of

cytochrome c (20,25). Cytochrome c that escapes the mitochondrion after the PTP opening activates the caspase family of proteases, which ultimately results in apoptosis (27-29).

Others maintain that the opening of the PTP initiates necrosis, but not apoptosis, and that a pro-apoptotic protein such as Bax, triggers the release of cytochrome c without mitochondrial swelling (25,30-31). Nevertheless, mitochondrion-associated hexokinase II clearly antagonizes the action of pro-apoptotic factors such as Bax (32) (33-34). Pro-apoptotic proteins (Bax, Bak, and Bim) interact with VDAC in the assembly of large pores that presumably serve as conduits for the release of cytochrome c (30-31,35). Indeed, over-expression of VDAC-1 causes apoptotic cell death (36-37). Hexokinase I and II, through their own associations with VDAC, may antagonize the formation of apoptotic channels. Some have gone so far as to label hexokinase as “guardian of the mitochondria” (38). Hexokinase colocalizes differentially with human VDAC1, 2 and 3 (39). Hexokinase binding to mitochondria inhibits ATP flux through VDAC-1 (40). Over expression of N-terminally truncated VDAC-1 did not induce cells to release cytochorme c and the cells were resistant to apoptosis (41). The N-terminal peptide of VDAC-1 and other VDAC-1 based peptides bind to immobilized HKI. These peptides prevented protection of cells by HKI (42). Chemical modification of Glu 72 eliminated the binding of HKI to mitochondria (36). Mutating Glu 72 and other residues abolished overexpressed HKI protection against apoptosis in different cancer cells (43). Adding HKI to VDAC-1 reconstituted in lipid membrane reduced the channel conductance (20). HKI addition to mutant (Glu 72 to glutamine) mouse VDAC reconstituted in

lipid membrane did not lessen channel conductance, indicating failure of HKI to bind to mutant VDAC-1 (43).

A number of small and physiological important ligands are capable of dissociating HKI from the mitochondrial outer membrane. These compounds include Glc-6-P and ATP (16). Skaff *et al.* (44) demonstrated a wild-type recombinant HKI with properties comparable to native brain hexokinase, including those of mitochondrial-binding and release. Their recombinant construct has an intact membrane targeting element and a formyl group attached to the amino terminus of the polypeptide chain. The release properties of mutant constructs demonstrated the significance of Glc-6-P binding to the N-terminal half of HKI in promoting the release of the mitochondrion-associated enzyme. The Glc-6-P release phenomenon adheres to a simple equilibrium model. To date, little is known regarding the mechanism of ATP-induced release of HKI from mitochondria (16,45-47). Three binding sites exist on HKI for adenine nucleotides: the active site at the C-terminal half (11), the P_i binding site at the N-terminal half at which the nucleotide may bind through its terminal phosphoryl group (48), and the nucleotide pocket of unknown function near the N-terminal membrane targeting element (48-49). Photoactive ATP analog, Bz-ATP (benzoyl-benzoyl-ATP), can bind to more than one sites on VDAC-1 with low and high affinities (50). Mutating residues in predicted nucleotide-binding site in VDAC-1 reduced ATP cellular levels and caused retarded cell growth (51).

The purpose of the present study was to investigate the mechanism of HKI release from mitochondria by adenosine nucleotides, and which, if any, of the adenine nucleotide binding sites of HKI or VDAC are responsible for that release. The

fluorescent ADP analog, 2′,3′-*O*-(2,4,6-trinitrophenyl) adenosine 5′-diphosphate (TNP-ADP), binds with high affinity to single sites at the C-terminal domain of HKI and to VDAC. Nevertheless, TNP-ADP releases the N-terminal domain of HKI (a domain to which it does not bind) from mitochondria. The data here are consistent with a site on VDAC that binds HKI and ADP-TNP in a mutually exclusive manner.

Experimental Procedures

Materials—ATP, ADP, chloramphenicol, deoxyribonuclease (DNase I), bovine serum albumin (BSA), leupeptin, protease cocktail inhibitor and phenylmethylsulfonyl fluoride came from Sigma. Kanamycin sulfate and 2′,3′-*O*-(2,4,6-trinitrophenyl)-derivatives of ATP, ADP, AMP, and CTP came from Invitrogen. DEAE HPLC was from Tosohaas. Nickel-nitrilotriacetic acid-agarose (NiNTA) and Rosetta (DE3) competent cells were from Novagen. Glucose-6-phosphate dehydrogenase was obtained from Roche Molecular Biochemicals. Isopropyl-1-thio-β-D-galactopyranoside (IPTG) came from Anatrace. His-tag anitbodies, N-terminal HKI antibodies and C-terminal HKI antibodies were from Abcam. Substrates for the 3,3′,5,5′-tetramethylbenzidine enzyme-linked imunoabsorbant assay (TMB-ELISA) and western blotting chemiluminescence came from Pierce. Oligonucleotides came from the Iowa IDT. Lauryldimethylamine-N-oxide (LADO) was purchased from Affymetrix.

Construction of Wild-type Hexokinase and N-domain Plasmids—Human brain hexokinase (HKI) was cloned into pET-24b vector with a 10-residue histidine tag at its C-terminus (pET-24b-HKI-10*x*His) as reported previously (44). Hexokinase

mutants were created through PCR modification. An NdeI cut site was created at Ala^{454} in pET-24b-HKI-10*x*His using the forward primer, 5'-GCAGCGGCAAGGGGGCTCATATGGTGACGGCGGTGGC-3', and its reverse complement. Mutant plasmid was digested with NdeI and then ligated to produce pET24b-N-HKI-10*x*His. This plasmid encodes residues 1-454 of HKI with a C-terminal polyhistidyl tag (hereafter N-domain HKI).

Mitochondrion Purification— Pig livers were obtained from the Iowa State University Meats Laboratory shortly after slaughter. Mitochondrial purification is described (52) with modification as discussed elsewhere (44). Both outer mitochondrial membrane (OMM) and inner mitochondrial membrane (IMM) integrities were measured as described previously (53-54). Mitochondria were stored at –80º C in the presence of 5% dimethyl sulfoxide.

Expression and Purification of Wild-Type HKI and N-domain HKI— E.coli strain Rosetta (DE3) cells were transformed with wild-type or N-domain HKI plasmids. Expression and purification HKI enzymes are discussed in detail by Skaff *et al* (44). The determination of protein concentration employed the Bradford method with bovine serum albumin as a standard (55).

HKI Activity Assay—Hexokinase activity was measured using the glucose 6-phosphate dehydrogenase (G6PDH)-coupled spectrophotometric assay. All assay solutions had 3mM $MgCl_2$, 3 mM DTT, 0.3 mM NADP, 10 μg/mL G6PDH and 50 mM Tris-HCl, pH 8.0. Concentrations of substrate (either glucose or ATP:Mg^{2+} at1:1 ratio) varied from 1/5 to 5 times K_m. NADPH production was monitored at 340 nm.

G6PDH was in sufficient excess so that a doubling of HKI concentration resulted in a doubling of initial velocity. Assays were initiated by addition of 0.5 µg HKI. Initial rates were determined from slopes of linear progress curves (monitored for 3 minutes). Initial-rate data were analyzed using the GraFit computer program (56). The mechanism of TNP-ADP inhibition was determined by assays in the presence of saturating glucose (1.6 mM) and systematic variations in the concentration of ATP:Mg^{2+} at1:1 (0.3-4.5 mM) and TNP-ADP (0-40µM). Mitochondrion-bound hexokinase was added to the assay cocktail with saturating glucose (1.6 mM) and saturating ATP:Mg^{2+}, 1:1 (6 mM). Initial velocity data were fit to models described in the Results section by nonlinear least squares using GraFit (56).

Mitochondrial Binding and Release— Purified HKI was dialyzed twice against mitochondrial-binding buffer (250 mM sucrose, 5 mM Glc, 50 mM NaCl, 5 mM $MgCl_2$ and 50 mM HEPES, pH 7.4), and then diluted to 2 mg/mL using the same buffer. Thirty mg wet weight of mitochondrion (0.24 mg mitochondrial protein), thawed on ice, was suspended in 1 mL of mitochondrial-binding buffer, and then collected by centrifugation at 11,000 × *g* for 5 minutes. Suspension and centrifugation steps were repeated twice. The pellet was suspended in 1 mL of mitochondrial-binding buffer with added HKI (2 mg/mL), protease cocktail inhibitor (0.25mg/mL) and PMSF (1 mM). After 60 minutes on ice, the mixture of HKI and mitochondria was centrifuged at 11,000 × *g* for 5 minutes. Unbound HKI in the supernatant fluid was decanted. Pelleted mitochondria were suspended in

mitochondrial-binding buffer, less the $MgCl_2$, NaCl, and Glc, and centrifuged again. This wash step was twice-repeated.

HKI-bound mitochondria, prepared as above, is suspended in release buffer (250 mM sucrose and 50 mM HEPES, pH 7.4). 100 μL aliquots of this suspension were distributed to plastic micro-centrifuge tubes, to which were added a release agent (ATP or TNP-nucleotide) at various concentrations. After 30 minutes at room temperature, the mitochondria were pelleted by centrifugation. HKI solubilized by nucleotide was removed by decanting the supernatant liquid. The mitochondrial pellet was suspended in wash buffer (250 mM sucrose and 5 mM HEPES, pH 7.4), and centrifuged. After discarding the supernatant fluid, pelleted mitochondria were suspended in 100 μL wash buffer and then assayed for hexokinase activity or suspended in 100 μL of coating buffer (100 mM sodium carbonate/bicarbonate, pH 9.6) for ELISA assays.

HKI ELISA Assay— Fifty μL of HKI-bound mitochondrial suspension in coating buffer (100 mM Na_2CO_3/$NaHCO_3$ pH 9.6) was loaded in each well of the ELISA plate and incubated overnight at 4 °C. Plates were washed four times with PBST (137mM NaCl, 2.7mM KCl, 8.1mM Na_2HPO_4, 1.76mM KH_2PO_4, pH 7.4, 0.05% Tween-20). Wells were blocked with 200 μL of 1% BSA in PBST at room temperature for 2 hours and then washed four times with 200 μL PBST. Wells were incubated with 100 μL of anti-His-tag primary antibodies (1:1000 dilution) for 2 hours at room temperature, and then washed four times with PBST. 100 μL of anti-rabbit IgG secondary antibodies solution (1:10000 dilution) was added to each well,

incubated for 2 hours at room temperature, and then washed four times with PBST. A volume of 100 μL of 1-Step Ultra TMB-ELISA solution was added to each well. A Biotek (Ceres 900) plate reader was used to measure change in absorbance at wavelength 620 nm. A reading was taken every 10 seconds, a total of 75 for each well. HKI was used as a positive control and mitochondria as a negative control. Slopes of linear progress curves were determined by regression analysis, and used in nonlinear least square fits (using GraFit) to models described in the Results section.

Mitochondria western blotting— Mitochondria with and without bound HKI were re-suspended in 15 μL water plus 3μL of loading buffer (1M Tris-HCl, pH 6.8, 10% SDS, 3% glycerol, 0.12 mg/mL bromophenol blue) and boiled for 5 minutes prior to polyacrylamide gel electrophoresis (SDS-PAGE). After removal of SDS, proteins were transferred by blotting from gel to nitrocellulose membranes (57). Membranes were blocked with 3% bovine serum albumin in 50 mM Tris, 150 mM NaCl, 0.05% Tween 20, pH 7.6, (TBST buffer) for one hour at room temperature and then washed three times with TBST buffer. Membranes were exposed to primary antibody (His-Tag antibodies, C-terminal HKI antibodies, or N-terminal HKI antibodies) in TBST buffer for one hour at room temperature, and then washed three times with TBST buffer. Membranes were subsequently treated with rabbit IgG secondary antibodies for one hour at room temperature and washed three times with TBST buffer. Finally, x-ray film was exposed for 1 minute to membranes treated with Pierce chemiluminescence substrate and then developed.

Cloning of Wild-Type human VDAC-1— A plasmid with the coding sequence of human VDAC-1 was purchased from Open Biosystems. NdeI and SacI cut sites

were created in the plasmid using the polymerase chain reaction (PCR) and NdeI primer 5'CGCGGCAGCCATATGATGGCTGTGCCACCCACG3' and SacI primer 5'GGACTGGAATTTCAAGCA TCGAGCTCCGTCGACAAGC3'. The PCR product and vector pET-24a were digested by NdeI and SacI restriction enzymes. After separation on agarose, the DNA fragment for human VDAC-1 was ligated to pET-24a. The construct was confirmed by DNA sequencing facility at Iowa State University.

Expression and Purification of Wild-Type human VDAC-1— Wild-type human VDAC-1 containing plasmid was transformed into *E. coli* strain BL21 (DE3). Cells were grown in LB media at 37 °C, kanamycin was added to a final concentration of (30 µg/mL). Growth was monitored by absorbance at wavelength 600 nm. At A_{600} of 0.9, the temperature was reduced to 16 °C and IPTG was added to a final concentration of 0.3 mM. Cells were collected after 16-20 hours of induction and suspended in lysis buffer (30mM Tris-HCl, pH8.0, 150mM NaCl, 1mM EDTA, and 1mM DTT). DNase (50 µg/mL), leupeptin (5 µg/mL), and PMSF (1 mM) were all added to the solution. Cells were lysed by sonication. Inclusion bodies were pelleted at 32460*g* for 1 hour. Pelleted inclusion bodies were subjected to the following procedures three times: separation from the supernatant fraction, suspension in wash buffer (30 mM Tris-HCl, pH 8.0, 150 mM NaCl, 1 mM EDTA, 1 mM DTT) and centrifugation at 15,000 rpm 32460*g* for 30 minutes. Inclusion bodies were suspended in 30 mL of wash buffer plus 1% Triton X-100, incubated for 30 minutes at 37 °C, and then suspended and washed twice with wash buffer.

Refolding of Wild-Type Human VDAC-1— HumanVDAC-1 purification and folding follows protocols in the literature (51, 58) with modifications. Washed

inclusion bodies were solubilized in 150 mL dissolving buffer (6 M guanidine hydrochloride, 10 mM DTT, 0.1 mM EDTA, 100 mM Tris-HCl, pH8.0) to a final protein concentration of 15 mg/mL. Inclusion bodies dissolved completely in 12 hr. at 4 °C. Twenty five milliters of unfolded human VDAC-1were diluted by slow addition into 300 mL of refolding buffer (0.1 mM EDTA, 1 mM DTT, 100 mM Tris-HCl, pH8.0, 2% LDAO) at 4 °C. Refolded protein was concentrated and dialyzed against 50 mM Tris-HCl. pH 7.5, 0.1% LDAO buffer for 24 hr at 4 °C. Solution was loaded onto a nickel-nitrilo triacetic acid (Ni^{2+}-NTA) column. The column was washed with buffers containing 50 mM Tris-HCl, pH7.5, 300 mM NaCl, 0.1% LDAO and 5 mM imidazole and then 50 mM imidazole. Finally, human VDAC-1 was eluted with the same buffer containing 300 mM imidazole.

HKI and VDAC-1 Fluorescence Experiments— Purified HKI and human VDAC-1 were dialyzed against 2 mM glucose and 50 mM Tris-HCl, pH 7.5. Flurescence measurements were made at room temperature using a 1-cm^2 quartz cuvette on a SLM Amico 8000 fluorometer with entrance/exit slits of 4 mm. For TNP-nucleotides the excitation wavelength was 409 nm, and emission scans were from 450 to 600 nm. Fluorescence scans (a total of three for each datum) were performed after additions of small volumes of TNP-nucleotide to 2 mL of 2.5 μM HKI or human VDAC-1. TNP-nucleotide displacement was accomplished by the addition of the alternative nucleotide to 1 mL solution of 2 .5 μM HKI or human VDAC-1 and 1 μM TNP-nucleotide. For each kind of experiment, the total concentration of added titrant did not exceed 5% of the initial volume of solution, and

the total concentration of titrant was corrected for volume changes. The analysis of fluorescence data followed the approach of Fallar (59), modified as described in the Results section, using GraFit to perform nonlinear least squares fitting.

Results

Mitochondria integrity and absence of native hexokinase— Cytochrome c oxidase activity indicated 90% integrity of OMM (data not shown). Uptake of carbocyanine dye JC-1 indicated intact IMM (data not shown). Western blotting of pig liver mitochondria and staining with polyclonal antibodies raised against HKI indicated the absence of native hexokinase (data not shown).

TNP-ADP inhibits HKI— Wild-type HKI (k_{cat} = 73 ± 4 s^{-1}, K_m^{Glc} = 77 ± 6 µM, K_m^{ATP} = 1.1 ± 0.1 µM) exhibited no measurable activity with TNP-ADP as a replacement substrate for ATP, placing an upper limit on k_{cat} of 0.001 s^{-1}. TNP-ADP has no effect on the activity glucose 6-phosphate dehydrogenase (coupling enzyme) up to a concentration of 100 µM. On the other hand, TNP-ADP is a competitive inhibitor with respect to ATP (K_i = 4.9 ± 0.5 µM) (Fig. 2.1).

TNP-nucleotide binding to Wild-type hexokinase I and displacement by ATP— The observed fluorescence from a mixture of TNP-ADP and HKI comes from free TNP-ADP, TNP-ADP bound to HKI, and HKI itself:

$$F_{obs} = F_{free} + F_{bound} + F_{protein} \qquad \text{Eq. 1}$$

$F_{protein}$ is small relative to other contributions as HKI has no native fluorophore sensitive to an excitation wavelength of 409 nm. $F_{free}=a + b[L] + c[L]^2$, where *a, b,* and *c* are determined by a fit of fluorescence versus [L] in the absence of protein

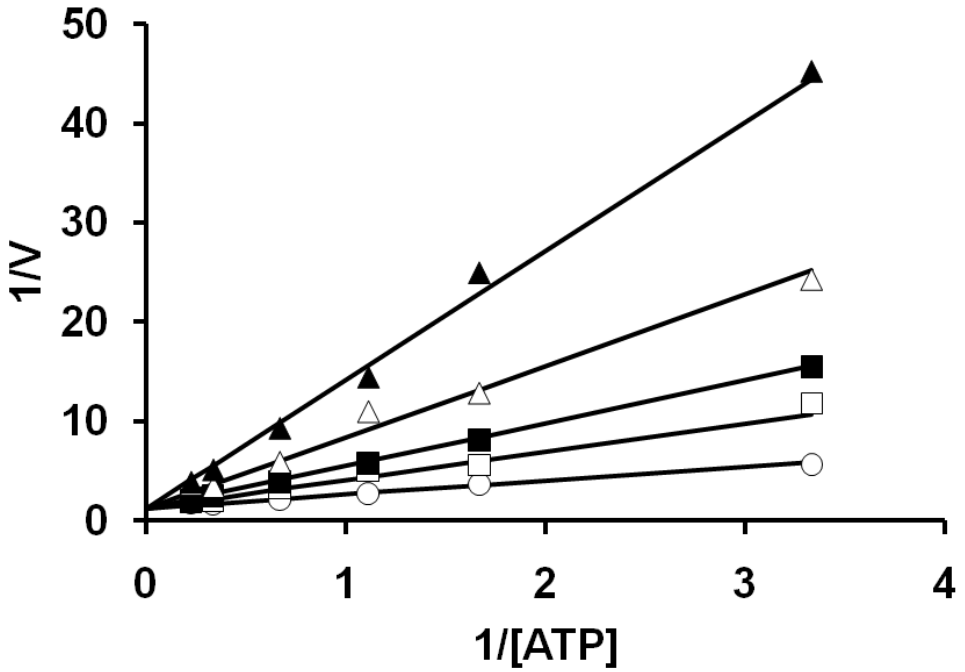

Fig. 2.1. TNP-ADP and ATP binding to WTHKI. TNP-ADP inhibition of HKI competitive with ATP HKI activity was measured using the Glc-6-P dehydrogenase assay in 100 mM Tris, pH 8.0, glucose 1.6 mM, ATP 0.3-4.5 mM and TNP-ADP 0 μM (○), TNP-ADP 2.5 μM (●), TNP-ADP 5 μM (□), TNP-ADP 10 μM (■), TNP-ADP 20 μM (Δ), and TNP-ADP 40 μM (▲).

under buffer conditions identical to those used in the tritation of HKI. $F_{bound} = \gamma b(L_o - [L])$, where γ is a fluorescence enhancement factor of the bound relative to the free state of the fluorescent ligand and L_o and [L] are the total and free concentrations of fluorescent ligand.

A single binding-site model adequately accounts for the observed fluorescence of the bound state and for the displacement of the TNP-nucleotide by a non-fluorescent nucleotide:

$P + L = PL, \qquad K_L = [P][L]/[PL]$

$P + A = PA, \qquad K_A = [P][A]/[PA]$

Scheme I

In Scheme I, L represents the TNP-nucleotide and A the displacing ligand. The equilibrium relationships of Scheme I with mass conservation relationships for L_o (total fluorophore concentration), A_o (total concentration of displacing ligand) and P_o (total concentration of protein) leads to a third-order equation in the concentration of free protein [P]. For circumstances here, $K_A >> [P]$, allowing an approximation that reduces the third-order equation to one of second order:

$$(1+ A_o/ K_A)[P]^2 + (K_A - P_o + A_o K_L/K_A + L_o)[P] - P_o K_L = 0 \qquad \text{Eq. 2}$$

The physical root of this quadratic relationship is the concentration of free protein, and determines the concentration of free fluorophore $[L] = L_o K_L/(K_L+[P])$ at a given total concentration of fluorophore, L_o. GraFit software optimizes the fit of the observed fluorescence to the right-hand side of Eq. 1 at fixed P_o and varying L_o and A_o by adjusting parameters K_A, K_L, γ and $F_{protein}$. TNP-ADP binds to wild-type HKI

with high affinity (K_L = 0.79 ± 0.09 µM, γ = 14.8 ± 0.3, and $F_{protein}$ = 0.017 ± 0.002) and weakly to the N-domain of HKI (K_L = 900 ± 800 µM) (Fig. 2.2). ATP displaces TNP-ADP from wild-type hexokinase (K_A = 190 ± 20 µM) (Fig. 2.3).

TNP-nucleotide binding to wild-type human VDAC-1 and displacement by nucleotides— Single binding site model of Scheme I also account for TNP-ADP binding to VDAC-1 and its displacement by ATP. Analog TNP-ADP binds to VDAC-1 with high affinity (K_L = 1.3 ± 0.1 µM, γ = 16.7 ± 0.3, $F_{protein}$ = 0.06 ± 0.02) (Fig. 2.4) and is displaced by ATP (K_A = 550 ± 40 µM) (Fig. 2.5). CDP does not displace TNP-ADP from VDAC-1 (Fig. 2.6). Analogs TNP-ATP, TNP-AMP and TNP-CTP bind to VDAC-1 similarly to TNP-ADP (Table 2.1).

Nucleotide release of wild-type HKI— Incubation times of twenty and sixty minutes produced identical release curves, indicating an equilibrium phenomenon. Scheme II represents the simplest equilibrium model that accounts for ATP-release of wild-type and mutant enzymes from mitochondria.

$E + Q = EQ$, $\quad K_1 = [EQ]/[E][Q]$

$E + P = EP$ $\quad K_2 = [EP]/[E][P]$

$Q + A = QA$ $\quad K_3 = [QA]/[Q][A]$

Scheme II

In Scheme II, K_1 and K_2 represent association constants for the binding of HKI (represented by E) to specific mitochondrial binding sites Q, and nonspecifically to the membrane at sites P. The association constant K_3 represents the binding of A competitively with E for the specific binding sites Q. The fraction of E bound to

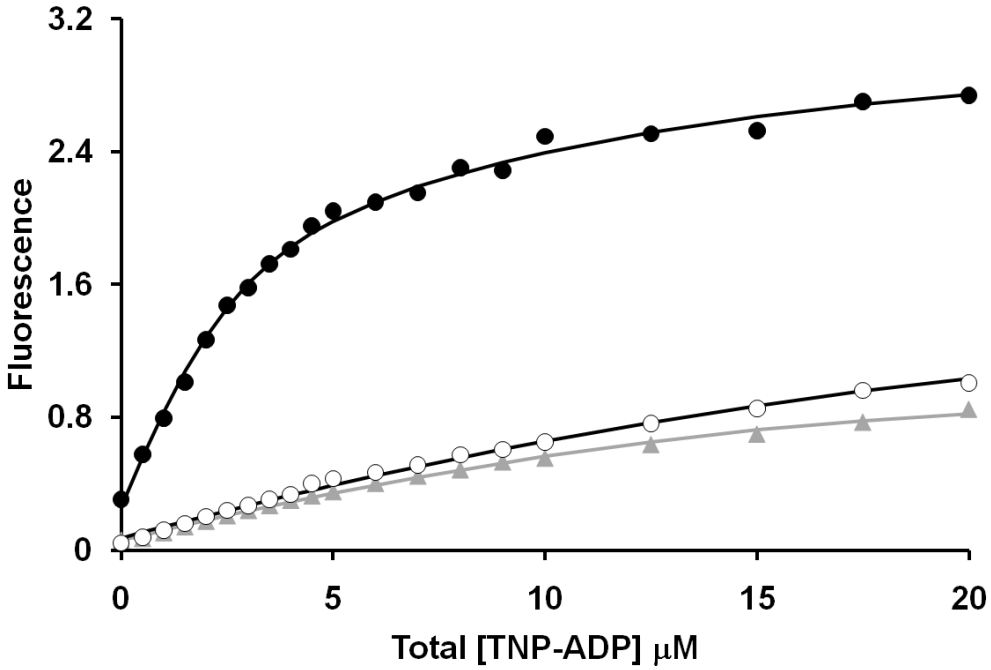

Fig. 2.2. Titration of HKI constructs with TNP-ADP. Plots represent the fluorescence at varying total concentrations of TNP-ADP in 2 mM glucose and 50 mM Tris-HCl, pH 7.5, with no protein (▲), wild-type HKI 2.5 μM (●), and N-domain HKI 2.5 μM (○). Black lines for wild-type and N-domain HKI represent Eq. 1 with A_o of 0 μM, P_o of 2.5 μM and parameters K_L, K_A, γ and $F_{protein}$ given in the Results section. The gray line is the fit of observed fluorescence in the absence of protein to the second-order polynomial, $a + b(L_o) + c(L_o)^2$.

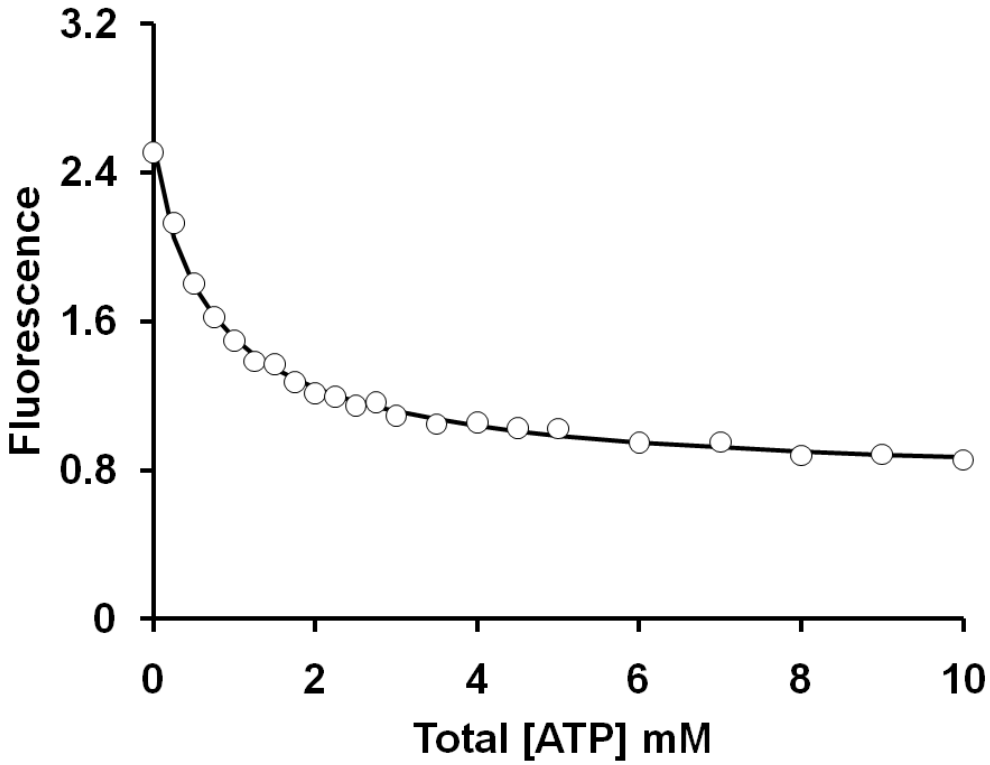

Fig. 2.3. Titration of wild-type HKI bound TNP-ADP with ATP. Plot represents the fluorescence at varying total concentrations of ATP (○) added to 2.5 μM wild-type HKI and 5 μM TNP-ATP in 2mM glucose and 50 mM Tris pH 7.5. The solid line represents is a fitted curve using Eq. 1 with L_o of 5 μM, P_o of 2.5 μM and parameters K_L, K_A, γ and $F_{protein}$ given in the Results section.

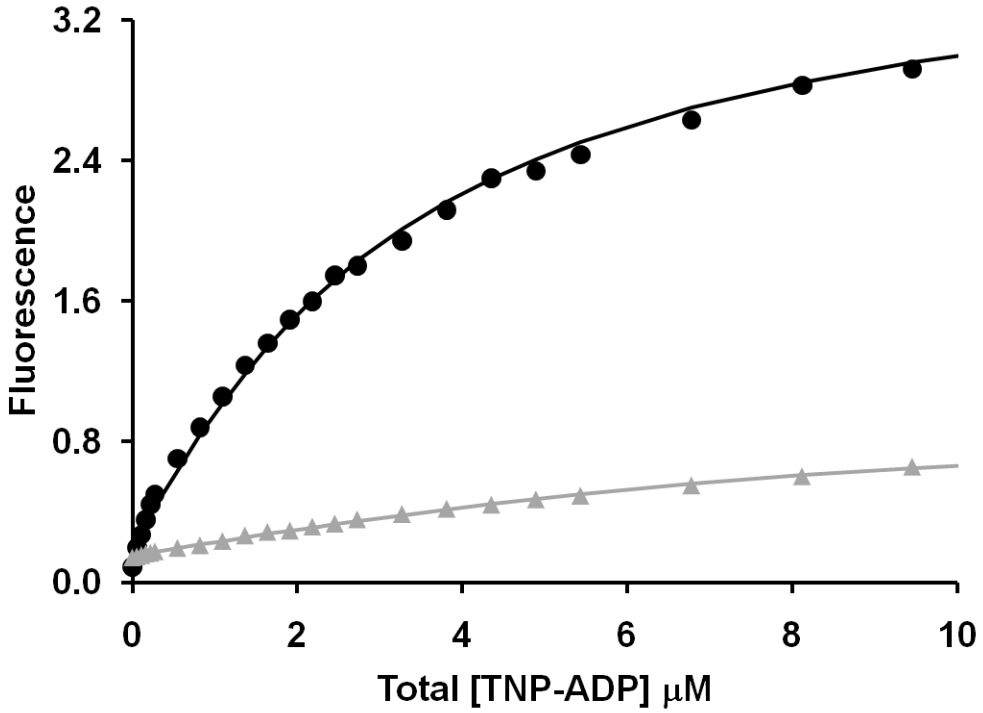

Fig. 2.4. Titration of wild-type human VDAC-1 with TNP-ADP. Plots represent the fluorescence at varying total concentrations of TNP-ADP in 2 mM glucose and 50 mM Tris-HCl, pH 7.5, with no protein (▲) or with wild-type human VDAC-1 2.0 μM (●). The black line represents Eq.1 with P_o of 2 μM, A_o of 0 μM and parameters K_L, K_A, γ and $F_{protein}$ given in the Results section. The gray line is the fit of observed fluorescence in the absence of protein to the second-order polynomial, $a + b(L_o) + c(L_o)^2$.

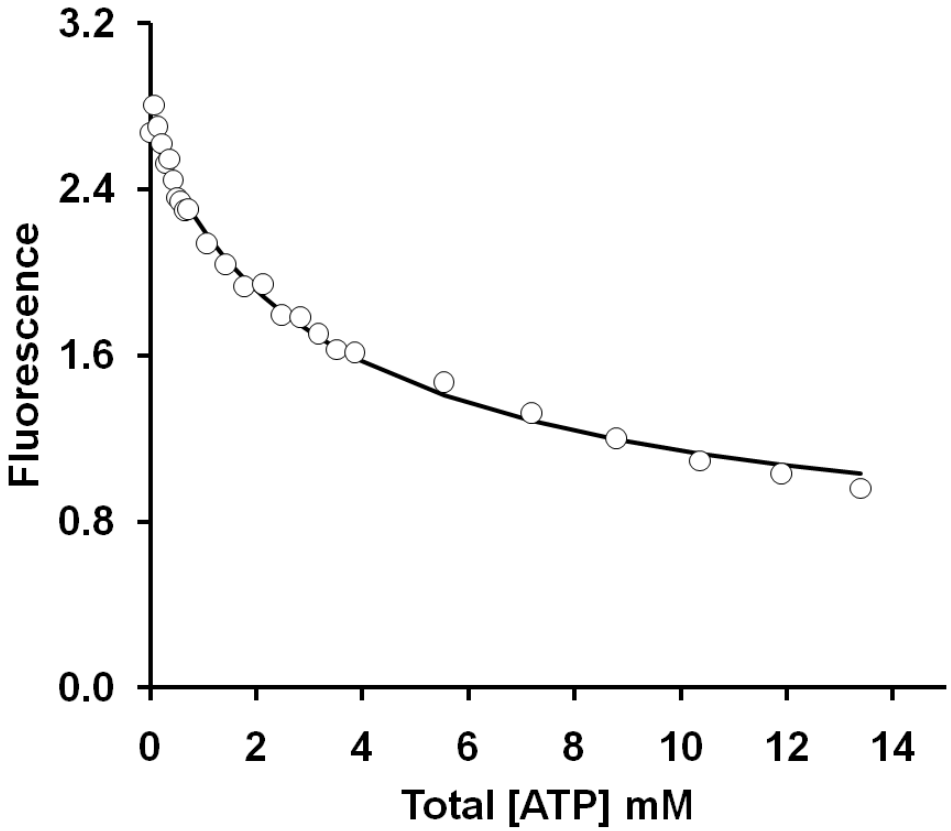

Fig. 2.5. Titration of wild-type human VDAC-1 bound TNP-ADP with ATP. Plot represents the fluorescence at varying total concentrations of ATP (○) added to 2.0 μM wild-type human VDAC-1 and 5 μM TNP-ATP in 2mM glucose and 50 mM Tris, pH 7.5. The black line represents Eq. 1 with P_o of 2 μM, L_o of 5 μM and parameters K_L, K_A, γ and $F_{protein}$ given in the Results section.

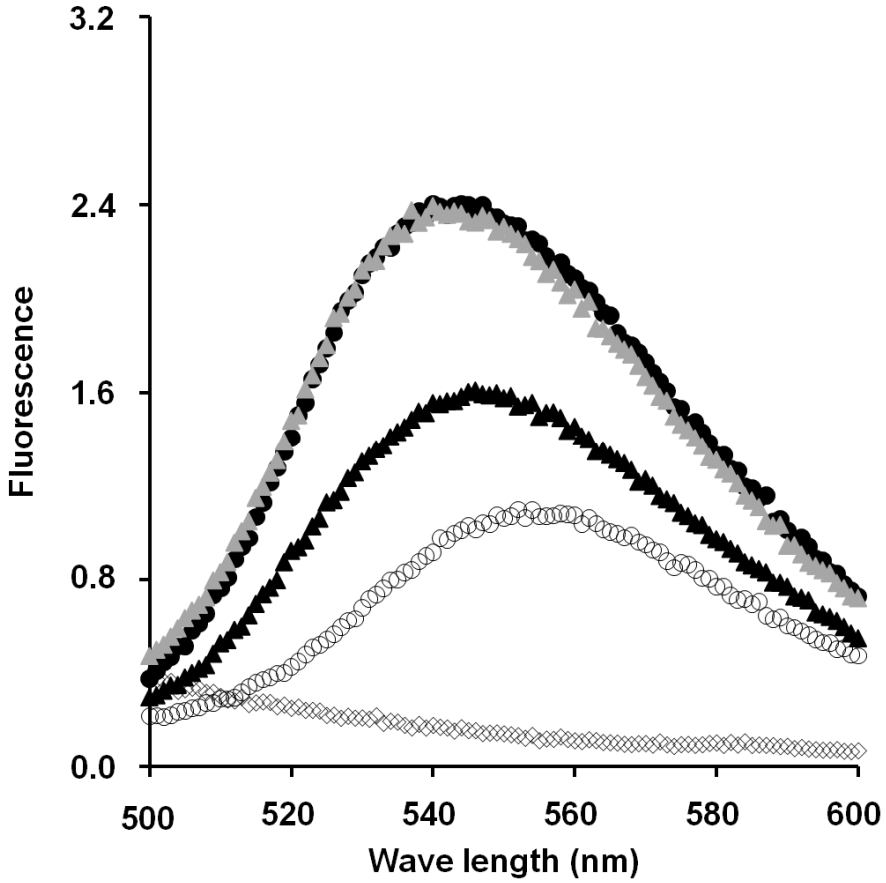

Fig. 2.6. Human VDAC-1 bound TNP-ADP displacement by nucleotides. Fluorescence scans of 2.0 µM human VDAC-1 in 2mM glucose and 50 mM Tris, pH 7.5. human VDAC-1 only (○), 5 µM TNP-ADP only (○), human VDAC-1 plus 5 µM TNP-ADP (●), human VDAC-1 plus 5 µM TNP-ADP and 10 mM ATP (▲), and human VDAC-1 plus 5 µM TNP-ADP and 10 mM CDP (▲).

Table 2.1. TNP-nucleotides binding to wild-type human VDAC-1.

TNP-nucleotide	K_L (μM)	γ	$F_{protein}$
TNP-ATP	0.5 (2)	16.4 (9)	0.40 (9)
TNP-ADP	1.3 (1)	16.7 (3)	0.06 (2)
TNP-AMP	2.0 (1)	20.4 (3)	0.13 (2)
TNP-CTP	0.7 (1)	11.2 (3)	0.22 (2)

Parameters are from a single binding site model. K_L, γ and $F_{protein}$ are constants for the dissociation of TNP-nucleotides from human VDAC-1. Fluorescence was measured at varying total concentrations of TNP-nucleotides in 2 mM glucose and 50 mM Tris-HCl, pH 7.5. Standard deviations in the last significant digits are given in parentheses.

mitochondria depends explicitly on the concentrations of Q and P, and implicitly on the concentration of A as follows:

$$R([A]) = (K_1[Q] + K_2[P])/(1+K_1[Q]+K_2[P]) = (K_1[Q] + K_2')/(1+K_1[Q]+K_2') \quad \text{Eq. 3}$$

The concentration of free nonspecific binding sites for hexokinase is overwhelmingly large allowing a pseudo constant K_2' to approximate the product $K_2[P]$. The concentration of free specific mitochondrial sites Q is itself a function of the concentrations of enzyme and competitive binding ligand. Algebraic manipulation of the equilibrium expression in Scheme II and relationships for mass conservation of total enzyme E_o and total specific sites Q_o results in a quadratic relationship in Q:

$$a[Q]^2 + b[Q] + c = 0$$

where $a = K_1(1+K_3[A])$, $b = K_1(E_o–Q_o)+(1+K_2')(1+K_3[A])$, and $c = –Q_o(1+K_2')$. The general solution to the quadratic equation gives $[Q]$:

$$[Q] = –\{K_1(E_o–Q_o)+(1+K_2')(1+K_3[A])\}/\{2K_1(1+K_3[A])\}$$
$$+\{K_1^2(E_o–Q_o)^2+2K_1(E_o+Q_o)+(1+K_2')(1+K_3[A])$$
$$+(1+K_2')^2(1+K_3[A])^2\}^{1/2}/\{2K_1(1+K_3[A])\} \quad \text{Eq. 4}$$

Substitution of Eq. 4 into Eq. 3 provides a relationship for the fraction of enzyme bound to the mitochondria $R([A])$, explicitly as a function of $[A]$.

The fitting relationship is $V = sR([A])$ (Eq. 5), where s is a proportionality constant that relates the fraction of bound enzyme $R([A])$ to velocity V in μmoles/min. Eq. 5 includes undefined quantities s, E_o, Q_o, K_1, K_2' and K_3; all six cannot be determined by a nonlinear least squares fit of data from a single experiment. Hence, values for some of these quantities must come from other determinations. Firstly, one assumes

the HKI-VDAC complex has an equal number of HKI and VDAC subunits. The value for Q_o ($7.1x10^{-8}$ M) then is an estimate based on 42,000 VDAC molecules per mitochondrion (60), $7.2x10^{9}$ mitochodria per 1 mg of total mitochondrial protein (61), and 0.014 mg of mitochondria in each 100 µL assay. In binding HKI to mitochondria, the concentration of enzyme (10^{-6} M) is 10-fold greater than the estimated concentration of specific binding sites. After washing away excess enzyme, we assume all specific sites have bound enzyme, and that the condition E_o=Q_o applies to the system. The release of HKI is complete at the highest levels of nucleotide, R([A]→∞) = 0, which requires $K_2' = 0$. Moreover, $s = Q_o$×(specific activity)×(assay volume), where the specific activity for HKI is $6x10^{9}$ µmole/min^{-1} mole^{-1} and the assay volume is liters. Hence, if the assumption of a 1:1 ratio of the HKI-VDAC complex is correct, then data can be fit to Eq. 5 using K_1 and K_3 alone as adjustable parameters. Moreover, as K_1 represents the binding affinity of HKI for the mitochondrion, all experiments using wild-type HKI should provide comparable values for K_1 regardless of the release agent. Listed in Table 2.2 are values for K_1 and K_3 for 8 release experiments involving ATP and ADP. Although correlations in K_1 and K_3 are evident, one finds values of K_1 within a single order with an average value of $4.1 \pm 1.0x10^{8}$ M^{-1}. In release experiments involving the HKI activity assay, K_1 is set to its average value, and only K_3 is optimized in fitting the data. The true uncertainty in K_3 then is on par with that for the average value of K_1; however, on a comparative basis the K_3 values in Table 2.3 accurately reflect the relative binding efficacies of nucleotides to VDAC. Characteristic release curves are in Fig. 2.7. All TNP-nucleotides tested were effective in the release of wild-type HKI from

Table 2.2. ATP and ADP release of wild-type HKI from pig liver mitochondria in the determination of K_1.

	K_1 (M^{-1})	K_3^{ATP} (M^{-1})	K_3^{ADP} (M^{-1})
Experiment 1	6.0×10^8 (1.2×10^8)	5.2×10^4 (1.7×10^4)	-
Experiment 2	5.1×10^8 (7.8×10^7)	4.9×10^4 (8.9×10^3)	-
Experiment 3	6.6×10^8 (2.4×10^8)	1.5×10^4 (6.1×10^4)	-
Experiment 4	8.1×10^8 (3.3×10^8)	1.7×10^5 (7.7×10^4)	
Experiment 5	1.3×10^8 (1.5×10^7)	3.6×10^4 (6.7×10^3)	
Experiment 6	1.2×10^8 (1.3×10^7)	3.7×10^4 (6.6×10^3)	
Experiment 7	2.7×10^8 (6.9×10^7)	-	9.6×10^3 (3.7×10^3)
Experiment 8	2.1×10^8 (4.4×10^7)	-	8.5×10^3 (2.6×10^3)

Parameters are from an equilibrium model in which the binding of nucleotide and WHKI and nucleotide to the mitochondrion is mutually exclusive. K_1, K_3^{ATP} *and* K_3^{ADP} are constants for the association in M^{-1} of HKI, ATP and ADP from the mitochondrion. Mitochondria with HKI bound in 250mM sucrose and 50 mM HEPES, pH7.5, were exposed to different nucleotides for 30 minutes. Remaining mitochondria bound HKI was measured by activity. Standard eviations in the last significant digits are given in parentheses.

Table 2.3. Release of wild-type HKI from pig liver mitochondria by TNP-nucleotides.

TNP-nucleotide	K_3 (M^{-1})
ATP	9.9×10^4 (3.0×10^3)
ADP	1.8×10^4 (3.5×10^3)
TNP-ATP	2.7×10^5 (2.7×10^4)
TNP-ADP	3.7×10^5 (5.2×10^4)
TNP-AMP	3.1×10^5 (5.2×10^4)
TNP-CTP	1.9×10^5 (4.8×10^4)

Parameters are defined in the Results section and by Scheme II. K_1 is set to its average value of $4.1x10^8$ M^{-1} and K_3 determined by fitting Eq. 5 to data as described in the Results section. Standard deviations in the last significant digit are given in parentheses

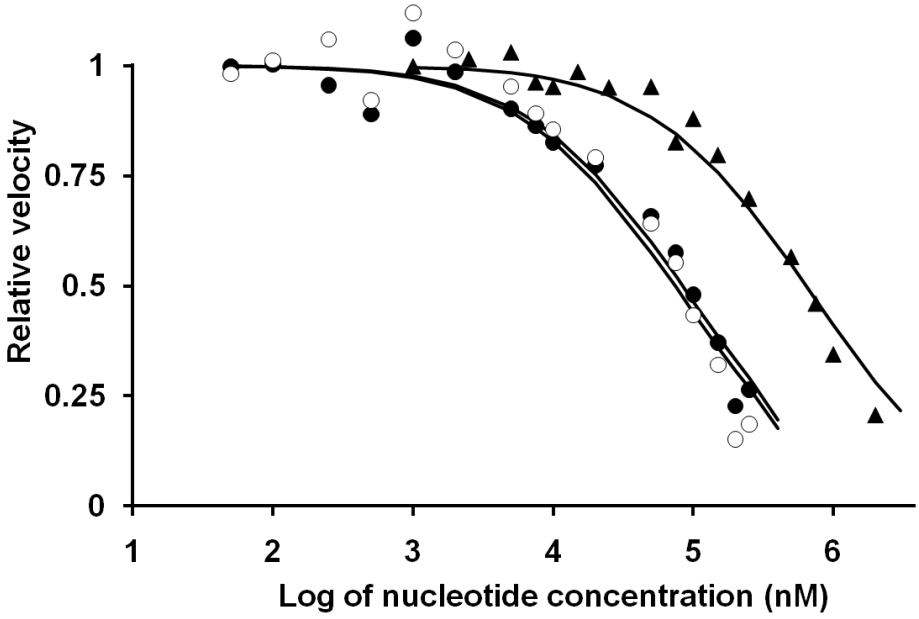

Fig. 2.7. Nucleotide-induced release of wild-type HKI from pig liver mitochondria. Mitochondria with HKI bound in 250 mM sucrose and 50 mM HEPES, pH 7.5, were exposed to different nucleotides for 30 minutes. Plots represent relative velocities from mitochondria-bound HKI that remains after exposure to varying concentrations of ATP (▲), TNP-ATP (○), or TNP-ADP (●). The solid lines represent fitted curves using Eq. 5 with parameters given in the Results section and Table 2.3.

mitochondria.

Nucleotide induced release of N-domain HKI from mitochondria— Validation of the ELISA assay is provided by Fig. 2.8. Release of wild-type HKI, determined as a percent of total release, is measured comparably by the ELISA and the HKI activity assays. Measures of nucleotide affinity constants come from the fitting data to Eq. 5. The parameter *s*, however, is difficult to determine, requiring the optical path length of a plate reader, and the assumption of one to one correspondences between the hexokinase construct, primary antibody, and secondary antibody/peroxidase components. Moreover, nonzero background levels in the presence of high concentrations of nucleotide require a nonzero K_2'. Hence, fitting of data from ELISA assays employs *s*, K_2' and K_3 as parameters. TNP-ADP and ATP release wild-type HKI and N-domain HKI from mitochondria to a comparable extent (Fig. 2.8), and provide values for K_3 that compare favorably to those of the determined from the HKI assays (Table 2.4).

Discussion

Previous reports demonstrated the release of HKI from mitochondria by ATP and other nucleotides at millimolar concentrations (16, 45-47). The importance of the hexokinase-mitochondrion interaction to apoptosis motivated our efforts to quantify and determine the mechanism of nucleotide release of HKI from mitochondria. Four general mechanisms can account for ATP-release of HKI from mitochondria (Fig. 2.9): ATP binds to the C-terminal domain of HKI causing release. ATP and HKI bind with mutual exclusion to human VDAC-1. ATP binds to the N-terminal domain of

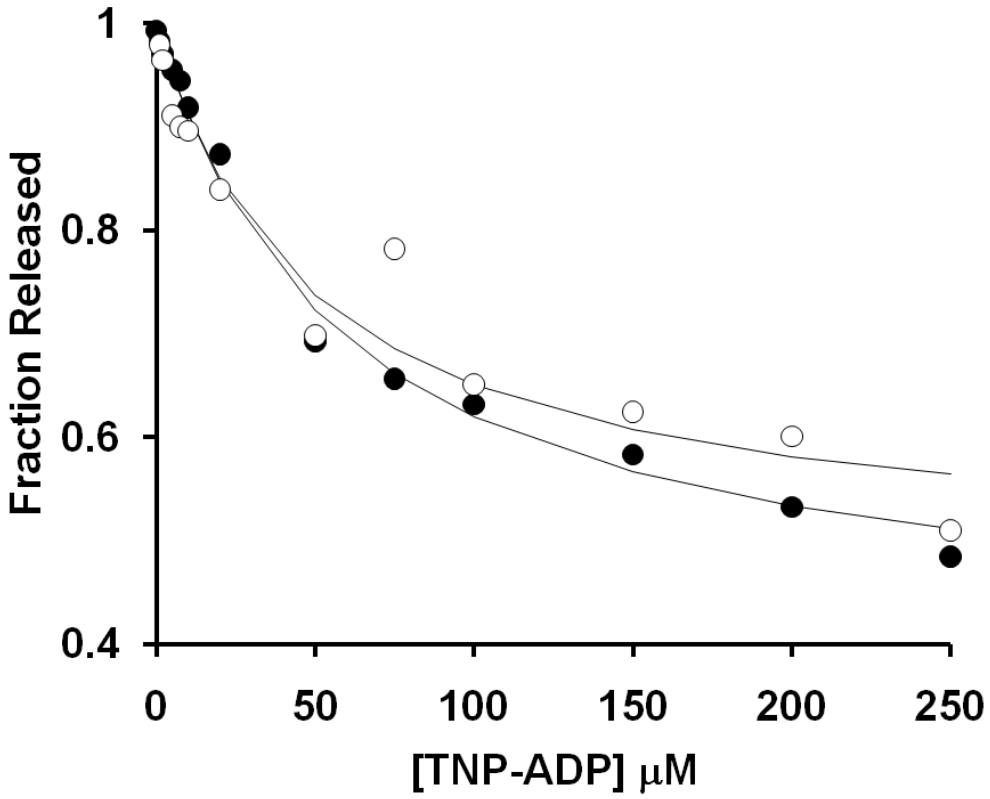

Fig. 2.8. Nucleotides induced release of wild-type HKI and N-domain HKI from pig liver mitochondria measured by kinetic ELISA. Mitochondria with HKI bound in 250 mM sucrose and 50 mM HEPES, pH 7.5, were exposed to different nucleotides for 30 minutes. Plots represent wild-type HKI (●) or N-domain HKI (○) that remains bound to mitochondria as measured by His-TAG antibodies and ELISA. The solid lines represent fitted curves using Eq. 5 with parameters given in the Results section and Table 2.4.

Table 2.4. Nucleotide-dependent release of HKI constructs from pig-liver mitochondria.

HKI Construct	Nucleotide	*s* (μmol/min)	K_2' (M^{-1})	K_3 (M^{-1})
Wild-type[a]	ATP	0.0213*	0**	3.1×10^4 (2.9×10^3)
	TNP-ADP	0.0213*	0**	2.3×10^5 (6.8×10^4)
Wild-type[b]	ATP	0.098 (3)	0.14 (3)	1.3×10^4 (8.2×10^3)
	TNP-ADP	0.110 (1)	0.24 (1)	1.8×10^5 (3.8×10^4)
N-domain[b]	ATP	0.190 (2)	0.44 (2)	2.8×10^4 (5.9×10^3)
	TNP-ADP	0.069 (1)	0.73 (2)	1.3×10^5 (4.1×10^4)

Parameters are defined in the Results section and by Scheme II. K1 is set to its average value $4.1x10^8$ M^{-1} and *s*, K_2' and K_3 determined by fitting to Eq.5 to data as described in the Results section. Mitochondria with HKI bound in 250 mM sucrose and 50 mM HEPES, pH 7.5, were exposed to different nucleotides for 30 minutes. Remaining mitochondria bound HKI was measured by activity and/or ELISA. Standard deviations in the last significant digit are in parentheses.

[a]Measured by HKI activity

[b]Measured by His-tag antibodies and kinetic-ELISA

* Calculated as described in the Results section

** Fixed at zero as described in the Results sectio

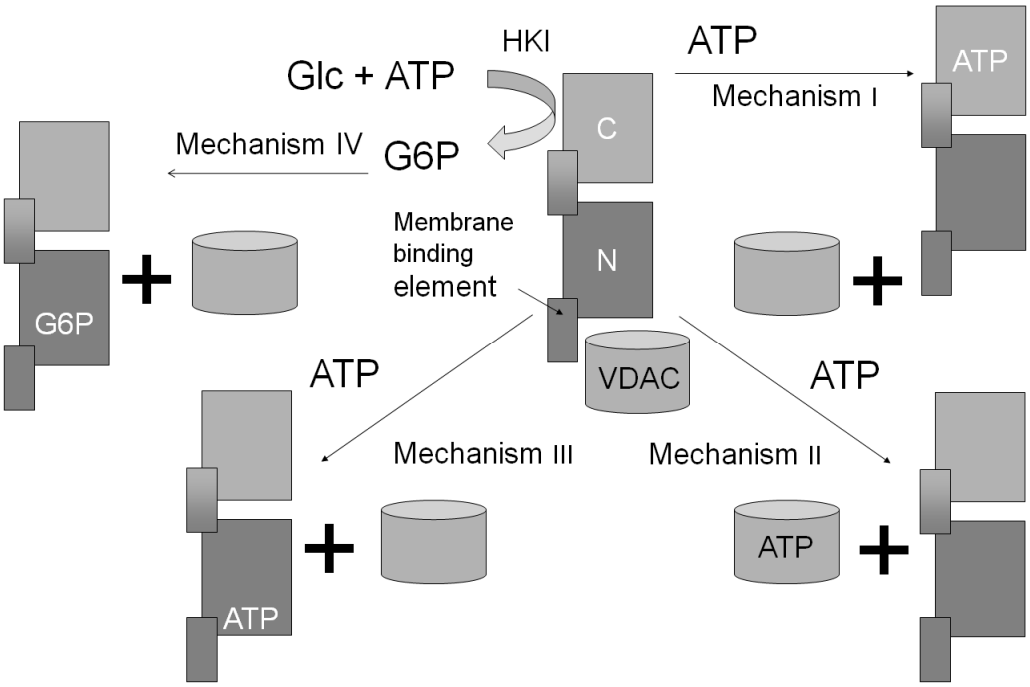

Fig. 2.9. Four mechanisms by which ATP could release HKI from mitochondria. VDAC-1 (cylinder) HKI (rectangles) interact directly. ATP binds to HKI, C-terminal half, (Mechanism I), to VDAC (Mechanism II), or to HKI, N-terminal half (Mechanism III) to disrupt the HKI-VDAC-1 complex. HKI produces glucose 6-phosphate from ATP, which in turn binds to N-terminal half of HKI (Mechanism VI) to disrupt the HKI-VDAC-1 complex.

HKI causing release. HKI converts ATP and glucose to Glc-6-P, which in turn binds to the N-terminal half of HKI triggering release.

The experimental protocols adopted here avoid the combination of glucose and ATP, which in the presence of Mg^{2+} and HKI would result in the generation of Glc-6-P. TNP-nucleotides are not substrates for HKI (current study) or for yeast hexokinase (62). TNP-ADP binds to HKI and yeast hexokinase at micromolar concentrations and is displaced by ATP. In the absence of Mg^{2+} both TNP-ADP and ATP release HKI from mitochondria. Under such conditions, the evolution of Glc-6-P from ATP and glucose is an unlikely cause for ATP release, and cannot be the mechanism by which TNP-ADP releases HKI from the mitochondrion (Mechanism IV).

A test of Mechanisms II and III requires an assay for N-domain HKI, which has no hexokinase activity. Data of Fig. 2.10 validate the kinetic ELISA assay to measure levels of N-domain HKI bound to mitochondria. The kinetic ELISA measures the HKI construct in any state (active or inactive), whereas the HKI activity assay measures only HKI in an active state. The presence of substantial peroxidase activity in the presence of high levels of nucleotide indicates residual HKI bound to the mitochondrion. This bound fraction of HKI must not be active, as it would be detected by the HKI activity assay. Blank samples (mitochondria not exposed to an HKI construct) in the ELISA assay have low peroxidase activity, consistent with Western blots which indicate no bound HKI on the surface of the pig-liver mitochondria. Released HKI, as a fraction of total released HKI, is nonetheless in excellent agreement for the two assay methods (Fig. 2.10).

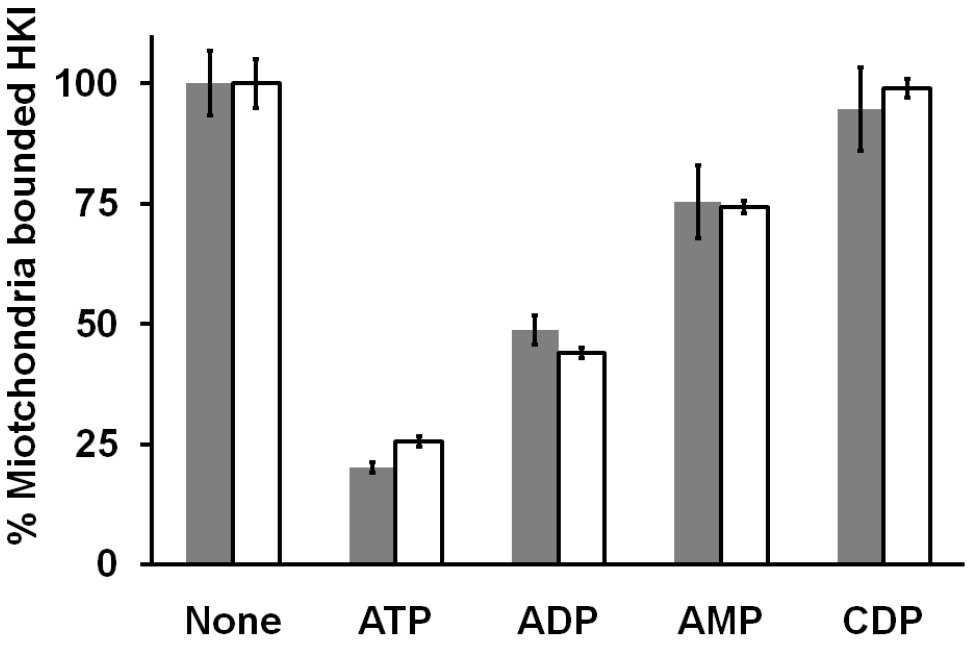

Fig. 2.10. Nucleotide release of wild-type HKI and N-domain HKI from pig liver mitochondria. Plots represent wild-type HKI (■) remained bound to mitochondria and measured by activity and N-domain HKI (□) remained bound to mitochondria and measured by His-tag antibodies and ELISA.

Release of HKI and N-domain HKI are indistinguishable by the kinetic ELISA assay (Fig. 2.8). Evidently, the C-terminal half of HKI plays no significant role in the binding of HKI to the mitochondrion. Indeed, other evidence is consistent with this view. Polyclonal antibodies directed to the C-terminal half of HKI do not release HKI from mitochondria, whereas antibodies directed toward the N-terminal half of HKI cause release (63). Mutations to the Glc-6-P binding site at the N-terminal half greatly diminish release of HKI by Glc-6-P, but mutation to the Glc-6-P site at the C-terminal half has little effect on release (44). The indistinguishable release of HKI and N-domain-HKI but ATP and TNP-ADP is inconsistent with Mechanism I, which attributes release to nucleotide association with the C-terminal half of HKI.

A single-site binding model accounts for TNP-ADP association with HKI. That binding site is not part of the N-terminal half, as TNP-ADP binds weakly to N-domain HKI. Potent competitive inhibitor of TNP-ADP with respect to ATP is consistent with a high-affinity site at or near the active site of the C-terminal half. TNP-ADP does not bind to N-domain HKI and yet releases N-domain HKI from mitochondria, observations clearly inconsistent with Mechanism III.

Although it is relatively straightforward to exclude mechanisms of release, to actually prove the remaining mechanism (Mechanism IV) requires the accumulation of overwhelming experimental evidence. The approach here is to demonstrate correlations between nucleotide release of HKI from mitochondria and high-affinity binding to human VDAC-1. In fact if Mechanism IV is correct, newly-discovered agents that bind to human VDAC-1 competitively with respect to TNP-ADP should

also release HKI from mitochondria. The TNP-nucleotides (TNP-ATP, TNP-ADP, TNP-AMP, and TNP-CTP) bind to human VDAC-1 with high affinity (Table 2.1), and each is effective in the release of HKI from the mitochondrion (Table 2.3). The affinity of TNP-nucleotides to the mitochondrion, as measure by the release experiments (K_3) and by fluorescence titrations (K_L) are in reasonable agreement. Moreover, CDP does not displace TNP-ADP from human VDAC-1, and is not effective as a release agent (Figs. 2.6 & 2.10). These findings are consistent with Mechanism IV. If the target protein is not VDAC, then it must be another protein of equal abundance, able to bind TNP-nucleotides with similar high affinities, but not CDP. As VDAC is reportedly the most abundant protein in the outer leaflet, another protein with these attributes seems a remote possibility.

One should note, however, an apparent discrepancy within the body of data presented here. Firstly, $1/K_3$ for ATP release of HKI is ~$5x10^{-5}$ M, whereas K_A for ATP measured by fluorescence is ~$5x10^{-4}$ M. The basis for this difference is unclear. Mg^{2+} is necessary for the association of HKI with mitochondria, and quite possibly ATP releases HKI not only through its interaction with VDAC, but also by chelation of Mg^{2+}. ATP and ADP, however, are nearly equal in efficacy of HKI release. Moreover, release of HKI by TNP-nucleotides show no dependence on the number of phosphoryl groups, release efficacies and binding affinities being linked to the trinitrophenol functionality. Although TNP-ADP does not bind to the N-terminal half of HKI, one cannot rule-out a release effect due to the binding of ATP (or ADP) to the N-terminal half. Mutations of residues at the ATP binding site of the N-terminal half, however, seem not to influence ATP release (Skaff, Honzatko, and Fromm,

unpublished). ATP could bind to an additional site on VDAC which does not exclude the binding of TNP-ADP. An azido photoaffinity label modifies VDAC at three positions that could map to distinct sites (50).

Although the focus here is on a mechanism of release, one can glean some basic understanding of the subunit stoichiometries in the HKI-VDAC-1 complex. Firstly, the ratio of HKI to VDAC must be at least one to one. If HKI is present at ratios less than unity with VDAC, then the observed reaction velocities in the absence of release agent are unachievable. A ratio of 1:2 HKI to VDAC requires a doubling of the estimated number of VDAC molecules in the mitochondrion. HKI forms dimers (15,48), and at least one report in the literature indicates a subunit tetramer of mitochondrion-bound hexokinase (64). An assumption of 4:1 HKI to VDAC for release data presented here decrease K_1 by 20-fold ($\sim 10^7$ M^{-1}) and K_3 by 4-fold, but the relative values of K_3 remain unchanged. Hence, the affinity constants presented here are fairly insensitive to radical departures from the assumed 1:1 subunit ratio of the HKI-VDAC complex.

Multimers of mitochondrion-bond HKI, to the extent that they form, must not involve interactions of C-terminal halves to be consistent with observations here. In fact, the simplest structural model consistent with release data is complex involving the N-terminal half of HKI with VDAC. Using the X-ray structure of mouse VDAC-1 (65), the N-terminal hydrophobic tail of HKI most likely interacts with lipid and the external surface of the VDAC β-barrel. TNP-ADP, however, is highly anionic, having at pH 7.5 formal charges on the phosphoryl and nitro groups. The most probably binding site for this anion is somewhere at the inner surface of the VDAC

barrel, which is lined with positively charged side chains. The model here is one of completion between TNP-ADP and HKI for VDAC, and leaves two possibilities: Either the binding of TNP-ADP cause such significant conformational change in VDAC as to disrupt interactions involving the N-terminal resides of HKI or another set of surfaces residues of the N-terminal half of HKI are essential to the stability of the HKI-VDAC complex.

Disruption of the hexokinase-mitochondrion association is the intention of potential anti cancer drugs (66). Hexokinases I&II are often over-expressed in cancer cell lines, presumably to block pro-apoptotic signals which act through the release of cytochrome c from the mitochondrion. Remove hexokinase from the mitochondrion, and cancer cell succumb to apoptosis or have heightened sensitivity to existing treatments for cancer. Small molecules such as clotrimazole, bifonazole (67), 3-bromopyruvate (68) and methyl jasmonate (69) dissociate hexokinase from the mitochondrion. In most cases, the mechanism of release has not been determined, as has been here for the TNP-nucleotides and for Glc-6-P (44). VDAC evidently is a target for small molecules that release mitochondrion-bound hexokinase. As the trinitrophenol group seems critical to binding affinity and not the phosphoryl groups or nucleotide base, one has a reasonable expectation of finding a molecule of high specificity and within the parameters that define substances of potential pharmacological value.

References

1. Katzen, H M; Schimke, R T. (1965) *Proc. Natl. Acad. Sci. U S A* **54**, 1218-25.

2. Lowry, O H; Passonneau, J V. (1964) *J. Biol. Chem.* **239**, 31-42.

3. Wilson, J E. (1980) *Curr. Top. Cell. Regul.* **16**, 1-54.

4. Crane, R K; Sols, A. (1954) *J. Biol. Chem.* **210**, 597-606.

5. Rose, I A; Warms, J V; O'Connell. (1964) *Biochem. Biophys. Res. Commun.* **15**, 33-7.

6. Ellison, W R; Lueck, J D; Fromm, H J. (1975) *J. Biol. Chem.* **250**, 1864-71.

7. Wilson, J E. (1995) *Rev. Physiol. Biochem. Pharmacol*. **26**, 65-198.

8. Wilson, J E. (2003*) J. Exp. Biol.* **206**, 2049-57.

9. Schwab, D A; Wilson, J E. (1989) *Proc Natl Acad Sci U S A* **86**, 2563-2567.

10. Ardehali, H; Yano, Y; Printz, R L; Koch, S; Whitesell, R R; May, J M; Granner, D K. (1996) *J. Biol. Chem.* **271**, 1849-52.

11. White, T K; Wilson, J E. (1989) *Arch. Biochem. Biophys.* **274**, 375-93.

12. Fang, T Y; Alechina, O; Aleshin, A E; Fromm, H J; Honzatko, R B. (1998) *J. Biol. Chem.* **273**, 19548-53.

13. Liu, X; Kim, C S; Kurbanov, F T; Honzatko, R B; Fromm, H J. (1999) *J. Biol. Chem.* **274**, 31155-9.

14. Tsai, H J; Wilson, J E. (1995) *Arch. Biochem. Biophys.* **316**, 206-14.

15. Aleshin, A E; Zeng, C; Bartunik, H D; Fromm, H J; Honzatko, R B. (1998) *J. Mol. Biol.* **282**, 345-57.

16. Rose, I A; Warms, J V. (1967) *J. Biol. Chem.* **242**, 1635-45.

17. Xie, G C; Wilson, J E. (1988) *Arch. Biochem. Biophys.* **267**, 803-10.

18. Lindén, M; Gellerfors, P; Nelson, B D. (1982) *FEBS Lett.* **141**, 189-92.

19. Fiek, C; Benz, R; Roos, N; Brdiczka, D. (1982) *Biochim. Biophys. Acta.* **688**, 429-40.

20. Azoulay-Zohar, H; Israelson, A; Abu-Hamad, S; Shoshan-Barmatz, V. (2004) *Biochem. J.* **377**, 347-55.

21. Beutner, G; Ruck, A; Riede, B; Welte, W; Brdiczka, D. (1996) *FEBS Lett.* **396**, 189-95.

22. Beutner, G; Rück, A; Riede, B; Brdiczka, D. (1997) *Biochem. Soc. Trans.* **25**, 151-7.

23. Vyssokikh, M Y; Brdiczka, D. (2003) *Acta. Biochim. Pol.* **50**, 389-404.

24. Vyssokikh, M Y; Goncharova, N Y; Zhuravlyova, A V; Zorova, L D; Kirichenko, W; Krasnikov, B F; Kuzminova, A E; Melikov, K C; Melik-Nubarov, N S; Samsonov, A V; Belousov, W; Prischepova, A E; Zorov, D B. (1999) *Biochemistry (Mosc).* **64**, 390-8.

25. Machida, K; Ohta, Y; Osada, H. (2006) *J. Biol. Chem.* **281**, 14314-20.

26. Zoratti, M; Szabò, I. (1995) *Biochim. Biophys. Acta.* **1241**, 139-76.

27. Crompton, M; Virji, S; Doyle, V; Johnson, N; Ward, J M. (1999) *Biochem. Soc. Symp.* **66**, 167-79.

28. Zamzami, N; Kroemer, G. (2003) *Curr. Biol.* **13**, R71-3.

29. Lemasters, J J; Qian, T; Bradham, C A; Brenner, D A; Cascio, W E; Trost, L C; Nishimura, Y; Nieminen, A L; Herman, B. (1999) *J. Bioenerg. Biomembr.* **31**, 305-19.

30. Shimizu, S; Narita, M; Tsujimoto, Y. (2000) *Nature* **399**, 483-87.

31. Shimizu, S; Matsuoka, Y; Shinohara, Y; Yoneda, Y; Tsujimoto, Y. (2001) *J. Cell*

Biol. **152**, 237-50.

32. Pastorino, J G; Shulga, N; Hoek, J B. (2002) *J. Biol. Chem.* **277**, 7610-8.

33. Majewski, N; Nogueira, V; Bhaskar, P; Coy, P E; Skeen, J E; Gottlob, K; Chandel, N S; Thompson, C B; Robey, R B; Hay, N. (2004) *Mol. Cell* **16**, 819-30.

34. Majewski, N; Nogueira, V; Robey, R B; Hay, N. (2004) *Mol. Cell. Biol.* **24**, 730-40.

35. Shimizu, S; Ide, T; Yanagida, T; Tsujimoto, Y. (2000) *J. Biol. Chem.* **275**, 12321-5.

36. Zaid, H; Abu-Hamad, S; Israelson, A; Nathan, I; Shoshan-Barmatz, V. (2005) *Cell Death Differ.* **12**, 751-60.

37. Abu-Hamad, S; Sivan, S; Shoshan-Barmatz, V. (2006) *Proc. Natl. Acad. Sci. U S A* **103**, 5787-92.

38. Robey, R B; Hay, N. (2005) *Cell Cycle* **4**, 654-8.

39. Neumann, D; Bückers, J; Kastrup, L; Hell, S W; Jakobs, S. (2010) *PMC Biophys.* **3**, 1-15.

40. Perevoshchikova, I V; Zorov, S D; Kotova, E A; Zorov, D B; Antonenko, Y N. (2010) *FEBS Lett.* **584**, 2397-402.

41. Abu-Hamad, S; Arbel, N; Calo, D; Arzoine, L; Israelson, A; Keinan, N; Ben-Romano, R; Friedman, O; Shoshan-Barmatz, V. (2009) *J. Cell Sci.* **122**, 1906-16.

42. Arzoine, L; Zilberberg, N; Ben-Romano, R; Shoshan-Barmatz, V. (2009) *J. Biol. Chem.* **284**, 3946-55.

43. Shoshan-Barmatz, V; Zakar, M; Rosenthal, K; Abu-Hamad, S. (2009) *Biochim. Biophys. Acta.* **1787**, 421-30.

44. Skaff, D A; Kim, C S; Tsai, H J; Honzatko, R B; Fromm, H J. (2005) *J. Biol. Chem.* **280**, 38403-9.

45. Wilson, J E. (1968) *J. Biol. Chem.* **243**, 3640-7.

46. Hochman, M S; Shimada, Y; Sacktor, B. (1974) *J. Neurochem.* **23**, 861-3.

47. Bustamante, E; Pedersen, P L. (1980) *Biochemistry,* **19**, 4972-7.

48. Aleshin, A E; Kirby, C; Liu, X; Bourenkov, G P; Bartunik, H D; Fromm, H J; Honzatko, R B. (2000) *J. Mol. Biol.* **296**, 1001-15.

49. Rosano, C; Sabini, E; M, Rizzi; Deriu, D; Murshudov, G; Bianchi, M; Serafini, G; M, Magnani; Bolognesi, M. (1999) *Structure* **7**, 1427-37.

50. Yehezkel, G; Hadad, N; Zaid, H; Sivan, S; Shoshan-Barmatz, V. (2006) *J. Biol. Chem.* **281**, 5938-46.

51. Yehezkel, G; Abu-Hamad, S; Shoshan-Barmatz, V. 2007, *J. Cell. Physiol.* **212**, 551-61.

52. Graham, J M. (1993) Methods Mol. Biol. **19**, 29-40.

53. Wojtczak, L; Zaluska, H; Wroniszewska, A; Wojtczak, A B. (1972) *Acta. Biochim. Pol.* **19**, 227-34.

54. Rice, J E; Lindsay, J G. (1997) in *Subcellular Fractionation, A Practical Approach* (Graham J M; Rickwood, D, ed) pp 107-142, Oxford University Press, New York, NY

55. Bradford, M M. (1976) *Anal. Biochem.* **72**, 248-54.

56. Leatherbarrow, R J. (2001) *GraFit*, Version 5, Erithacus Software Ltd., Horley, UK

57. Towbin, H; Staehelin, T; Gordon, J. (1979) *Proc. Natl. Acad. Sci. U S A.* **76**, 4350–4.

58. Engelhardt, H; Meins, T; Poynor, M; Adams, V; Nussberger, S; Welte, W; Zeth, K. (2007) *J. Membrane Biol.* **216**, 93-105.

59. Fallar, L D. (1990) *Biochemistry* **29**, 3179-86.

60. Aleshin, A E; Fromm, H J; Honzatko, R B. (1998) *FEBS Lett.* **434**, 42-6.

61. Estabrook, R W; Holowinsky A. (1961) *J. Biophys. Biochem. Cytol.* **9**, 19-28.

62. Arora, K K; Shenbagamurthi, P; Fanciulli, M; Pedersen, P L. (1990) *J. Biol. Chem.* **265**, 5324-8.

63. Smith, A D; Wilson, J E. (1991) *Arch. Biochem. Biophys.* **287**, 359-66

64. Xie, G and Wilson, J E. (1990) *Arch. Biochem. Biophys.* **276**, 285-93

65. Ujwal, R; Cascio, D; Colletier, J P; Faham, S; Zhang, J; Toro, L; Ping, P; Abramson, J. (2008) *Proc. Natl. Acad. Sci. USA* **105,** 17742-7

66. Mathupala, S P, Ko; Y H; Pedersen, P L. (2006) *Oncogene* **25**, 4777-86.

67. Penso, J; Beitner, R. (1998) *Eur. J. Pharmacol.* **342**, 113-7.

68. Kim, W; Yoon, J H; Jeong, M; Cheon, G J; Lee, T S; Yang, J I; Park, S C; Lee, H S. (2007) *Mol. Cancer Ther.* **6**, 2554-62.

69. Cohen, S; Flescher, E. (2009) *Phytochemistry* **70**, 1600-9.

CHAPTER 3: SINGLE-RESIDUE DETERMINANTS IN THE BINDING OF RECOMBINANT HUMAN BRAIN HEXOKINASE TO THE MITOCHONDRION[1]

A paper to be submitted to the Journal of Biological Chemistry

Nimer Mehyar[2], Nidhi Shah, Lu Shen, Dong Yan, and Richard B. Honzatko[2,3]

Abstract

The N-terminal segment (residues 1-15) of hexokinase I (HKI) is essential for the binding of HKI to the outer membrane of the mitochondrion. Whether the N-terminal segment is merely a hydrophobic anchor to the membrane or has specific residues that are key determinants in the mitochondrion-HKI interaction is unclear. Recombinant wild-type HKI binds to mitochondria, but the removal of residues 1-15 abolishes such binding. Mutations A4L, A8L and Q5P individually cause a 10-fold decreases (relative to wild-type enzyme) in HKI binding to mitochondria. In contrast, mutations Q5A, Y10L and T12I decrease binding by approximately twofold. The mutations did not affect the catalytic properties of the enzyme, and all HKI constructs remained monomeric to concentrations as high as 10 micomolar. Results here are consistent with a helical conformation for the N-terminus of HKI, with residues A4

[1]This research was supported in part by National Institute of Health Research Grant NS 10546

[3]To whom correspondence should be addressed.

and A8 defining a contiguous surface that does not tolerate large hydrophobic side chains.

Introduction

Hexokinases catalyze glucose phosphorylation by adenosine tri-phosphate (ATP) to produce glucose 6-phosphate (Glc-6-P). Mammals have four isozymes of hexokinase: I, II, III and IV (1). Hexokinase I (HKI) or brain hexokinase regulates glucose metabolism in brain tissue and the red blood cell (2). Hexokinases (I-III) have molecular masses of approximately 100 kDa (1), consisting of C- and N-terminal halves with significant levels of sequence identity to each other and to yeast hexokinase (3). Hexokinase IV (glucokinase) is a 50 kDa protein with a sequence similar to both C-terminal and N-terminal halves of hexokinase I-III and to yeast hexokinase (4). Similarities between mammalian isoenzymes evidently originate from the duplication and fusion of a primodial hexokinase gene similar to that of yeast hexokinase (5). A number of ligands inhibit HKI; however, Glc-6-P is probably the primary physiological inhibitor of the type-I enzyme (6). Glc-6-P inhibits HKI catalysis by binding with high affinity to either the C- or N-terminal halves (7,8). Under normal physiological conditions, inorganic orthophosphate (P_i) decreases Glc-6-P inhibition (9). P_i binds tightly to the N-terminal half of HKI and relieves Glc-6-P inhibition by an allosteric mechanism that couples both halves of the enzyme (10) (11). At elevated levels, P_i inhibits HKI by binding to the active site (12).

Despite structural similarities, hexokinases (I-III) are functionally different. Both halves of HKII support catalysis and are each sensitive to inhibition by Glc-6-P

(13), whereas only the C-terminal half of HKI and HKIII supports activity (14,15). Nonetheless, P_i can relieve Glc-6-P inhibition of HKI alone (4,7-8,12).

HKI co-localizes on the outer mitochondrial membrane (OMM) in brain tissue preferentially close to newly formed ATP inside the mitochondrion (16,17). In tumor cells, mitochondrion-associated HKII antagonizes Bax-induced cytochrome c release and in turn inhibits apoptosis (18-20). Bax interacts with permeability transition pore (PTP) resulting in loss of membrane potential, triggering of mitochondrial membrane permeabilization (MPP) and release of cytochrome c (21). Pro-apoptotic proteins such as Bax, Bak, and Bim interact with voltage-dependent anion channel (VDAC) forming an assembly of large channels likely used for cytochrome c passage from mitochondrion matrix to cytoplasm (22-24). VDAC is part of PTP, which in addition to VDAC, includes the adenylate translocator (ANT) of the inner mitochondrion membrane (IMM) (25-29), and cyclophilin D of the inner mitochondrion matrix (30-32). Released cytochrome c activates the caspase family of proteases in cytoplasm, which in turn triggers apoptosis (32-34). VDAC-1 overexpression causes apoptotic cell death (35,36). Hexokinase I and II, in association with VDAC, likely antagonize the formation of apoptotic channels. Some have gone so far as to label hexokinase as “guardian of the mitochondria” (37).

Over expression of N-terminally truncated VDAC-1 did not induce cells to release cytochorme c, and such cells were resistant to apoptosis (38). N-terminus peptide and other VDAC-1 based peptides bind to immobilized HKI, these peptides prevent HKI-protection of cells (39). Chemical modification of Glu 72 prevents HKI from binding to mitochondria (35). Mutating Glu 72 and other residues abolishes

HKI-protection against apoptosis in cancer cells (40). Adding HKI to VDAC-1 reconstituted in lipid membrane reduced the channel conductance (25); however, the addition of HKI to mutant mouse VDAC-1 E72Q reconstituted in lipid membrane did not block conductance in patch clamp experiments, indicating failure of HKI to bind to mutant VDAC-1 (40).

A number of small and physiological important ligands are capable of dissociating HKI from the mitochondrial outer membrane. These compounds include Glc-6-P and ATP (16). Skaff *et al.* (41) demonstrated wild-type recombinant HKI with properties comparable to native brain hexokinase including those of mitochondrial-binding and release. The recombinant construct has an intact membrane targeting element and a formyl group attached to the amino terminus of the polypeptide chain. The release properties of mutant constructs demonstrated the significance of Glc-6-P binding to the N-terminal half of HKI in promoting the release of the mitochondrion-associated enzyme. Nucleotide-induced release, on the other hand, follows a competitive binding model between HKI and nucleotides a binding site on VDAC1 (unpublished data).

Early studies showed that digesting hexokinase I with proteases resulted in loss of mitochondrial binding properties (16). Rapid purification of rat brain hexokinase using HPLC decreased the portion of HKI devoid of mitochondria-binding properties (42,43). Rat-brain hexokinase with mitochondrion-binding properties intact is more hydrophobic than the non-bindable form (44). The two enzyme forms (with and without mitochondrial binding properties) have similar molecular weights and kinetic properties (45). N-terminal sequence of rat brain

hexokinase was determined as a critical determinant of mitochondrial binding of HKI (46). The N-terminus of HKI from native tissue is putatively blocked by an acetyl group (47). Xie and Wilson (1988) proposed a helical conformation of the first 11 residues of HKI N-terminus. This conformation allows the insertion of the N-terminus in a lipid bilayer (46,48). The effect of monoclonal antibodies against rat brain hexokinase varied from blocking mitochondrial binding to inhibiting Glc-6-P release (49). Mitochondrial-bound rat brain hexokinase was released upon exposure to monoclonal antibodies raised against the N-terminus (50).

Although some studies stress that hexokinase binding to mitochondria is determined by the hydrophobicity of the tail (51,52), HKI cellular co-localization with VDAC on OMM (17) implies more complex and specific interactions than general hydrophobic interactions with lipid. To date, no single residue has been proven essential to hexokinase association with the mitochondrion. Yet inspection of the putative N-terminal helix of HKI reveals amino acids with small side chains localize to only one face of the helix, whereas large side chains occupy all other faces. Does the helix surface defined by small side chains make critical contacts with a protein binding partner (presumably VDAC) in the outer membrane of the mitochondria? Indeed, the mutation of Ala 4 and Ala 8 to leucine abolished hexokinase association with the mitochondrion, whereas mutations at other residues have little or no effect. The discovery of a localized surface critical to hexokinase association with the mitochondrion provides a useful constraint in modeling possible HKI-VDAC complexes.

Experimental Procedures

Materials—ATP, Glc-6-P, ampicillin, deoxyribonuclease (DNase I), bovine serum albumin (BSA), leupeptin, protease cocktail inhibitor and phenylmethylsulfonyl fluoride (PMSF) came from Sigma. DEAE HPLC resin was a product of Tosohaas. *E.coli* strain BL21 (DE3) competent cells were from Novagen. Glucose-6-phosphate dehydrogenase was obtained from Roche Molecular Biochemicals. Isopropyl-1-thio-β-D-galactopyranoside (IPTG) came from Anatrace. Sequencing PVDF membranes (ProSorb sample preparation cartridge) were purchased from Applied Biosystems.

Construction of Wild-type Hexokinase and Mutant Plasmids—Human brain hexokinase (HKI) had been cloned into pET-11a as reported in a previous study (41). Hexokinase mutants were created through PCR modification with oligonucleotide primers synthesized at the Iowa State University DNA Sequencing and Synthesis Facility. Mutants Ala4Leu, Ala8Leu, Thr12Ile, Gln5Ala and Gln5Pro were created with the following forward primers (and their reverse compliments) respectively:

5'CATATGATCGCCCTGCAGCTCCTGGCC-3';

5'CGCAGCTCCTGCTCTATTACTTCACGGAGC-3';

5'GCCTATTACTTCATTGAGCTGAAGGATG-3';

5'GATCGCCGCGGCGCTCCTGGCC-3';

5'GATCGCCGCGCCGCTCCTGGCC-3'.

Iowa State University DNA Sequencing and Synthesis Facility confirmed all final constructs by sequencing the DNA of the entire gene. Mutant Y10L was used in previous studies (unpublished data).

Expression and Purification of Wild-Type and Mutant Hexokinases— Wild-type or mutant pET-211a-HKI plasmids were transformed into *E.coli* strain BL21 (DE3). Expression and purification of HKI enzymes were previously discussed (41). Protein concentrations employed the Bradford method with bovine serum albumin as a standard (53).

Pig Liver Mitochondria Purification— Pig livers were obtained from the Iowa State University Meats Laboratory shortly after slaughter. Mitochondrial purification is described (54) with modifications as discussed elsewhere (41). Both outer mitochondrial membrane (OMM) and inner mitochondrial membrane (IMM) integrities were measured as described previously (55, 56). Mitochondria were stored at –80º C in the presence of 5% dimethyl sulfoxide.

The HKI Activity Assay— Hexokinase activity was measured using the glucose 6-phosphate dehydrogenase (G6PDH)-coupled spectrophotometric assay. Assay solutions have 3mM $MgCl_2$, 3 mM DTT, 0.3 mM NADP and 10 μg/mL G6PDH in 50 mM Tris-HCl, pH 8.0, and concentrations of glucose and ATP:Mg^{2+} that varied from 1/5 *x* K_m to 5 *x* K_m. NADPH production was monitored at 340 nm wavelength. Reaction was initiated by the addition of enzyme and linear progress curves monitored for 3 minutes. Slopes were used to calculate initial rates in umole/min. The capacity of the coupling enzymes was verified by observing a

twofold increase in velocity with a doubling of added hexokinase. Initial rate data were analyzed using GraFit (57).

Mitochondrial Binding and Release— Purified HKI was dialyzed twice against mitochondrial-binding buffer (250 mM sucrose, 5 mM Glc, 50 mM NaCl, 5 mM $MgCl_2$ and 50 mM HEPES, pH 7.4), and then diluted to 2 mg/mL using the same buffer. Thirty mg wet weight of mitochondrion, thawed on ice, was suspended in 1 mL of mitochondrial-binding buffer, and then collected by centrifugation at 11,000 × *g* for 5 minutes. Suspension and centrifugation steps were repeated twice. The pellet was suspended in 1 mL of mitochondrial-binding buffer with added HKI (2 mg/mL), protease cocktail inhibitor (0.25 mg/mL) and PMSF (1 mM). After 60 minutes on ice, the mixture of HKI and mitochondria was centrifuged at 11,000 × *g* for 5 minutes. Unbound HKI in the supernatant fluid was decanted. Pelleted mitochondria were suspended in mitochondrial-binding buffer, less the $MgCl_2$, NaCl, and glucose, and centrifuged again. This wash step was twice-repeated.

HKI-bound mitochondria, prepared as above, is suspended in release buffer (250 mM sucrose and 50 mM HEPES, pH 7.4). 50 μL aliquots of this suspension were distributed to plastic micro-centrifuge tubes, to which were added a release agent (ATP, TNP-nucleotide, or Glc-6-P) at various concentrations. After 30 minutes at room temperature, the mitochondria were pelleted by centrifugation. HKI solubilized by nucleotide was removed by decanting the supernatant liquid. The mitochondrial pellet was suspended in wash buffer (250 mM sucrose and 5 mM HEPES, pH 7.4), and centrifuged. After discarding the supernatant fluid, pelleted

mitochondria were suspended in 100 μL wash buffer and then assayed for hexokinase activity.

Results

Mitochondria integrity— The outer membrane integrity of the mitochondrion preparation was 90% as indicated by the cytochrome c oxidase activity assay (data not shown). Inner membrane integrity was confirmed by mitochondrial uptake of the cationic carbocyanine dye JC-1 (data not shown).

Rationale for the selection of HKI mutants—Xie and Wilson (46) predicted a helical structure for the first 11 residue sequence of rat brain HKI, which was confirmed subsequently the structure of the rat HKI (58) (Fig. 3.1). This sequence is identical to that of human brain HKI (Fig. 3.1). The helical conformation for these initial residues puts Ala 4, Ala 8 and Thr 12 on the same face of the helix (Fig. 3.1). Other faces of the helix have predominantly residues with large hydrophobic side chains. The alignment of small residues on one face of the N-terminal helix could facilitate packing of the helix against a relatively uniform surface of on the β-barrel of VDAC1. If so, then mutations of position 4, 8, and 12 to larger hydrophobic residues should decrease the binding of HKI to mitochondria. The mutation of position 5 to proline should destabilize the helix and thereby disrupt mitochondrial association.

Size exclusion— Size exclusion chromatography of wild-type HKI and mutants (Fig. 3.2) revealed a major band corresponding to a protein of mass 100 kDa (Table 3.1).

A. *B.*

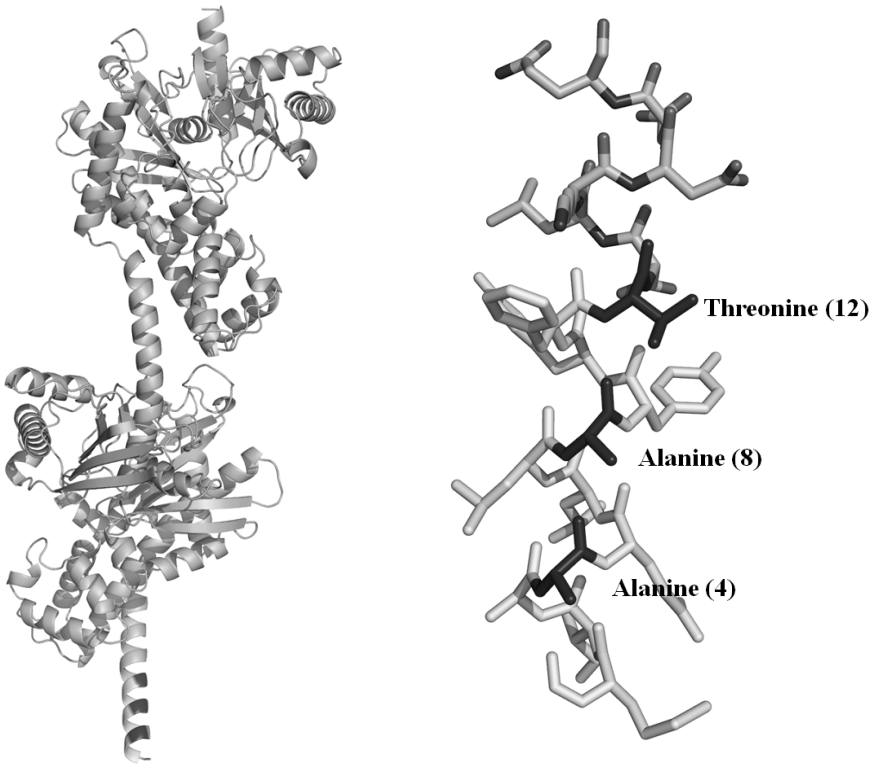

C.

```
                10        20        30        40        50        60
Human   MIAAQLLAYYFTELKDDQVKKIDKYLYAMRLSDETLIDIMTRFRKEMKNGLSRDFNPTAT
        :::::::::::::::::::::::::::::::: :::.:::.:::::::::::::::::.
Rat     MIAAQLLAYYFTELKDDQVKKIDKYLYAMRLSDEILIDILTRFKKEMKNGLSRDYNPTAS
                10        20        30        40        50        60
```

Fig. 3.1 Structure of HKI. *A.* Ribbon of HKI. The image shows the N-terminal α-helix with positions 4, 8, and 12 in dark gray. *B.* Stick model of the N-terminal helix (light gray). Residues targeted for mutation (dark gray) lie on one side of the helix. Model adapted from crystal structure of HKI (PDB ID 1CZA). *C.* Human brain hexokinase (NCBI Reference Sequence: NP_000179.2) and rat brain hexokinase (GenBank: AAC20075.1) aligned by LALIGN (59).

A.

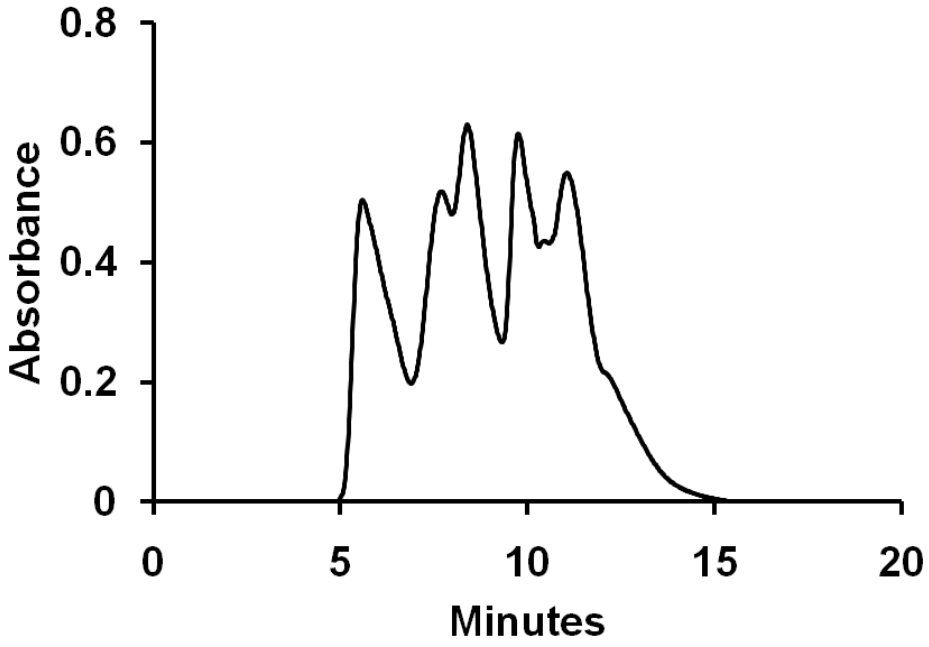
0.8
0.6
0.4
0.2
0
Absorbance
0
5
10
15
20
Minutes

B.

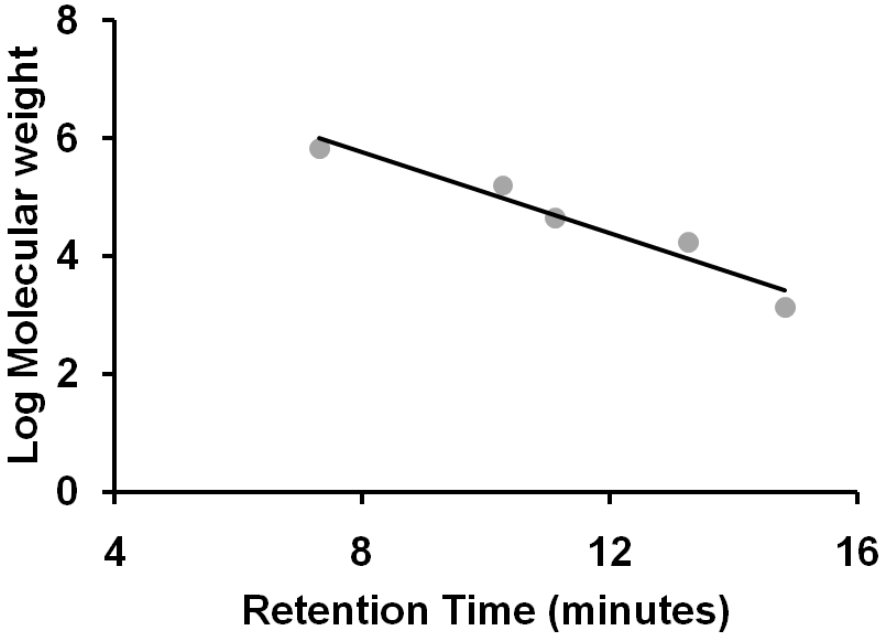
8
6
4
2
0
Log Molecular weight
4
8
12
16
Retention Time (minutes)

C.

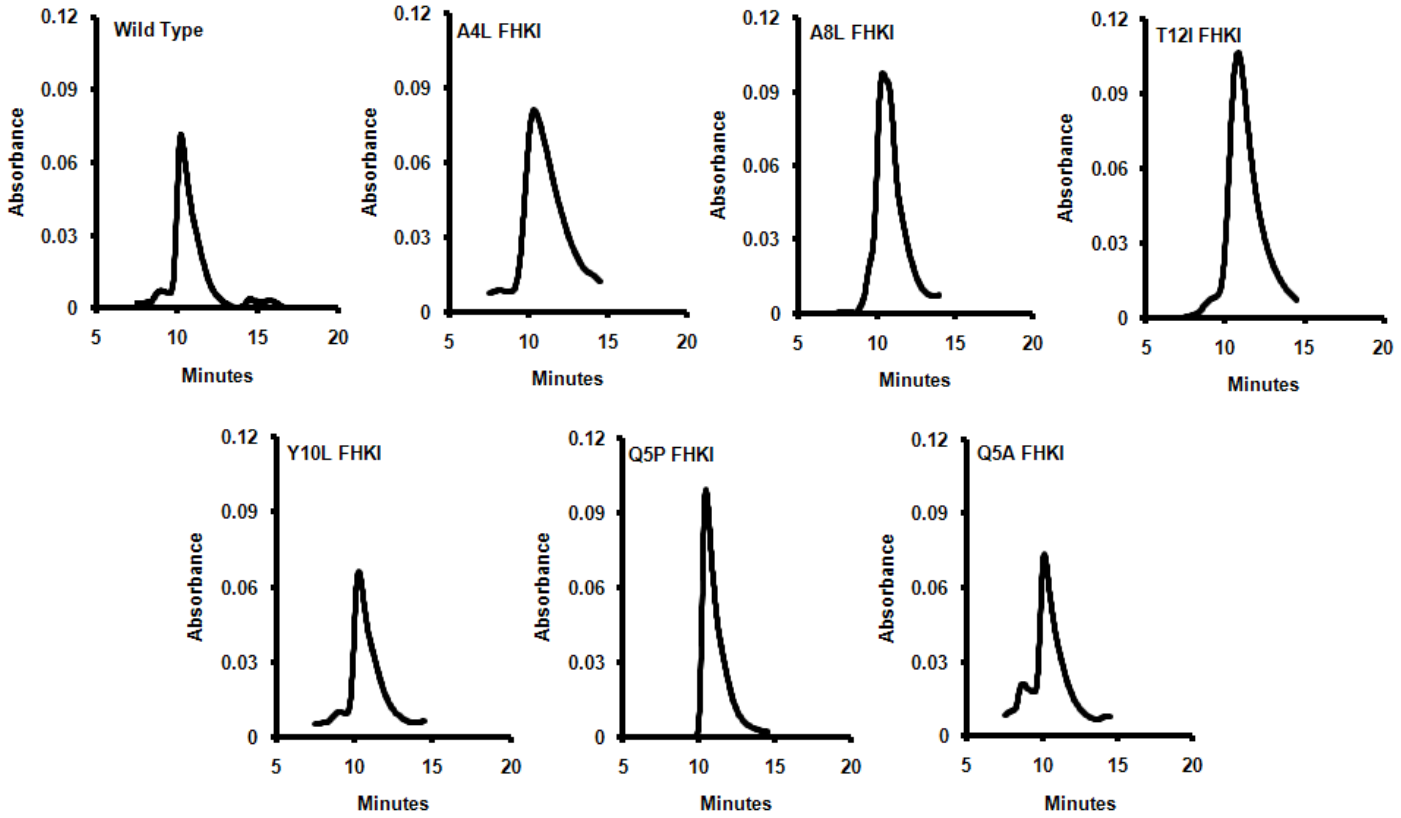

Fig. 3.2. Size exclusion chromatography profiles of HKI constructs. *A.* Elution profiles of standard proteins. *B.* Calibration curve made from plots log molecular weights of standard proteins logarithm versus retention times. *C.* Elution profiles of wild-type and mutant HKI. The concentration of wild-type and mutant HKI was 1 mg/mL. A sample of volume 100 µL was injected onto a TSK-G3000SW type size-exclusion column. Size exclusion was done in the presence of 5 mM glucose, 1 mM DTT, and 25 mM KPi, pH 7.4. Absorbance was monitored at 280 nm.

Table 3.1. Apparent molecular weights of wild-type and mutant hexokinases as determined by size exclusion chomatography.

	HKI construct						
	WT	Y10L	A4L	A8L	T12I	Q5A	Q5P
MW (kDa)	105 (7)	96 (4)	100 (6)	99 (9)	115 (10)	103 (6)	95 (5)

Linear regression equation of calibration curve (Figure 1) was used to calculate apparent molecular weights of wild type and mutant HKI. Size exclusion was done in the presence of 5 mM glucose, 1 mM DTT, and 25 mM KPi, pH 7.4. Absorbance was monitored at 280 nm.

HKI and mutants properties— Purified proteins here were at least 95% pure on the basis of sodium dodecylsulfate polyacrylamide gel electrophoresis (SDS-PAGE). Each hexokinase was prepared twice, and used immediately upon purification in mitochondrial binding, gel-filtration and kinetics experiments. Mutant hexokinases have k_{cat}, K_m^{Glc} and K_m^{ATP} comparable to those of wild-type HKI (Table 3.2). Edman degradation of wild-type and mutant hexokinases (400 picomole of purified enzyme) either provided no sequence information or weak signals for sequences beginning at residues 10 and 12. The vast majority of enzyme molecules in each sample had blocked N-terminal residues that resisted Edman degradation. Efforts to deformylate the N-terminus by incubation with 0.6 M HCl failed.

Wild-type and mutant hexokinase I binding to mitochondria— Scheme I represents the simplest equilibrium model that accounts for the binding of wild-type and mutant hexokinases to the mitochondria:

$$E + Q = EQ, \qquad K_1 = [EQ]/[E][Q]$$

Scheme I

In Scheme I, K_1 represents an association constant for the binding of the HKI construct (represented by E) to specific mitochondrial binding sites Q. As demonstrated by previous work nonspecific binding to the mitochondrion by HKI does not occur at significant levels. The ratio of enzyme bound to total E_o is as follows:

$$R([E]) = (K_1[E])/(1+K_1[E]) \qquad \text{Eq. 1}$$

The concentration of free specific mitochondrial sites Q is itself a function of the

Table 3.2. Kinetic properties of HKI constructs

HKI construct	k_{cat} (s^{-1})	K_m^{ATP} (mM)	K_m^{Glc} (μM)
Wild-type	92 (11)	0.58 (6)	40 (5)
Y10L	95 (15)	0.54 (4)	19 (3)
A4L	93 (7)	0.99 (8)	24 (3)
A8L	103 (15)	0.87 (7)	24 (5)
T12I	89 (9)	0.57 (5)	23 (4)
Q5A	98 (10)	0.60 (4)	20 (4)
Q5P	77 (4)	0.82 (2)	24 (6)

Determination of k_{cat} employed concentrations of Glc and ATP of 1.6 mM and 9 mM. Determination of K_m^{ATP} employed a Glc concentration of 1.6 μM and concentrations of ATP of 0.3–7.5 mM. Determination of K_m^{Glc} employed an ATP concentration of 9 mM and concentrations of Glc of 10–600 μM.

concentration of enzyme. Algebraic manipulation of the equilibrium expression in Scheme I and relationships for mass conservation of total enzyme E_o and total specific sites Q_o results in a quadratic relationship in E:

$$a[E]^2 + b[E] + c = 0$$

where $a = K_1$, $b = K_1(Q_o–E_o)+1$, and c = $–E_o$. The physical root of the quadratic equation gives [E]:

$$[E] = –\{K_1(Q_o–E_o)+1\}/2K_1 + \{K_1^2(E_o–Q_o)^2+2K_1(E_o+Q_o)+1\}^{1/2}/2K_1 \qquad \text{Eq. 2}$$

Substitution of Eq. 2 into Eq. 1provides a relationship for the fraction of enzyme bound to the mitochondria as a function of E_o, Q_o and K_1.

The fitting relationship is $V = s\mathrm{R}(E_oQ_oK_1)$ (Eq. 3), where s is a proportionality constant that relates the fraction of bound enzyme R to velocity V in μmoles/min. Undefined quantities s, E_o, Q_o, and K_1 cannot be determined by a nonlinear least squares fit of the data from a single experiment. Hence, values for some of these quantities must come from other determinations. Firstly, one assumes the HKI-VDAC complex has an equal number of HKI and VDAC subunits. The value for Q_o ($7.1x10^{-8}$ M) then is an estimate based on 42,000 VDAC molecules per mitochondrion (60), $7.2x10^9$ mitochodria per 1 mg of total mitochondrial protein (61), and 0.014 mg of mitochondria in each 100 μL assay. Moreover, $s = Q_o$×(specific activity)×(assay volume), where the specific activity for HKI is $6x10^9$ μmole/min^{-1} mole^{-1} and the assay volume is liters. Hence, if the assumption of a 1:1 ratio of the HKI-VDAC complex is correct, then data can be fit to Eq. 3 using K_1 alone as an adjustable parameter. Data fit by this method appears in Fig. 3.3. Listed in Table 3.3 are values for K_1 for wild-type and mutant constructs of HKI.

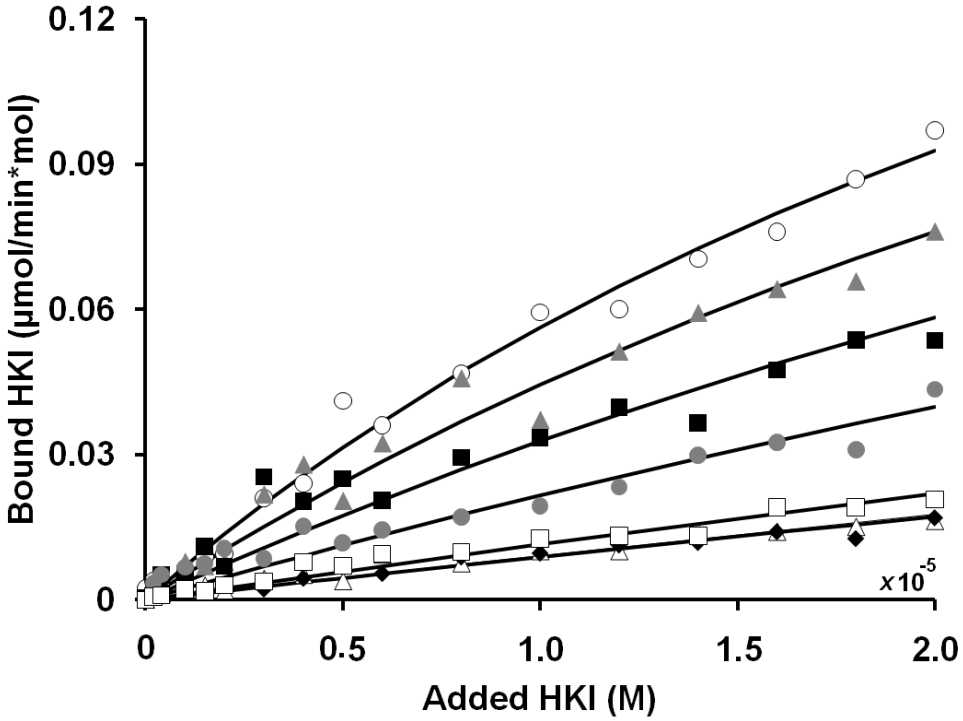

Fig. 3.3. HKI binding to pig liver mitochondria. Plots represent velocities from varying concentrations of wild-type (○), T12I (▲), Y10L (■), Q5A (●), Q5P (□), A4L (Δ) or A8L (♦) bound to 1.8 mg, wet weight mitochondria (each fraction) in 250 mM sucrose and 50 mM HEPES, pH 7.5. The solid lines represent fitted curves using Eq. 3 with parameters given in the Results section and Table 3.3.

Table 3.3. Fitted parameters for wild type and mutant FHKI binding to pig liver mitochondria.

FHKI construct	Apparent dissociation constant K_1 (M^{-1})
WT	2.7×10^4 (6.5×10^2)
Y10L	1.4×10^4 (7.3×10^2)
A4L	3.6×10^3 (1.6×10^2)
A8L	3.5×10^3 (1.5×10^2)
T12I	2.0×10^4 (7.0×10^2)
Q5A	8.9×10^3 (4.3×10^2)
Q5P	4.5×10^3 (1.5×10^2)

Parameter K_1 is defined in the Result section. HKI bound to 1.8 mg, wet weight mitochondria (each fraction) in 250 mM sucrose and 50 mM HEPES, pH 7.5 was measured by activity. Standard deviations in the last significant digits are given in parenthesis.

Glc-6-P induced release of Wild-type and mutant hexokinase I from mitochondria— Glc-6-P releases wild-type HKI from mitochondria as well as Thr12Ile, Tyr10Leu and Gln5Ala (Table 3.4). The model and fitting is as described previously (41). Release experiments could not be done for the A4L, A8L, and Q5P constructs due to poor binding to the mitochondrion.

ATP-induced release of Wild-type and mutant hexokinase I from mitochondria— ATP released wild-type, Thr12Ile, Tyr10Leu and Gln5Ala hexokinases from the mitochondrion likely (Table 3.5 and Fig. 3.4.). The model and fitting is as described in Chapter 2 of this thesis. Release experiments could not be done for the A4L, A8L, and Q5P constructs due to poor binding to the mitochondrion.

Discussion

K_1 of Scheme I represents binding affinity of HKI for the mitochondrion, but binding sites on the mitochondrion may be heterogeneous. VDAC molecules may exist as monomers, dimers, or in assemblies of large number. Nonetheless each class obeys the relationships of Scheme I, provided that HKI binds without cooperativity to large aggregates of VDAC. For a dispersive system, K_1 becomes a weighted average of association constants for each class of binding site:

$$K_1 = (\sum^{i} K_1[Q_i])/\sum[Q_i]$$

where the summations extend over *i* classes of binding sites with association constants ${}^{i}K_1$ and $[Q_i]$ is the concentration of mitochondrial binding sites in each class. The effect of site heterogeneity is a K_1 that depends on the concentrations of total enzyme E_o and mitochondrial sites Q_o. For instance, high ratios of E_o to Q_o will

Table 3.4. Fitted parameters for Glc-6-P-induced release of mitochondrial wild type and mutant HKI.

HKI construct	*a* ($\mu M S^{-1}$)	*b*	*c* (μM^{-1})	K_{ii} (*mM*)	$I_{0.5}$ (μM)	Relative velocity at $I_{0.5}$	Limiting release %
WT	0.035 (7)	6 (2)	1.1 (4)	0.2 (1)	3 (1)	0.70 (5)	47 (3)
T12I	0.040 (6)	5 (2)	1.1 (3)	0.3 (1)	2.7 (3)	0.67 (6)	48 (3)
Y10L	0.028 (4)	4 (2)	0.9 (2)	0.4 (2)	2.8 (4)	0.63 (5)	54 (6)
Q5A	0.047 (1)	8 (1)	1.5 (1)	0.3 (1)	3.4 (4)	0.74 (2)	40 (2)

Parameters *a, b, c*, $K_{ii,}$ and $I_{0.5}$ previously described (41). Mitochondria with HKI bound in 250 mM sucrose and 50 mM HEPES, pH 7.5, were exposed to varying Glc-6-P concentrations for 30 minutes. Remaining mitochondria bound HKI was measured by activity. Standard deviations in the last significant digit are given in parentheses.

Table 3.5. ATP-dependent release of HKI from pig liver mitochondria.

FHKI construct	K_1 (M^{-1})	K_3 (M^{-1})
WT	2.5×10^6 (7.3×10^4)	3.0×10^3 (4.1×10^2)
T12I	1.7×10^6 (6.3×10^4)	8.0×10^3 (1.2×10^2)
Y10L	4.9×10^6 (1.9×10^5)	3.0×10^3 (5.0×10^2)
Q5A	2.4×10^6 (1.0×10^5)	1.0×10^4 (1.7×10^3)

Parameters are from an equilibrium model in which the binding of nucleotide and HKI to the mitochondrion is mutually exclusive. K_1 and K_3 are constants for the dissociation in M^{-1} of HKI and ATP from the mitochondrion. Mitochondria with HKI bound in 250mM sucrose and 50 mM HEPES, pH7.5, were exposed to varying concentrations of ATP for 30 minutes. Remaining mitochondria bound HKI was measured by activity. Standard deviations in the last significant digits are given in parentheses.

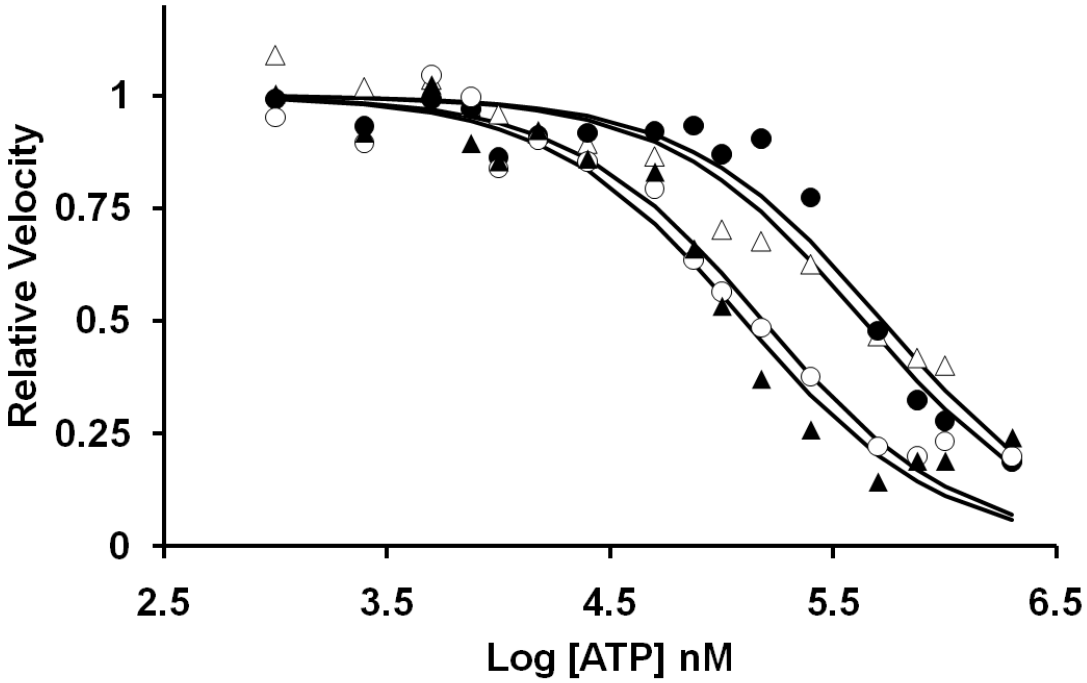

Fig. 3.2. ATP-induced release of wild-type and mutant HKI from pig liver mitochondria. Mitochondria with bound wild type (Δ), T12I (○), Y10L (●) or Q5A (▲) in 250mM sucrose and 50 mM HEPES, pH7.5, were exposed to varying concentrations of ATP . Plots represent relative velocities from mitochondria-bound bound HKI that remains after exposure to varying concentrations of ATP. The solid lines represent fitted curves using fitting model previously described in chapter 2 of this thesis.

result in low values for K_1, as subclasses of binding sites with low association constants contribute to the ensemble average. Wilson et al. (46) have published the only binding curve for which the number of mitochondrial binding sites Q_o is in great excess over E_o. Applying the model used here to these data yields a K_1 of $1.4x10^6$ M^{-1}. The number determined from (46) agrees well with the K_1 of nucleotide release assays (Table 3.5), but is 100-fold higher than the K_1 determined from binding assays (Table 3.3). The discrepancy lies in the relative abundance of HKI and mitochondria for the release and binding assays. Specifically for all data points in release assays [HKI] $\leq Q_o$, whereas for binding assays [HKI] $\geq Q_o$. The consequence of different experimental conditions is a K_1 that differs by 100-fold.

Pittler *et. al.* (47) proposed that an *N*-acetyl group blocks the N-terminus of native rat-brain hexokinase. In the present study, the N-termini of wild-type and mutant hexokinases resist Edman degradation. Deformylation of C-terminal His-tagged human HKI removed the blocking group, resulting in a clear hexokinase sequence beginning with the N-terminal methionine (41). The same procedure, however, did not deblock recombinant HKI, used here, which is expressed from a vector which does not incorporate a C-terminal His-tag. There are now many reports of recombinant proteins expressed in *E. coli* with an N-acteyl group at the N-teminus (62). The status of the N-terminus of HKI constructs is critical, because the loss of either the blocking group or N-terminal residues could greatly alter the binding affinity toward the mitochondrion. Each of the constructs here has a blocked N-terminus, and hence, changes in binding properties relative to the wild-type enzyme must be a consequence of a specific mutation.

Several mechanisms could be responsible for the disruption of HKI binding affinity to the mitochondrion. Mutations could cause global conformational change in the protein; however, kinetic parameters clearly indicate active enzyme with wild-type properties. Moreover, the removal of residues from the N-terminus has no effect on the kinetic properties of HKI (or hexokinase Type-II) from human and other sources (63,64). Mutations could also change the state of aggregation of HKI, and thereby impede association with the mitochondrion, but constructs here are monomers up to peak concentrations used in mitochondrial binding assays. Hence, decreased binding affinities observed here are due the effect of the mutation on the specific interactions with the mitochondrion.

Although HKI binds to hydrophobic surfaces (48), specific binding of HKI to mitochondria cannot be explained merely by hydrophobic interactions with a lipid bilayer (46). Mutations at positions 4 and 8 identify the first single-residue determinants essential for the interaction of HKI with the mitochondrion. The loss of binding properties due to the Gln5→Pro mutation infers a helical conformation for the N-terminal residues of mitochondrion-bound HKI. Hence, positions 4 and 8 define a contiguous surface that does not allow large residues, even if these residues are hydrophobic. Other positions seem less important, and allow conservative changes in the type of amino acid side chain, but no mutation improved mitochondrial binding.

Cyclic AMP-dependent protein kinase, D-AKP1, binding to mitochondria and endoplasmic reticulum is also controlled by a 15-residue N-terminal sequence homologous to that of HKI (52). Small hydrophobic side chains on residues

corresponding to residues Ala^4 and Ala^8 in HKI tail are necessary for mitochondrial targeting (52). Moreover, the amount of HKI that binds to the mitochondrion diminishes as residues are removed from the N-terminal sequence (51). Thr^{12} is on the same helical face as Ala^4 and Ala^8, but the mutation of position 12 to isoleucine has less impact on mitochondrial binding properties of HKI; however, the steric bulk at position 12 increases by only single methyl group, whereas positions 4 and 8 have additions of isopropyl groups. Ala4 and Ala8 are not likely critical for lipid interactions, but would define a relatively flat surface on the N-terminal helix. Such a surface would pack favorably against a flat exterior surface of the β-barrel of VDAC. Preliminary coarse grain modeling (Yang Gao and Richard Honzatko, unpublished results) indicates a preferred placement of the surface defined by positions 4 and 8 on the barrel of VDAC. This placement puts the N-terminal domain of HKI over the opening of the anion pore of VDAC, consistent with the channel-blocking properties of HKI.

Although N-terminal residues are essential for HKI association with the mitochondria, one cannot exclude the possibility of other residues elsewhere on HKI playing an essential role (65). Nucleotide (Chapter 2) and Glc-6-P (41) release of mitochondrion-bound HKI implicate the pore of VDAC and the Glc-6-P binding pocket of the N-terminal half of HKI in the VDAC-HKI recognition. If VDAC favors an open conformation for the N-terminal half of HKI, then Glc-6-P could disrupt essential contacts by driving the N-terminal domain to its closed conformation. The binding of nucleotides to VDAC could alter the conformation of the pore, disrupting the same VDAC-HKI interactions. Finally, the N-terminal hydrophobic helix of HKI

continues beyond residue 15 and becomes highly charged with acid and basic side chains. Some of these charged residues are in position to interact with VDAC. Given the current work establishes a method of quantifying the effects of a mutation on mitochondrion binding affinity, one can systematically mutate residues suggested by a HKI-VDAC model to locate additional residues on HKI critical to mitochondrion-binding.

References

1. Katzen, H M; Schimke, R T. (1965) *Proc. Natl. Acad. Sci. U S A* **54**, 1218-25

2. Lowry, O H; Passonneau, J V. (1964) *J. Biol. Chem.* **239**, 31-42

3. Schwab, D A; Wilson, J E. (1989) *Proc. Natl. Acad. Sci. U S A* **86**, 2563-7

4. Wilson, J E. (1995) *Rev. Physiol. Biochem. Pharmacol.* **126**, 65-198

5. Wilson, J E. (2003) *J. Exp. Biol.* **206**, 2049-57

6. Crane, R K; Sols, A. (1954) *J. Biol. Chem.* **210**, 597-606

7. Ureta, T. (1975) in *Isozymes III* (Markert, C L, ed) pp 575-601, Academic Press Inc., New York, NY.

8. Fromm, H J. (1981) in *The Regulation of Carbohydrate Formation and Utilization in Mammals* (Veneziale, C M, ed) pp 45-68, University Park Press, Baltimore, MD.

9. Rose, I A; Warms, J V; O'Connell. (1964) *Biochem. Biophys. Res. Commun.* **15**, 33-7

10. Tsai, H J; Wilson, J E. (1995) *Arch. Biochem. Biophys.* **316**, 206-14

11. Aleshin, A E; Zeng, C; Bartunik, H D; Fromm, H J; Honzatko, R B. (1998) *J. Mol. Biol.* **282**, 345-57

12. Ellison, W R; Lueck, J D; Fromm, H J. (1975) *J. Biol. Chem.* **250**, 1864-71

13. Ardehali, H; Yano, Y; Printz, R L; Koch, S; Whitesell, R R; May, J M; Granner, D K. (1996) *J. Biol. Chem.* **271**, 1849-52

14. White, T K; Wilson, J E. (1989) *Arch. Biochem. Biophys.* **274**, 375-93

15. Arora, K K; Filburn, C R; Pedersen, P L. (1993) *J. Biol. Chem.* **266**, 18259-66

16. Rose, I A; Warms, J V. (1967) *J. Biol. Chem.* 242, 1635-45

17. Lindén, M; Gellerfors, P; Nelson, B D. (1982) *FEBS Lett.* **141**, 189-92

18. Pastorino, J G; Shulga, N; Hoek, J B. (2002) *J. Biol. Chem.* **277**, 7610-8

19. Majewski, N; Nogueira, V; Bhaskar, P; Coy, P E; Skeen, J E; Gottlob, K; Chandel, N S; Thompson, C B; Robey, R B; Hay, N. (2004) *Mol. Cell* **16**, 819-30

20. Majewski, N; Nogueira, V; Robey, R B; Hay, N. (2004) *Mol. Cell. Biol.* **24**, 730-40

21. Narita, M, Shimzu, S; Ito, T; Chittenden, T; Lutz, R; Matsuda, H; Tsujimoto, Y (1998) *Proc. Natl. Acad. Sci. U S A*, Vol. **95**, 14681–6

22. Shimizu, S; Narita, M; Tsujimoto, Y. (2000) *Nature* **399**, 483-7

23. Shimizu, S; Matsuoka, Y; Shinohara, Y; Yoneda, Y; Tsujimoto, Y. (2001) *J. Cell Biol.* **152**, 237-250

24. Shimizu, S; Ide, T; Yanagida, T; Tsujimoto, Y. (2000) *J. Biol. Chem.* **275**, 12321-12325

25. Azoulay-Zohar, H; Israelson, A; Abu-Hamad, S; Shoshan-Barmatz, V. (2004) *Biochem. J.* **377**, 347-55

26. Fiek, C; Benz, R; Roos, N; Brdiczka, D. (1982) *Biochim. Biophys. Acta.* **688**,

429-40

27. Beutner, G; Rück, A; Riede, B; Brdiczka, D. (1997) *Biochem. Soc. Trans.* **25**, 151-7

28. Vyssokikh, M Y; Brdiczka, D. (2003) *Acta. Biochim. Pol.* **50**, 389-404

29. Vyssokikh, M Y; Goncharova, N Y; Zhuravlyova, A V; Zorova, L D; Kirichenko, W; Krasnikov, B F; Kuzminova, A E; Melikov, K C; Melik-Nubarov, N S; Samsonov, A V; Belousov, W; Prischepova, A E; Zorov, D B. (1999) *Biochemistry (Moscow)* **64**, 390-8

30. Machida, K; Ohta, Y; Osada, H. (2006) *J. Biol. Chem.* **281**, 14314-20

31. Zoratti, M; Szabò, I. (1995) *Biochim. Biophys. Acta.* **1241**, 139-76

32. Crompton, M; Virji, S; Doyle, V; Johnson, N; Ward, J M. (1999) *Biochem. Soc. Symp.* **66**, 167-79

33. Zamzami, N and Kroemer, G. (2003) *Curr. Biol.* **13**, 71-3

34. Lemasters, J J; Qian, T; Bradham, C A; Brenner, D A; Cascio, W E; Trost, L C; Nishimura, Y; Nieminen, A L; Herman, B. (1999) *J. Bioenerg. Biomembr.* **31**, 305-19

35. Zaid, H; Abu-Hamad, S; Israelson, A; Nathan, I; Shoshan-Barmatz, V. (2005) *Cell Death Differ.* **12**, 751-60

36. Abu-Hamad, S; Sivan, S; Shoshan-Barmatz, V. (2006) *Proc. Natl. Acad. Sci. U S A* **103**, 5787-92

37. Robey, R B; Hay, N. (2005) *Cell Cycle* **4**, 654-8

38. Abu-Hamad, S; Arbel, N; Calo, D; Arzoine, L; Israelson, A; Keinan, N; Ben-Romano, R; Friedman, O; Shoshan-Barmatz, V. (2009) *J. Cell Sci.* **122**, 1906-16

39. Arzoine, L; Zilberberg, N; Ben-Romano, R; Shoshan-Barmatz, V. (2009) *J. Biol. Chem.* **284**, 3946-55

40. Shoshan-Barmatz, V; Zakar, M; Rosenthal, K; Abu-Hamad, S. (2009) *Biochim. Biophys. Acta.* **1787**, 421-30

41. Skaff, D A; Kim, C S; Tsai, H J; Honzatko, R B; Fromm, H J. (2005) *J. Biol. Chem.* **280**, 38403-9

42. Felgner, P L and Wilson, J E. (1976) *Biochem. Biophys. Res. Commun.* **68**, 592-7

43. Polakis, P G and Wilson, J E. (1982) *Biochem. Biophys. Res. Commun.* **107**, 937-43

44. Kurokawa, M, Tokoyama, K; Kaneko, M; Ishibashi, S (1983) *Biochem. Biophys. Res. Comm.* **115**, 1101-7

45. Ceccaroli, P, Fiorani, M; Buffalini, M; Piccoli, G; Biagiarelli, B; Stocchi, V (1995) *Biochem. Mol. Biol. Int.* **37**, 665-74

46. Xie, G C; Wilson, J E. (1988) *Arch. Biochem. Biophys.* **267**, 803-10

47. Pittler, S J, Kozak, L P and Wilson, J E. (1985) *Biochim. Biophys. Acta.* **843**, 186-92

48. Ehsani-Zonouz, A, Golestani, A and Nemat-Gorgani, M. (2001) *Mol. Cell. Biochem.* **223**, 81-7

49. Finney, K G, Messer, J L; DeWitt, D L; Wilson, J E (1984) *J. Biol. Chem.* **259**, 8232-7

50. Smith, A D and Wilson, J E. (1991) *Arch. Biochem. Biophys.* **287**, 359-66

51. Gelb, B D; Adams, V; Jones, S N; Griffin, L D; MacGregor, G R; McCabe, E R

(1992) *Proc. Natl. Acad. Sci. U S A* **89**, 202-6

52. Ma, Y and Taylor, S. (2002) *J. Biol. Chem.* **277**, 27328-36

53. Bradford, M M. (1976) *Anal. Biochem.* **72**, 248-254

54. Graham, J M. (1993) *Methods. Mol. Biol.* **19**, 29-40

55. Wojtczak, L; Zaluska, H; Wroniszewska, A; Wojtczak, A B. (1972) *Acta. Biochim. Pol.* **19**, 227-34

56. Rice, J E; Lindsay, J G. (1997) in *Subcellular Fractionation, A Practical Approach* (Graham, J.M.; Rickwood, D. , ed) pp 107-42, Oxford University Press, New York, NY.

57. Leatherbarrow, R J. (2001) *GraFit*, Version 5, Erithacus Software Ltd., Horley, UK

58. Mulichak, A M; Wilson, J E; Padmanabhan, K; Garavito, R M. (1998) *Nat Struct Biol*. **5**, 555-560.

59. Myers, E W; Miller, W. (1988) *Comput. Appl. Biosci.* **4**, 11-7.

60. Aleshin, A E; Fromm, H J; Honzatko, R B. (1998) *FEBS Lett.* **434**, 42-6.

61. Estabrook, R W and Holowinsky A. (1961) *J. Biophys. Biochem. Cytol.* **9**, 19-28.

62. Charbaut, E, Redeker, V; Rossier, J; Sobel, A (2002) *FEBS Lett.* **529**, 341-5

63. Ma, H, Bloom, L M; Dakin, S E; Walsh, C T; Botstein, D (1989) *Proteins* **5**, 218-23

64. Bianchi, M, Serafini, G; Bartolucci, E; Giammarini, C; Magnani, M (1998) *Mol. Cell. Biochem.* **189**, 185-93

65. Sui, D and Wilson, J E. (1997) *Arch. Biochem. Biophys.* **345**, 111-25

CHAPTER 4: TRINITROPHENYL NUCLEOTIDE ANALOGS BINDING TO WILD-TYPE AND MUTANT HUMAN BRAIN HEXOKINASES[1]

A paper to be submitted to the Journal of Biological Chemistry

Nimer Mehyar[2] and Richard B. Honzatko[2,3]

Abstract

Fluorescent nucleotide analogue 2′,3′-*O*-(2,4,6-trinitrophenyl) adenosine 5′-diphosphate (TNP-ADP) binds with high affinity to the active site of HKI. Nucleotides displace TNP-ADP from HKI with different efficiencies. Adenosine 5′-triphosphate (ATP) is the most potent displacement nucleotide. Magnesium divalent ion (Mg^{2+}) has no effect on TNP-ADP binding to HKI. Glucose affects TNP-ADP binding to HKI, and also affects it displacement by glucose 6 phosphate (Glc-6-P). TNP-ADP binding to HKI under kinetic assay conditions is weaker that under fluorescence assay conditions. Results here are consistent two conformations of HKI in slow equilibrium. One conformation binds TNP nucleotides with high affinity, but under conditions of assay HKI adopts a conformation that binds TNP nucleotides with less affinity.

Introduction

Hexokinase (ATP: D-hexose-6-phosphotransferase, EC 2.7.1.1) catalyzes first step of glycolysis. Hexokinases catalyze the use of ATP to phosphorylate glucose at

[1]This research was supported in part by National Institute of Health Research Grant NS 10546

[3]To whom correspondence should be addressed.

its 6-hydroxyl position (1). Mammals have four isoenzymes: I, II, III, and IV (2). Although hexokinases (I-III) have similar molecular weights (~100 kDa) and share 70% sequence identity (3) they have distinct kinetic properties (4). Brain hexokinase (HKI) is the major isoenzyme in brain tissue and red blood cell (5). The primary physiological inhibitor of the Type-I enzyme is glucose 6-phosphate (Glc-6-P) (6). Under normal physiological conditions, inorganic orthophosphate (P_i) is capable of relieving inhibition by Glc-6-P (4). At high concentrations, P_i can bind to the active site and inhibit HKI (7). Hexokinase II (HKII) is functionally similar to HKI; however, P_i does not relieve Glc-6-P inhibition of the Type-II (3) or Type-III (8) isoenzymes. Hexokinases have evolved by the duplication and fusion of a primodial hexokinase gene similar to that of yeast hexokinase (9). The Glc-6-P binding site has evolved putatively from a primordial catalytic site (3). Both halves of HKII support catalysis and are each sensitive to inhibition by Glc-6-P (10), whereas only the C-terminal half of HKI supports activity (11). Glc-6-P binds to either half and inhibits activity (12-13). P_i allosterically relieves Glc-6-P inhibition by binding with high affinity to the N-terminal half of HKI (14-15).

HKI and HKII associate with the outer mitochondrial membrane in brain tissue (16). This interaction requires fifteen, largely hydrophobic amino acid residues at its N-terminus (17). HKI association with outer mitochondrial membrane allows preferential access to newly formed mitochondrial ATP (16). HKI likely interacts with the voltage-dependent anion channel (VDAC) of the outer mitochondrial membrane (18-19). HKI binding to the mitochondrion prevents the opening of the permeability transition pore (PTP) (20). Opening of the PTP results in loss of

membrane potential, organelle swelling, cytosolic acidification, and release of cytochrome c (20-21). Cytochrome c that escapes the mitochondrion activates the caspase family of proteases, which ultimately results in apoptosis (22-24). Mitochondrion-associated hexokinase II clearly antagonizes the action of pro-apoptotic factors such as Bax (25-27). A number of small and physiological important ligands are capable of dissociating HKI from the mitochondrial outer membrane. Skaff *et al.* (28) demonstrated the significance of Glc-6-P binding to the N-terminal half of HKI in promoting the release of the mitochondrion-associated enzyme. The Glc-6-P release phenomenon adheres to a simple equilibrium model. ATP-induced release of HKI from mitochondria (16,29-31) is linked to nucleotide binding to VDAC (Chapter 2, this thesis).

Glucose 6 phosphate inhibition of HKI is explained by two models. Glc-6-P competes with ATP for the active site of HKI (32-36) or alternatively, Glc-6-P inhibits HKI by binding to the N-half of the enzyme (37-41). The three dimensional structure of human HKI revealed two almost identical binding sites for Glc-6-P at the C- and N-terminal halves (15,42-44). Mutational analysis revealed that both sites bind Glc-6-P with high affinity and each site can inhibit HKI (13). To date, no experiment has clearly ruled out either model for Glc-6-P inhibition.

Human HKI has up to three adenine nucleotide binding sites: the active site at the C-terminal half (11), the P_i binding site at the N-terminal half at which the nucleotide may bind through its terminal phosphoryl group (42), and the nucleotide pocket of unknown function near the N-terminal membrane targeting element identified by x-ray crystallography (42,45). Since there is no three dimensional

structure of HKI with ATP in the active site, homology with yeast hexokinase and other nucleotide binding proteins was used to develop a model for ATP binding (46). Several residues at the HKI active site were tested by site directed mutation, some were shown to have a crucial role in stabilizing the transition state (39,47-48); however, none of the mutations eliminated ATP binding completely. Mutations in the vestigial nucleotide binding site at N-half caused significant loss of P_i-induced relief of Glc-6-P inhibition (48). Although $[ATP\text{-}Mg]^{2-}$ is the true substrate for HKI, the enzyme can uses Mg^{2+} complexes of other triphosphate nucleosides, albeit less efficiently (49). ATP^{4-} (50-51) and other pyrimidine nucleotides (52) compete with $[ATP\text{-}Mg]^{2-}$ for the active site of HKI. In addition to binding to the active site, purine nucleotides, particularly ADP, can also inhibit HKI allosterically (4,32,50-54). In contrast to kinetic data, HKI-bound flourescent nucleotide analog tetraiodofluorescein (TIF), a competitive inhibitor versus $[ATP\text{-}Mg]^{2-}$, is competitively displaced by ATP, ADP and Glc-6-P (55). Fluorescent nucleotide analogs proved to be a useful tool to study yeast hexokinase inhibition mechanisms and measure the specificity of different inhibitors toward HKI (56). The purpose of this paper is to use trinitrophenyl nucleotides to measure ligand specificty toward HKI.

Experimental Procedures

Materials—ATP, ADP, AMP, GDP, CDP, 2'-deoxy-ATP, glycerol-3-phosphate, chloramphenicol, deoxyribonuclease (DNase I), bovine serum albumin (BSA), leupeptin, protease cocktail inhibitor and phenylmethylsulfonyl fluoride (PMSF) came from Sigma. Kanamycin sulfate was purchased from Invitrogen. TNP-ATP,

TNP-ADP and TNP-AMP came from Invitrogen. TNP-CTP came from Jena Biosciences. DEAE HPLC resin was a product of Tosohaas. Nickel-nitrilotriacetic acid-agarose (NiNTA) resin and Rosetta (DE3) competent cells were from Novagen. Glucose-6-phosphate dehydrogenase was obtained from Roche Molecular Biochemicals. Isopropyl-1-thio-β-D-galactopyranoside (IPTG) came from Anatrace.

Construction of Wild-type Hexokinase and Mutant Plasmids—Human brain hexokinase (HKI) had been cloned into pET-24b with a 10-residue histidine tag at its C-terminus as reported in a previous study (28). Full length HKI (57), mHKI (46), triple mutant HKI: E280 A, R283A, and G284Y (42), α + 2 HKI and N384R HKI (28) were all available from previous studies. Hexokinase mutants were created through PCR modification with oligonucleotide primers synthesized at the Iowa State University DNA Sequencing and Synthesis Facility.

Truncated HKI was created by introducing a NdeI cut site before Thr^{12} in the pET24b-HKI-10-histidine tag using the following forward primer (and its reverse compliment):
5’CTCCTGGCCTATTACTTCACGGAGCATATGGATGACCAGGTCAA AAAGATTGA-3’. Mutated plasmid was digested with NdeI and then ligated to produce pET24b-truncated HKI with a 10-histidine tag. This plasmid encodes a truncated tail form of HKI starting from residue 12. G747 and S788M were prepared using the following forward primers and their reverse complements: 5'-GGTATGAGAAGATGAT CAGTCTGATGTACCTGGGTGAAATCGTC-3' for G747L and 5'GAGACCAAGTTT CTCATGCAGATC GAGAGTGACCGA-3' for S788M.

Expression and Purification of Wild-Type HKI and N-domain HKI— Wild-type or mutant HKI plasmids were transformed into *E.coli* strain Rosetta (DE3). Expression and purification HKI enzymes are discussed in detail by Skaff *et al* (28). Determination of protein concentrations employed the Bradford method with bovine serum albumin as a standard (58).

The HKI Activity Assay— Hexokinase activity was measured using the glucose 6-phosphate dehydrogenase (G6PDH)-coupled spectrophotometric assay. Assay solutions have 3 mM $MgCl_2$, 3 mM DTT, 6 mM ATP:Mg^{2+}, 1.6 mM Glucose, 0.3 mM NADP and 10 μg/mL G6PDH in 50 mM Tris-HCl, pH 8.0. NADPH production velocity was monitored at 340 nm wavelength. Reactiosn were initiated by the addition of enzyme. Linear reaction progress curves were monitored for 3 minutes, the slopes of which were used to calculate initial rates. When the amount of HKI was doubled, reaction rate was also doubled without affecting the linearity of the reaction. Initial rate data were analyzed using GraFit (59). TNP-nucleotide inhibition was measured using the same assay conditions.

HKI fluorescence experiments— Prior to the experiment, purified HKI and hVDAC-1 were dialyzed twice against 50 mM Tris-HCl, pH 7.5, and 2 mM glucose. SLM Amico 8000 fluorometer was used to measure fluorescence in a 1-cm^2 quartz cuvette. Fluorometer entrance and exit slit widths were set at 4 nm. Experiments were done at room temperature. TNP-ADP was exited at 409 nm and emission was scanned between wavelengths 450 to 600 nm. Fluorescence titrations were performed by successive addition of small volumes of TNP-ADP to 1 mL of 2.5 μM HKI, and then the emission spectrum was scanned three times. Total added titrant

volume did not exceed 5% of the total volume. Displacement experiments were performed by accumulative addition of nucleotide to 1 mL of 2 .5 μM HKI and 1μM TNP-ADP solution. Total volume of added nucleotide did not exceed 5% of the total volume. Observed fluorescence was corrected for titrant dilution. Fallar (60) approach to Analysis of fluorescence data followed the approach of Fallar (60), using a single-site binding model described in Chapter 2 of this thesis and GraFit for nonlinear least squares fitting.

RESULTS

TNP-nucleotides binding to Wild-type and mutant HKI and displacement by ATP and other nucleotides— Binding of ATP and TNP-ADP to HKI is mutually exclusive. ATP displaces HKI-bound TNP-ADP. Observed fluorescence as a result of TNP-ADP binding to HKI is the summation of fluorescence from free ligand, bound ligand, and protein (HKI), that is $F_{obs}=F_{free}+F_{bound}+F_{protein}$. Parameters K_A , K_L,γ and $F_{protein}$ were used for fitting. These parameters are defined in Chapter 2 of this thesis. Analog TNP-ADP binds with high affinity to wild type HKI and Hisis-tag HKI equivalently (Table 4.1) and also ATP displaces TNP-ADP efficiently from constructs (Table 4.1). ADP, AMP, 2'-deoxy-ATP, and GDP, displace TNP-ADP from wild type HKI (Table 4.2), but CDP and glycerol-3-phosphate do not. Trinitrophenyl nucleotides (TNP-ATP, TNP-ADP, TNP-AMP and TNP-CTP) bind to wild-type HKI similarly, and all are displaced by ATP (Table 4.3).

TNP-nucleotides inhibit wild type hexokinase I— Wild-type HKI (k_{cat}=73±4 s^{-1}, K_m^{Glc}=77±6 μM, and K_m^{ATP}=1.1±0.1 μM) was used in these experiments. When

ATP was replaced by TNP-ADP under assay conditions where free Mg^{2+} levels are 2 mM, no product evolution was observed even for prolonged times (data not shown). All TNP-nucleotides compete with ATP causing enzyme inhibition ($K_i^{TNP\text{-}ATP}$=4.5±0.4, $K_i^{TNP\text{-}ADP}$=4.9±0.5, $K_i^{TNP\text{-}AMP}$=4.7±0.6, $K_i^{TNP\text{-}CTP}$=2.6±0.2).

Glc-6-P displacement of TNP-nucleotides bound to wild-type HKI— Neither Glc-6-P nor glucose affect TNP-ADP fluorescence in the absence of HKI (data not shown). Glc-6-P displaces TNP-ADP bound to wild-type HKI (Fig. 4.1). In the presence of glucose, Glc-6-P displaces TNP-ADP more effectively (no glucose, K_A=480±50 µM *versus* 2 mM glucose, K_A=6.3±0.9 µM). Glucose has little effect on TNP-ADP binding affinity (no glucose, K_L=2.1±0.2 µM *versus* 2 mM glucose K_L=0.78±0.8 µM) (Fig. 4.2) or ATP displacement of TNP-ADP (no glucose, K_A=170±20 µM, *versus* 2 mM glucose

Table 4.1. TNP-ADP and ATP binding to HKI constructs in the presence of 50 μM Glc-6-P.

HKI Construct	K_L (μM)	K_A (mM)	γ	$F_{protein}$
Wild-type[a]	3.6 (5)	0.49 (6)	12.3 (4)	0.032 (2)
Wild-type	4.9 (8)	1.0 (1)	27 (1)	0.022 (4)
Triple	2.7 (4)	1.2 (1)	13.5 (4)	0.019 (2)
Truncated[a]	3.6 (4)	1.7 (2)	13.1 (4)	0.021 (2)
α+2[a]	1.4 (1)	1.2 (1)	8.1 (2)	0.010 (2)
N384R[a]	1.4 (3)	1.5 (3)	8.4 (3)	0.011 (3)
mHKI[a]	4.9 (7)	0.9 (1)	28 (1)	0.027 (4)

Parameters are from a single binding site model. K_L, K_A, γ and $F_{protein}$ are respectively the dissociation constant for TNP-nucleotide (TNP-ADP), the dissociation constant for displacing ligand (ATP), fluorescence enhancement factor attributed to the bound *versus* free state of the TNP-nucleotide, and the intrinsic fluorescence from the protein. Fluorescence was measured at varying total concentrations of TNP-nucleotides and ATP in 2 mM glucose, 50 μM Glc-6-P and 50 mM Tris-HCl, pH 7.5. Standard deviations in the last significant digits are given in parentheses.

[a]C-terminal His-tagged construct.

Table 4.2. TNP-nucleotide binding to wild-type C-terminal His-tagged HKI.

TNP-nucleotide	K_L (μM)	K_A (μM)	γ	$F_{protein}$
TNP-ATP	1.2 (2)	130 (20)	11.7 (3)	0.003 (1)
TNP-ADP	0.78 (9)	190 (20)	14.8 (3)	0.017 (2)
TNP-AMP	0.5 (1)	130 (30)	14.3 (5)	0.012 (2)
TNP-CTP	0.75 (3)	110 (10)	13.9 (4)	0.032 (2)

Parameters are from a single binding site model. K_L, K_A, γ and $F_{protein}$ are as defined in Table 4.1 Fluorescence was measured at varying total concentrations of TNP-nucleotides and ATP in 2 mM glucose and 50 mM Tris-HCl, pH 7.5. Enzyme concentration is 2.5 μM wild-type C-terminal His-tagged HKI. Standard deviations in the last significant digits are given in parentheses.

Table 4.3. Displacement of TNP-ADP from wild-type HKI by different nucleotides.

	Nucleotide				
Parameter	ATP	ADP	AMP	GDP	GMP
K_L (μM)	0.78 (9)	0.73 (7)	0.8 (1)	0.67 (8)	0.65 (8)
K_A (μM)	190 (20)	260 (20)	810 (80)	5000 (700)	7000 (1000)
γ	11.7 (3)	15.0 (2)	14.8 (3)	15.1 (3)	15.1 (3)
$F_{protein}$	0.003 (1)	0.015 (2)	0.018 (2)	0.014 (2)	0.014 (2)

Parameters are from a single binding site model. K_L and K_A, are constants for the dissociation of TNP-ADP and nucleotide indicated in the column heading from wild-type HKI. $F_{protein}$ and γ are defined in Table 4.1. Fluorescence was measured at varying total concentrations of TNP-nucleotides and ATP in 2 mM glucose and 50 mM Tris-HCl, pH 7.5. Enzyme concentration is 2.5 μM C-terminal His-tagged HKI. Standard deviations in the last significant digits are given in parentheses.

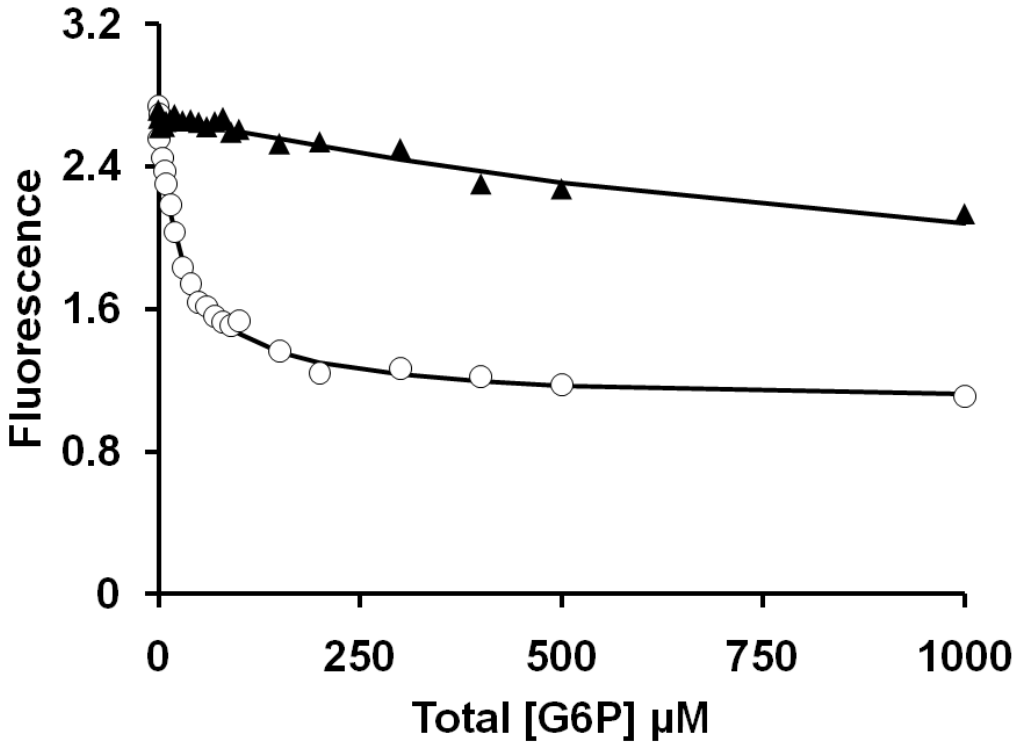

Fig. 4.1. Effect of glucose on TNP-ADP displacement by Glc-6-P. Plots are fluorescence at varying total concentrations of Glc-6-P added to 2.5 µM wild-type C-terminal His-tagged HKI and 5 µM TNP-ATP, 50 mM Tris, pH 7.5, plus 2 mM glucose (○) or 0 mM glucose (▲). Solid lines represent fitted curves using parameters K_A, K_L, γ and $F_{protein}$ as defined in Table 4.1. Parameters values are in results section.

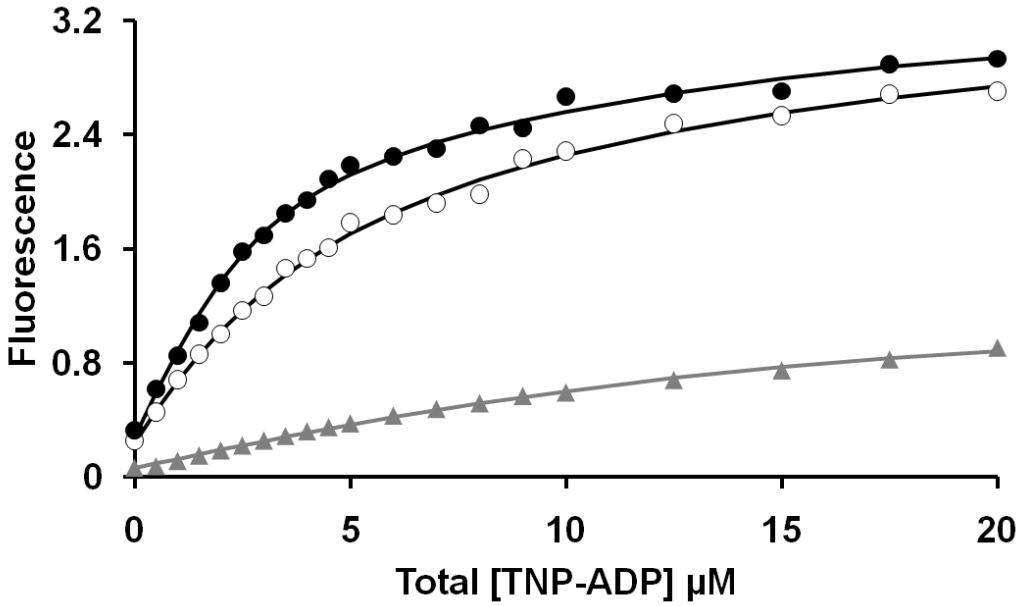

Fig. 4.2. Effect of glucose on TNP-ADP binding. Plots are fluorescence at varying total concentrations of TNP-ADP in 50 mM Tris-HCl, pH 7.5, with no protein (▲), wild-type C-terminal His-tagged HKI 2.5 µM plus 2 mM glucose (●) or plus 0 mM glucose (○). The solid lines represent fitted curves using parameters K_L, γ and $F_{protein}$. Parameters values are listed in the results section.

K_A=190±20 µM). 50 µM Glc-6-P weakened TNP-ADP binding to wild-type HKI (50 µM Glc-6-P, K_L=3.6±0.5 µM versus no Glc-6-P, K_L=0.8±0.1) and weakened the binding of other nucleotides (no Glc-6-P, see Table 4.3 *versus* 50 mM Glc-6-P, K_A^{ATP}=500±60 µM, K_A^{ADP}=1800±300 µM, K_A^{AMP}=6000±1000 µM, $K_A^{deoxy\ ATP}$=800±100 µM, K_A^{GDP}=5000±2000 µM) (Fig. 4.3). Glycerol-3-phosphate and CDP do not displace TNP-ADP.

pH and Mg2+ effects on TNP-ADP binding and displacement— Neither pH nor $MgCl_2$ affect TNP-ADP fluorescence in the absence of HKI (data not shown). When 2mM glucose is present, binding affinity of TNP-ADP to wild type HKI slightly increased as the pH increased to 8.0 (Fig. 4.4) (pH 8, K_L=0.27±0.07 µM *versus* pH 7.5 K_L=0.8±0.1). Raising the pH to 8.0 did not affect TNP-ADP displacement by ATP (K_A=140±30 µM) or Glc-6-P (K_A=6.2±0.5 µM). In the absence of glucose, adding Mg^{2+} did not affect TNP-ADP binding to wild-type HKI (K_L=2.5±0.2 µM, γ=11.5±0.2, $F_{protein}$=0.013±0.001) (Fig. 4.5).

TNP-ADP binding to hexokinase I mutants G747L and S788M and displacement by ATP and Glc-6-P— Catalytic activity of mutants G747L and S788M decreased significantly compared to the wild-type HKI; however, binding affinities for the substrates were not affected (Table 4.4). TNP-ADP binding is not affected by S788M ($K_L^{TNP\text{-}ADP}$=1.6±0.2 µM, γ=9.7±0.2, $F_{protein}$=0.032±0.001). Mutant G747L binds to TNP-ADP with significantly less affinity ($K_L^{TNP\text{-}ADP}$=22±7 µM, γ=19±3, $F_{protein}$=0.030±0.003) (Fig. 4.6). Glc-6-P concentrations required to displace TNP-

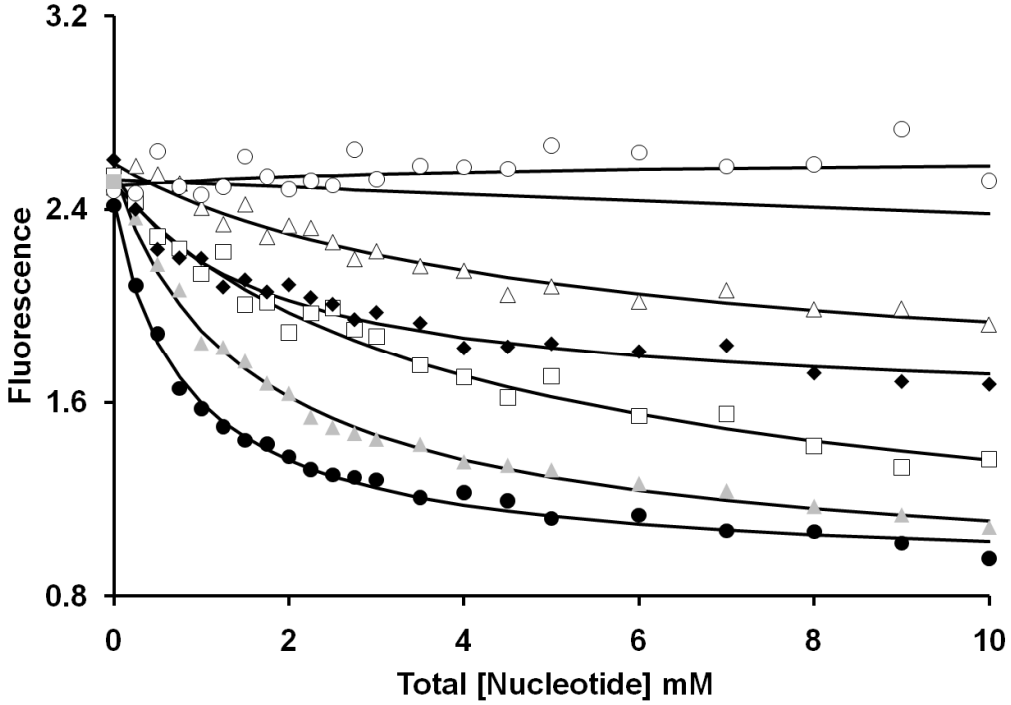

Fig. 4.3. Effect of Glc-6-P on nucleotide displacement of TNP-ADP. Plots are the fluorescence at varying total concentrations of different nucleotides: ATP (●), ADP (□), AMP (♦), 2'-deoxy-ATP (▲), GDP (Δ), CDP (■), and glycerol-3-phosphate (○) added to 2.5 μM wild-type C-terminal His-tagged HKI and 5 μM TNP-ATP, 2mM glucose, 50 mM Glc-6-P and 50 mM Tris buffer, pH 7.5. The solid lines represent fitted curves using parameters K_A, K_L, γ and $F_{protein}$ Parameters values are listed in results.

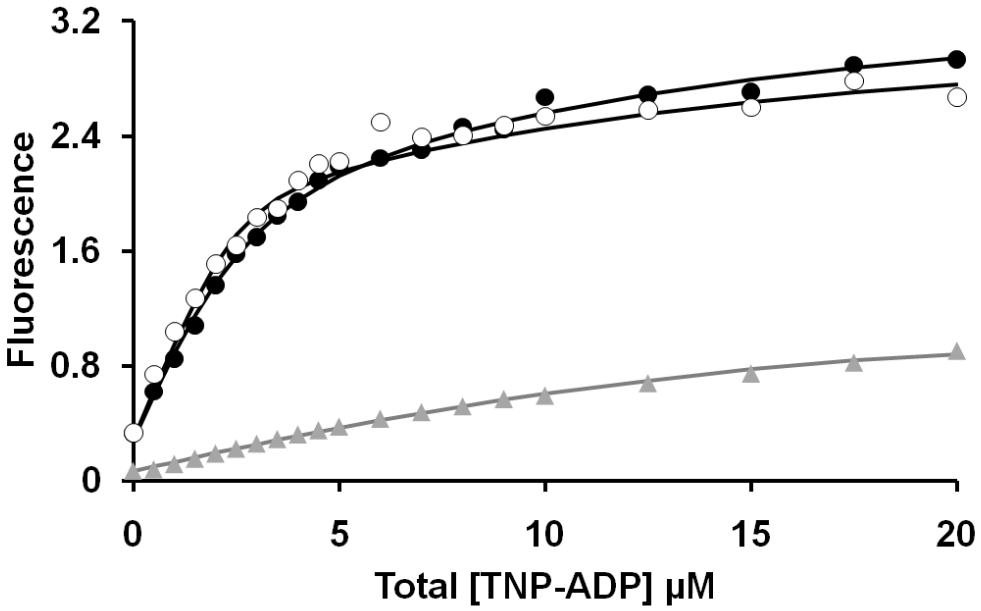

Fig. 4.4. Effect of pH on TNP-ADP binding to wild-type HKI. Plots represent the fluorescence at varying total concentrations of TNP-ADP in 50 mM Tris-HCl with no protein (▲), wild-type C-terminal His-tagged HKI 2.5 µM, pH 7.5 (●) or pH 8.0 (○). The solid lines represent fitted curves using parameter K_L,γ and $F_{protein}$. Parameter values are listed in the results section.

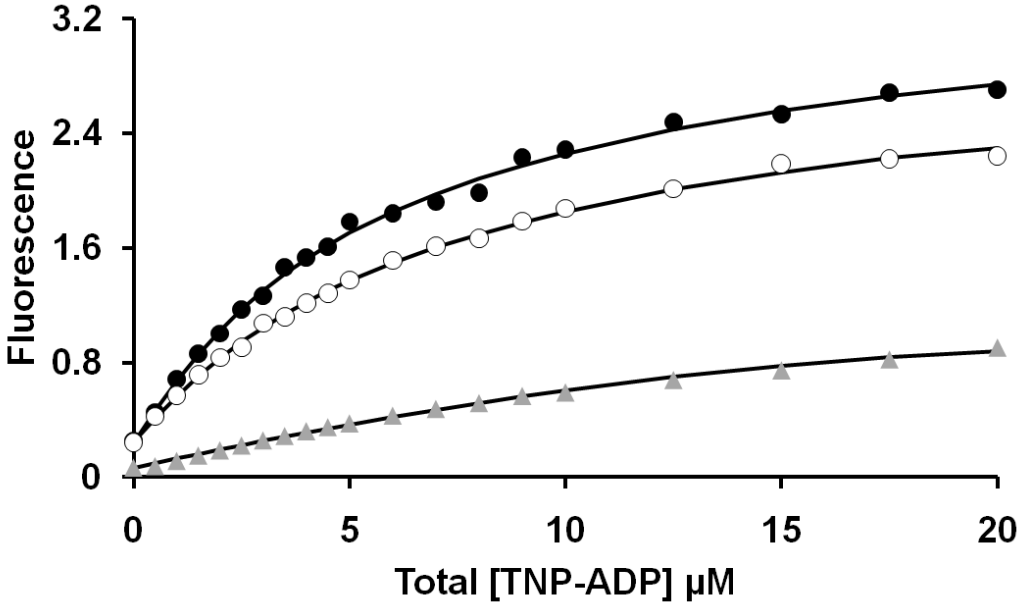

Fig. 4.5. Mg^{2+} effect on TNP-ADP binding to wild-type HKI. Plots represent the fluorescence at varying total concentrations of TNP-ADP in 50 mM Tris-HCl, pH 7.5, with no protein (▲), wild-type C-terminal His-tagged HKI 2.5 µM plus 2 mM $MgCl_2$ (○) or 0 mM $MgCl_2$ (●). Solid lines represent fitted curves using parameter K_L ,γ and $F_{protein}$. Parameter values are listed in results section.

Table 4.4. Kinetic parameters for wild-type and mutant HKI constructs.

HKI mutant	k_{cat} (s^{-1})	K_m^{ATP} (mM)	K_m^{Glc} (μM)
G747L	2.7 (4)	1.1 (1)	200 (10)
S788M	17 (3)	3.8 (6)	110 (10)

Assays are described in the experimental section. Determination of k_{cat} employed mutant C-terminal His-tagged HKI and concentrations of Glc and ATP of 1.6 mM and 9 mM. Determination of K_m^{ATP} employed a glucose concentration of 1.6 μM and concentrations of ATP of 0.3–7.5 mM. Determination of K_m^{Glc} employed an ATP concentration of 9 mM and concentrations of glucose of 10–600 μM.

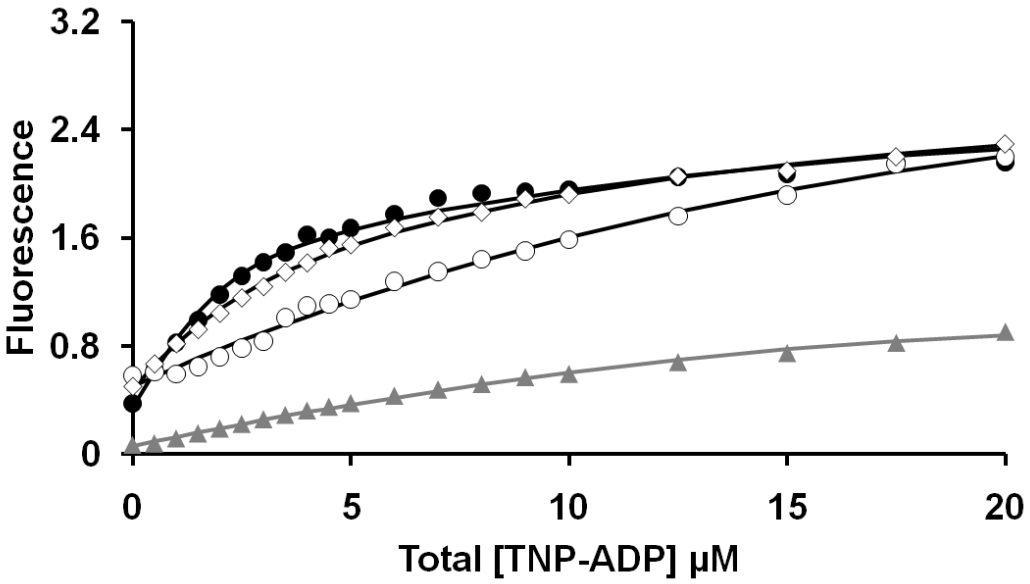

Fig. 4.6. Titration of wild type HKI and mutants G747L and S788M with TNP-ADP. Plots represent the fluorescence at varying total concentrations of TNP-ADP in 2 mM glucose and 50 mM Tris-HCl pH 7.5, with no protein (▲), wild-type HKI 2.0 µM (●), G747L HKI 2.0 µM (○),and S788M HKI 2.0 µM (◊). All HKI constructs have C-terminal His-tags. The solid lines represent fitted curves using parameters K_L, γ and $F_{protein}$ Parameters values are listed in results.

Table 4.5. TNP-ADP and ATP binding to mutant HKI.

HKI mutant	$K_L^{TNP\text{-}ADP}$ (μM)	K_A^{ATP} (μM)	$K_A^{Glc\text{-}6\text{-}P}$ (μM)	γ	$F_{protein}$
G747L	22 (7)	300 (200)	130 (70)	19 (3)	0.030 (3)
S788M	1.6 (2)	1400 (100)	5.1 (7)	9.7 (2)	0.032 (1)

Parameters are from a single binding site model. K_d, K_A^{ATP}, γ and $F_{scatter}$ are constants for the dissociation in μM of TNP-nucleotides. Fluorescence was measured at varying total concentrations of TNP-nucleotides and ATP in 2 mM glucose and 50 mM Tris-HCl pH 7.5. Enzyme concentration is 2.5 μM mutant C-terminal His-tagged HKI. Standard deviations in the last significant digits are given in parentheses.

ATP increased significantly for mutant G747L and was not affected for mutant S788M (Table 4.5). TNP-ADP displacement by ATP is twofold weaker for mutant G747L and ten-fold weaker for mutant S788M (Table 4.5).

Disscusion

Trinitrophenyl nucleotides bind to wild-type human HKI as previously reported (Chapter 2, this thesis). The TNP-ADP binding site on HKI does not involve the His tag or residues at the N-terminus involved in the binding of HKI to mitochondria. Tight binding of TNP-ADP to N384R HKI indicates that the N-domain ADP site revealed by crystallography (42) is not a binding site for the TNP-nucleotide. Triple mutant HKI (E280A, R283A, and G284Y) does not dimerize even at high concentrations of protein (42). TNP-ADP binding to triple mutant HKI eliminates the possibility a binding site stabilized by dimerization. Mini-HKI, an active construct consisting of the C-terminal half and transition helix (46), binds to the probe as does wild-type HKI. These data are consistent with a binding site on the C-terminal half of HKI. This agrees with previous reports of weak binding of TNP-ADP to N-domain HKI (Chapter 2, this thesis). Competitive inhibition behavior of TNP-nucleotides with respect to ATP identifies the HKI active site as a potential binding site for TNP-nucleotides (Chapter 2, this thesis). In contrast to yeast hexokinase (56) different TNP-nucleotides showed no variation in binding affinity or inhibition of wild-type HKI. The involvement of nitrophenyl group in binding TNP-nucleotides to wild-type HKI cannot be disregarded. TIF, a fluorescent molecule

binds specifically to rat HKI (55) and has similar structural and chemical properties as the nitrophenyl group.

A ten-fold difference between K_i and K_L was observed for all TNP-nucleotides. Although the published TIF inhibition of HKI (K_i=25 μM) (61) matches TIF binding affinity to HKI (K_L=15 μM) with a 6- to 7-fold fluorescence enhancement (55), the model used to fit fluorescence data in that study does not correct the observed fluorescence for contributions from free fluorophore and protein (62). Fitting the data from reference (55) with the model used in this study resulted in an enhancement factor (γ=7.5) and a binding affinity (K_L=1.7 μM). The difference between the reported TIF K_i and the TIF K_L is more than ten-fold, and similar to the difference reported here for TNP-ADP K_i and K_L. What is the cause of significant differences in K_i from kinetics and K_L from fluorescence titrations?

Three conditions are different between kinetic and florescence assays: (*i*) pH, (*ii*) presence of Mg^{2+} and (*iii*) length (duration) of the assay. Raising the pH of the fluorescence assay to that of the kinetic assay (pH 8.0) slightly decreases K_L for TNP-ADP and makes the discrepancy more significant. The addition of Mg^{2+} to fluorescence titrations does not affect TNP-ADP binding to wild-type HKI, and similarly, does not affect TNP-ATP binding to yeast hexokinase (56) or TIF binding to rat-brain hexokinase (55). The combination of Mg^{2+} and ATP in the kinetics assay, however, generates $[ATP\text{-}Mg]^{2-}$, which is not present in fluorescence titrations. In comparison to magnesium chelates of other nucleoside triphosphates, $[ATP\text{-}Mg]^{2-}$ is most effective in protecting the C-terminal half of rat-brain hexokinase against tryptic digestion (55,65). In the absence of Mg^{2+}, ATP, UTP, CTP and GTP protect

hexokinase equally (65) and Mg^{2+} alone does not protect hexokinase against tryptic digestion (38). Indeed, $[ATP\text{-}Mg]^{2-}$ is the favored substrate of HKI and could well stabilize HKI in a conformation less favorable for the binding of TNP-ADP. Moreover, fluorescence titrations compared to activity assays expose HKI to TNP-ADP for long times. If the binding of TNP-ADP requires a slow conformational change in HKI that is antagonized by $[ATP\text{-}Mg]^{2-}$, then the tight binding affinity observed in fluorescence titrations may not be observed in kinetics (Fig. 4.7).

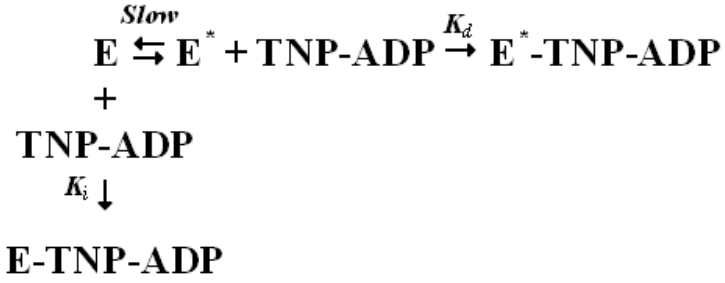

Figure 4.7. Proposed model for TNP-ADP binding to HKI.

Adenosine triphosphate displaced TNP-ADP from wild type most efficiently. Removing 2'-hydroxyl group did not affect ATP binding, however, removing the γ phosphoryl or both γ- and β-phosphoryl groups attenuates ATP binding significantly. Nitrogen bases contribute to nucleotide binding specificity. Purines displace TNP-ADP from wild-type HKI better than pyrimidines. A phosphotriose is unable to compete with TNP-ADP as measure by the lack of displacement by glycerol-3-

phosphate. Nucleotide binding specificity observed in this study matches the inhibition specificity observed in kinetics studies (52). TNP-ADP displacement by ATP is consistent with a model of mutual exclusion. Kinetics investigations indicate ATP^{4-} is a competitive inhibitor with respect to substrate $[ATP\text{-}Mg]^{2-}$ (52). Baijal and Wilson (55) report that ATP, ADP or ATP plus ADP displaced 50-70% of bound TIF from HKI. Due to the partial displacement of TIF and lack of accumulative effect of ATP plus ADP these authors concluded that ADP displaces TIF competitively by binding to the active site. Corrections for fluorescence contributions from high concentrations of HKI (6-12 μM) and free fluorophore were not made in reference (55), and without such corrections dissociation constants are erroneously high and estimates of displacement are erroneously low.

ADP displacement data in the current study does not rule out the possibility of ADP binding to a second binding site; however, binding to such a site does not displace TNP-ADP. This does not agree with kinetic data, which indicate two binding sites for ADP consistent with a model of mixed inhibition (51). The previously proposed model (Fig. 4.7) can also explain the different response to ADP in kinetic assays versus fluorescence assays. In this model, ADP binds effectively only to the active site of E* conformation, on the other hand, ADP can effectively bind to both active and allosteric sites of E conformation.

Glc-6-P displaces TNP-ADP from wild type HKI efficiently in the presence of glucose. Removing glucose significantly decreases Glc-6-P displacement of TNP-ADP. Glc-6-P also displaces TIF from rat brain hexokinase (55). This agrees with previously observed synergistic binding of glucose and Glc-6-P (11,36). Glc-6-P

displacement of TNP-ADP from wild-type HKI can be explained either by direct competition for the active site or by the binding of Glc-6-P to an allosteric site at the N-terminal half of HKI.

The mutation G747L introduces a bulky side chain in the putative ribosyl-binding pocket of ATP. Not surprisingly this mutation increases K_L for TNP-ADP by as much as 100-fold (using K_L for TNP-ADP in the presence of glucose); however, the mutation decreases Glc-6-P affinity (K_A rises 25-fold compared to wild-type HKI), but has little effect on ATP affinity. Gly747 is part of a structural element that may play a central role in the allosteric (N-terminal half) mechanism of Glc-6-P inhibition of HKI. Hence, the displacement of TNP-ADP by Glc-6-P may be due to the binding of Glc-6-P to the N-terminal half, rather than the direct binding of Glc-6-P to the C-terminal half. The absence of a significant effect on the K_A for ATP indicates that ATP can bind (the K_m for ATP also is unaffected by the G747L mutation), but that the binding differs in some way from the catalytically productive mode (k_{cat} is diminished by 98%). The mutation S788M introduces a bulky side chain in the base-binding pocket of ATP. This mutation has little effect on the affinity of TNP-ADP, no effect on Glc-6-P affinity and but decreases ATP affinity (K_A rises 8-fold compared to wild-type HKI). These observations can be reconciled if the base of TNP-ADP does not occupy the base-binding pocket of ATP. Hence, the data here suggest TNP-ADP, and presumably other TNP-nucleotides are not analogs of ATP, but that they still bind at a site that is subject to the action of Glc-6-P as an allosteric inhibitor. A detailed understanding of TNP-ADP binding could provide important insights regarding the mechanism of allosteric Glc-6-P inhibition.

References

1. Katzen, H M. (1967) *Adv. Enzyme. Regul.* **5**, 335-56.

2. Katzen, H M; Schimke, R T. (1965) *Proc. Natl. Acad. Sci. U S A.* **54**, 1218-25.

3. Wilson, J E. (1995) *Rev. Physiol. Biochem. Pharmacol.* **26**, 65-198.

4. Grossbard, L; Schimke, R T;. (1966) *J. Biol. Chem.* **241**, 3546-60.

5. Lowry, O H; Passonneau, J V. (1964) *J. Biol. Chem.* **239**, 31-42.

6. Crane, R K; Sols, A. (1954) *J. Biol. Chem.* **210**, 597-606.

7. Ellison, W R; Lueck, J D; Fromm, H J. (1975) *J. Biol. Chem.* **250**, 1864-71.

8. Magnani, M; Stocchi, V; Serafini, N; Piatti, E; Dachà, M; Fornaini , G. (1983) *Arch. Biochem. Biophys.* **226**, 377-87.

9. Wilson, J E. (2003) J. Exp. Biol. **206**, 2049-57.

10. Ardehali, H; Yano, Y; Printz, R L; Koch, S; Whitesell, R R; May, J M; Granner, D K. (1996) *J. Biol. Chem.* **271**, 1849-52.

11. White, T K; Wilson, J E. (1989) *Arch. Biochem. Biophys.* **274**, 375-93.

12. Fang, T Y; Alechina, O; Aleshin, A E; Fromm, H J; Honzatko, R B. (1998) *J. Biol. Chem.* **273**, 19548-53.

13. Liu, X; Kim, C S; Kurbanov, F T; Honzatko, R B; Fromm, H J. (1999) *J. Biol. Chem.* **274**, 31155-9.

14. Tsai, H J; Wilson, J E. (1995) *Arch. Biochem. Biophys.* **316**, pp. 206-14.

15. Aleshin, A E; Zeng, C; Bartunik, H D; Fromm, H J; Honzatko, R B. (1998) *J. Mol. Biol.* **282**, 345-57.

16. Rose, I A; Warms, J V. (1967) J. Biol. Chem. **242**, 1635-45.

17. Xie, G C; Wilson, J E. (1988) *Arch. Biochem. Biophys.* **267**, 803-10.

18. Lindén, M; Gellerfors, P; Nelson, B D. (1982) *FEBS Lett.* **141**, 189-92.

19. Fiek, C; Benz, R; Roos, N; Brdiczka, D. (1982) *Biochim. Biophys. Acta.* **688**, 429-40.

20. Azoulay-Zohar, H; Israelson, A; Abu-Hamad, S; Shoshan-Barmatz, V. (2004) *Biochem. J.* **377**, 347-55.

21. Machida, K; Ohta, Y; Osada, H. (2006) J. Biol. Chem. **281**, pp. 14314-20.

22. Crompton, M; Virji, S; Doyle, V; Johnson, N; Ward, J M. (1999) *Biochem. Soc. Symp.* **66**, 167-79.

23. Zamzami, N; Kroemer, G. (2003) Curr. Biol. **13**, R71-3.

24. Lemasters, J J; Qian, T; Bradham, C A; Brenner, D A; Cascio, W E; Trost, L C; Nishimura, Y; Nieminen, A L; Herman, B. (1999) *J. Bioenerg. Biomembr.* **31**, 305-19.

25. Pastorino, J G; Shulga, N; Hoek, J B. (2002) *J. Biol. Chem.* **277**, 7610-8.

26. Majewski, N; Nogueira, V; Bhaskar, P; Coy, P E; Skeen, J E; Gottlob, K; Chandel, N S; Thompson, C B; Robey, R B; Hay, N. (2004) *Mol. Cell* **16**, 819-30.

27. Majewski, N; Nogueira, V; Robey, R B; Hay, N. (2004) *Mol. Cell. Biol.* **24**, 730-40.

28. Skaff, D A; Kim, C S; Tsai, H J; Honzatko, R B; Fromm, H J. (2005) *J. Biol. Chem.* **280**, 38403-9.

29. Wilson, J E. (1968) *J. Biol. Chem.* **243**, 3640-7.

30. Hochman, M S; Shimada, Y; Sacktor, B. (1974) *J. Neurochem.* **23**, 861-3.

31. Bustamante, E; Pedersen, P L. (1980) *Biochemistry* **19**, 4972-7.

32. Fromm, H J; ZEWE, V. (1962) *J. Biol. Chem.* **237**, 1661-7.

33. Arora, K K; Filburn, C R; Pedersen, P L. (1993) *J. Biol. Chem.* **266**, 18259-66.

34. Magnani, M; Bianchi, M; Casabianca, A; Stocchi, V; Daniele, A; Altruda, F; Ferrone, M; Silengo, L. (1992) *Biochem. J.* **285**, 193-9.

35. Jarori, G K; Iyer, S B; Kasturi, S R; Kenkare, U W. (1990) *Eur. J. Biochem.* **188**, 9-14.

36. Mehta, A; Jarori, G K; Kenkare, U W. (1988) *J. Biol. Chem.* **263**, 15492-7.

37. White, T K; Wilson, J E. (1987) *Arch. Biochem. Biophys.* **259**, 402-11.

38. White, T K; Wilson, J E. (1990) *Arch. Biochem. Biophys.* **277**, 26-34.

39. Baijal, M; Wilson, J E. (1995) *Arch. Biochem. Biophys.* **321**, 413-20.

40. Hutny, J; Wilson, J E. (2000) *Acta. Biochim. Pol.* **47**, 1045-60.

41. Sebastian, S; Wilson, J E; Mulichak, A; Garavito, R M. (1999) *Arch. Biochem. Biophys.* **362**, 203-10.

42. Aleshin, A E; Kirby, C; Liu, X; Bourenkov, G P; Bartunik, H D; Fromm, H J; Honzatko, R B. (2000) *J. Mol. Biol.* **296**, 1001-15.

43. Aleshin , A E; Fromm, H J; Honzatko, R B. (1998) *FEBS Lett.* **434**, 42-6.

44. Aleshin, A E; Zeng, C; Bourenkov, G P; Bartunik , H D; Fromm, H J; Honzatko, R.B. (1998) *Structure* **6**, 39-50.

45. Rosano, C; Sabini, E; M, Rizzi; Deriu, D; Murshudov, G; Bianchi, M; Serafini, G; M, Magnani; Bolognesi, M. (1999) *Structure* **7**, 1427-37.

46. Zeng, C; Fromm, H J. (1995) *J. Biol. Chem.* **270**, 10509-13.

47. Zeng, C; Aleshin, A E; Hardie, J B; Harrison , R W; Fromm, H J. (1996)

Biochemistry **35**, 13157-64.

48. Zeng, C; Aleshin, A E; Chen, G; Honzatko, R B; Fromm, H J. (1998) *J. Biol. Chem.* **273**, 700-4.

49. Purich, D L; Fromm, H J; Rudolph, F B. (1973) *Adv. Enzymol. Relat. Areas. Mol. Biol.* **39**, 249-326.

50. Purich, D L; Fromm, H J. (1972) *Biochem. J.* **130**, 63-9.

51. Purich, D L; Fromm, H J. (1971) *J. Biol. Chem.* **246**, 3456-63.

52. Ning, J; Purich, D L; Fromm, H J. (1969) *J. Biol. Chem.* **244**, 3840-6.

53. Kosow, D P; Rose, I A. (1970) *J. Biol. Chem*. **245**, 198-204.

54. Copley , M; Fromm, H J. (1967) *Biochemistry* **6**, 3503-9.

55. Baijal, M; Wilson, J E. (1982) *Arch. Biochem. Biophys.* **218**, 513-24.

56.. Arora, K K; Shenbagamurthi, P; Fanciulli, M; Pedersen, P L. (1990) *J. Biol. Chem.* **265**, 5324-8.

57. Liu, F; Dong, Q; Myers, A M; Fromm, H J. (1991) *Biochem. Biophys. Res. Commun.* **177**, 305-11.

58. Bradford, M M. (1976) *Anal. Biochem.* **72**, 248-54.

59. Leatherbarrow, R J. *GraFit Version 5, Erithacus Software Ltd.* Horley, UK 2001.

60. Fallar, L D. (1990) *Biochemistry* **29**, 3179-86.

61. Wilson, J E. (1978) *Biochem. Biophys. Res. Commun.* **82**, 745-9.

62. McClure, W O; Edelman, G M. (1967) *Biochemistry* **6**, 559-66.

63. Solheim, L P; Fromm, H J. (1980) *Biochemistry* **19**, 6074-80.

64. Lewis, B E; Schramm, V L. (2003) *J. Am. Chem. Soc.* **125**, 4672-3.

65. Smith, A D; Wilson, J E. (1991) Arch. *Biochem. Biophys*. **291**,59-68.

CHAPTER 5: GENERAL CONCLUSIONS

This study provides the mechanism of nucleotide release of HKI from the mitochondrion. TNP-ADP and ATP significantly released HKI from the mitochondrion in the absence of Mg^{2+}. HKI does not utilize TNP-nucleotides as substrates. Consequently TNP-ADP release is not due Glc-6-P production. TNP-ADP is a competitive inhibitor of HKI with respect to ATP. TNP-ADP competes with ATP^{4-} and ATP-Mg^{2-} for a binding at the C-terminal half of HKI. TNP-ADP binding to the N-terminal half of HKI is weak or absent altogether, and yet TNP-ADP releases both wild-type and N-domain HKI from the mitochondrion. Evidently, the binding site for TNP-ADP at the C-terminal half is also not responsible for HKI release from the mitochondrion. Hence, TNP-ADP release of HKI must be due to its binding to the mitochondrion.

VDAC-1 is a possible mitochondrion binding site for nucleotides. TNP-nucleotides bind to VDAC-1 similarly high affinities. They are also equally effective in the release of HKI from the mitochondrion. ATP displaces TNP-ADP from VDAC-1 and also releases HKI from mitochondria. CDP is unable to displace TNP-ADP from VDAC-1, and it is also unable to displace HKI from the mitochondrion. The VDAC-1 binding site for TNP-nucleotides strongly interacts with the TNP moiety. The base and phosphoryl groups of TNP-nucleotides seem to play a secondary role in the high-affinity association of these nucleotides. ATP seems more effective that ADP in the release of HKI from the mitochondrion, indicating some preference for the triphosphoryl over the diphosphoryl group.

TNP-nucleotides competitively inhibit HKI and are equally effective in binding and inhibition. Evidently, the nitrophenyl group plays a dominant role in interactions with HKI. The TNP-ADP dissociation constant measured by fluorescence is 10-fold smaller than the inhibition constant determined by activity assays. The difference could be attributed to conformational states of HKI that are mutually exclusive, one favoring interactions with TNP-nucleotides and the other favoring the substrate $[ATP\text{-}Mg]^{2-}$ of HKI. These two conformations of HKI would necessarily be in slow exchange.

In agreement with synergistic binding of glucose and Glc-6-P to HKI, Glc-6-P displaces TNP-ADP from HKI more effectively in the presence than in the absence of glucose. Displacement of TNP-ADP can be explained by the binding of Glc-6-P to the active site or to the N-terminal half allosteric site. The reduction Glc-6-P binding affinity in the mutant G747L HKI, a mutation outside of the C-terminal half binding pocket for Glc-6-P, indicates TNP-ADP displacement by Glc-6-P may be by the allosteric mechanisms. The absence of a significant effect on the dissociation constant of TNP-ADP due to the S788M mutation indicates the base-binding pocket of ATP is not used by TNP-ADP. TNP-ADP then is not an analog of ATP, but binds at a site at the C-terminal half that is sensitive to the allosteric action of Glc-6-P.

Loss of mitochondrial binding properties due to the loss of the 15 N-terminal residues of rat-brain HKI suggests that one or more of these residues are necessary for the binding of HKI to the membrane. No single-residue determinant of HKI mitochondrial-binding are known, this study reports two residues are essential for binding. Selective mutations amongst the first 15 residues have no effect on kinetic

properties of HKI, and wild-type and mutant enzymes behave identically as monomers in solution. The N-terminus in all constructs is block by unknown functional group that prevents sequencing by Edman degradation. Mutant enzymes A4L and A8L do not bind to the mitochondrion. These residues define a contiguous surface of the N-terminal helix of HKI. That surface does not tolerate large hydrophobic side chains, indicating a close contact between it and a mitochondrial binding partner (VDAC-1).

The work here provides a new (displacement of TNP-ADP for VDAC-1), which can be used in a high-throughput screen for molecules that displace TNP-ADP from VDAC-1. These molecules should also displace HKI from the mitochondrion, and indeed, molecules are currently known that do displace HKI from mitochondrion, but the mechanism by which these molecules function is unknown.. Work here also defines a surface of contact between HKI and VDAC-1 that can serve as a basis for modeling the complex of VDAC-1 with HKI. That model should predict additional points of interaction that can be confirmed by mutation.

ACKNOWLEDGMENTS

I would like to thank Dr. Richard Honzatko, my major professor, for his guidance through my graduate career. I would like to thank him for his encouragement and support as a teacher and a mentor, and above all, I thank him for his friendship. My appreciation extends to my colleagues: Lu Shen, Muneaki Watanabi, Yang Gao, Nidhi Shah, Nathanial Ginder, Danny Binkawsky, Andrew Skaff, and Justin Hines for their help and support. In addition, I would like to express my gratitude to Dr. Raji Joseph for here help and useful advises. Thanks extend to Dr. Marit Nelson-Hamilton and Dr. Lee Bendickson for their help using their laboratory ELISA plate reader. Also thanks for Dr. Gaya Amarasinghe for his support and advice. Special thanks for my committee member for their encouragement and help through the years of my research.

Finally I thank my wife, three children, mother and sister for their patience, understanding and support.